STRUCTURE AND MECHANISM OF HORMONE PERCEPTION AND SIGNAL TRANSDUCTION BY ABSCISIC ACID RECEPTORS

NG LEY MOY (HUANG LIMEI)

B.Sc. (Hons.), Nanyang Technological University

A THESIS SUBMITTED FOR THE DEGREE OF DOCTOR OF PHILOSOPHY

NUS GRADUATE SCHOOL FOR INTEGRATIVE SCIENCES AND ENGINEERING

NATIONAL UNIVERSITY OF SINGAPORE

2013

DECLARATION

I hereby declare that this thesis is my original work and it has been written by me in its entirety. I have duly acknowledged all the sources of information which have been used in the thesis.

This thesis has also not been submitted for any degree in any university previously.

_____

NG LEY MOY

25 June 2013

ACKNOWLEDGEMENTS

First and foremost, I would like to express my gratitude to my supervisors, Professor Yong Eu Leong, Dr Eric Xu and Dr Karsten Melcher for providing me the opportunity to embark on this valuable research experience and nurturing me over the years. I appreciate the unfailing support from my main supervisor Professor Yong and co-supervisor Dr Li Jun, allowing me to pursue and explore alternative topics of interest and giving me advice and assistance when needed. I have been deeply inspired by my mentors, Dr Eric Xu and Dr Karsten Melcher whom I have benefitted immensely from under their close guidance during my attachment in Van Andel Institute (VAI).

I would like to acknowledge and thank NGS for providing me with the 4-year PhD scholarship as well as approval and additional financial support allowing me to perform my research in VAI under the "2+2" collaborative scheme. I would also like to acknowledge the Department of Obstetrics & Gynaecology for hosting and supporting my studies in NUS. I would like to thank my TAC chairperson, Assoc. Prof. K Swaminathan and TAC member, A/Prof. Gong Yinhan for their advice in my PhD qualifying examination and thesis.

I am deeply grateful to VAI for hosting my overseas attachment. The two years I spent working in VAI has been one of the most valuable and memorable experiences in my life so far. I have met many wonderful people who have helped me in my work and/or made my overseas living a smooth and enjoyable experience. I appreciate Margie, Ajian, Gao Xiang and Cathy for their help with my settling-in at the new location. I am thankful to Kelly

for her patience and kindness in teaching me the basic techniques when I first started working in VAI. I am grateful to be part of the "ABA team", consisting of Dr Eric, Dr Karsten, Dr Edward, Jasmine, Amanda, Kelly and Dr Xu Yong, in which we have worked closely and tirelessly to stay ahead in the intense competition. I would like to thank all members of Dr Eric Xu's lab for being such helpful and approachable colleagues. I have made many friends during my stay in Grand Rapids, who have given me much fun, laughter and encouragement. Although I regret that I am not able to list all of them here, I would make a special mention to Amanda, Kelly, Jennifer, Shiva, Kuntal, Krishna, Ting Ting, Jasmine, Eileen, Xiaodan, Lili, Cynthia and AK. I was also deeply touched by the warm reception and sumptuous delicacies I have received from the families of Amanda, Karsten, Eric, Ajian and Jinming in their homes. Many thanks for the wonderful times!

Back in my Singapore homeland, I have been treated to a warm welcome by the lab of Professor Yong. I am fortunate to have worked with my wonderful colleagues Dr Inthrani, Dr Sun Feng, Bao Hui, Ryan, Vanessa, Seok Eng and Zhi Wei, all whom I have became friends with. Thanks for always being very helpful and offering a listening ear whenever I needed.

I would also extend my gratitude to everyone else who have supported me in one way or another, including my previous mentors and colleagues. Also, a special mention here to Kah Ying and Terence.

Last but not least, I would like to thank my family and friends for being understanding and encouraging when I had been away from them in the pursuit of my PhD. Thanks for believing in me and standing by me. Finally, I would like to dedicate this thesis to my parents and brothers.

TABLE OF CONTENTS

SUMMARY

Adverse environmental conditions are a threat to agricultural yield, which in turn affect livelihood, health and economy worldwide. Abscisic acid (ABA) is a vital plant hormone that regulates abiotic stress tolerance, allowing plants to cope with environmental stresses. Upon ABA induction, several members of Snf1-related protein kinases (SnRKs) are activated and mediate the ABA response. Under basal conditions, a group of type 2C protein phosphatases (PP2Cs) act as negative regulators to silence the ABA signalling pathway, apparently by inhibiting SnRKs. The identity of the ABA receptor has been controversial until at least 2 recent studies independently discovered the same group of 14-member PYR/PYL/RCAR (in this thesis referred to as PYL for simplicity) family to be the likely ABA receptors. It has been proposed that ABA induces PYLs to inhibit PP2Cs, resulting in the activation of SnRKs and the ABA response, although the mechanisms have been unknown.

In this study, the structures of representative PYLs in apo and ABA-bound forms were determined using X-ray crystallography, providing evidence for the role of PYLs as ABA receptors. Comparison of the structures of ABA-bound and unbound receptors revealed conformational changes in 2 receptor loops, termed ‘gate’ and ‘latch’ loops, upon hormone binding. The functional importance of these loops and key pocket residues involved in ABA recognition were validated by biochemical assays of mutant receptors.

Subsequently, the structures of representative apo PP2C and PYL–ABA–PP2C complexes were determined. Analyses of these structures

revealed that while the overall PP2C conformation remains unchanged in PYL interaction, the receptor undergoes ABA-induced structural changes in the gate and latch regions that promote PP2C binding. In the PYL–ABA–PP2C structure, a conserved PP2C tryptophan residue inserts into the PYL pocket, acting as a molecular lock that stabilizes the receptor-phosphatase interaction. In this conformation, PYL sterically blocks the PP2C active site, which explains for the ABA-induced PYL inhibition of the phosphatase. Hence, we identified a 'gate-latch-lock' mechanism of hormone binding and signal transduction by the PYL ABA receptor. These structural observations were supported by interaction and phosphatase activity assays with mutant PYLs and PP2Cs.

Consistent with previous findings, we showed that pyrabactin, a synthetic ABA agonist, selectively activates or inhibits specific members of the PYL family. Here, the crystal structures of representative pyrabactin-activated and pyrabactin-antagonized PYL complexes were determined. Comparison of these structures revealed the molecular mechanisms underlying the selective PYL activation and repression, providing a basis for future design of specific ABA receptor agonists and antagonists.

Together, these data contribute significantly to the understanding of the molecular mechanisms controlling ABA responses. Such advancement will be valuable for developments in plant biotechnology to solve worldwide agriculture-implicated issues and may also contribute to the understanding of similar intracellular signalling mechanisms in humans.

LIST OF TABLES

LIST OF FIGURES

LIST OF ABBREVIATIONS

AAO3	Abscisic aldehyde oxidase
ABA	Abscisic acid
ABA–GE	ABA glucosyl ester
ABF	ABRE-binding factor
ABI	ABA-insensitive
ABRE	ABA-responsive element
AGI	Arabidopsis Genome Initiative
AMPK	Adenosine monophosphate (AMP)-activated protein kinase
AREB	ABRE-binding protein
cDNA	Complementary DNA
CDPK	Calcium-dependent proteins kinase
Da	Dalton
DMSO	Dimethyl sulfoxide
DNA	Deoxyribonucleic acid
DPA	Dihydrophaseic acid
EC_{50}	Half-maximal effective concentration
ER	Endoplasmic reticulum
GST	Glutathione-S-transferase
HAB	Homology to ABI
HSQC	Heteronuclear single quantum coherence
IC_{50}	Half-maximal inhibitory concentration
IPTG	Isopropyl β-D-1-thiogalactopyranoside
ITC	Isothermal titration calorimetry
K_d	Dissociation constant

kD	kilo Dalton
MBP	Maltose binding protein
MCS	Multiple cloning site
MW	Molecular weight
NCED	9-cis-epoxycarotenoid dioxygenase
NMR	Nuclear magnetic resonance
ORF	Open reading frame
OST1	Open stomata 1
PA	Phaseic acid
PCR	Polymerase chain reaction
PI	Isoelectric focusing point
PP2C	Type 2C protein phosphatase
PYL	PYR1-like
PYR1	Pyrabactin Resistance 1
RCAR	Regulatory Component of ABA Receptor
RMSD	Root-mean-square deviation
SD	Standard deviation
SEC	Size exclusion chromatography
Snf1	Sucrose nonfermenting
SnRK	Snf1-related protein kinase
SPA	Scintillation proximity assay
StAR	Steroidogenic acute regulatory protein
STARD	START domain protein
START	Steroidogenic acute regulatory (StAR)-related lipid transfer
ZEP	Zeathanxin epoxidase

LIST OF PUBLICATIONS

1. Melcher K, **Ng LM***, Zhou XE, Soon FF, Xu Y, Suino-Powell KM, Park SY, Weiner JJ, Fujii H, Chinnusamy V, Kovach A, Li J, Wang Y, Li J, Peterson FC, Jensen DR, Yong EL, Volkman BF, Cutler SR, Zhu JK, Xu HE. A gate-latch-lock mechanism for hormone signalling by abscisic acid receptors. *Nature.* 2009 Dec 3;462(7273):602-8.

2. Melcher K, Xu Y, **Ng LM***, Zhou XE, Soon FF, Chinnusamy V, Suino-Powell KM, Kovach A, Tham FS, Cutler SR, Li J, Yong EL, Zhu JK, Xu HE. Identification and mechanism of ABA receptor antagonism. *Nat Struct Mol Biol.* 2010 Sep;17(9):1102-8.

3. **Ng LM***, Soon FF, Zhou XE, West GM, Kovach A, Suino-Powell KM, Chalmers MJ, Li J, Yong EL, Zhu JK, Griffin PR, Melcher K, Xu HE. Structural basis for basal activity and autoactivation of abscisic acid (ABA) signaling SnRK2 kinases. *Proc Natl Acad Sci U S A.* 2011 Dec 27;108(52):21259-64.

4. Soon FF, **Ng LM***, Zhou XE, West GM, Kovach A, Tan MH, Suino-Powell KM, He Y, Xu Y, Chalmers MJ, Brunzelle JS, Zhang H, Yang H, Jiang H, Li J, Yong EL, Cutler S, Zhu JK, Griffin PR, Melcher K, Xu HE. Molecular mimicry regulates ABA signaling by SnRK2 kinases and PP2C phosphatases. *Science.* 2012 Jan 6;335(6064):85-8.

5. Zhou XE, Soon FF, **Ng LM***, Kovach A, Suino-Powell KM, Li J, Yong EL, Zhu JK, Xu HE, Melcher K. Catalytic mechanism and kinase interactions of ABA-signaling PP2C phosphatases. *Plant Signal Behav.* 2012 May 1;7(5):581-8.

Notes and author contributions:

*Co-first author.

The scope of this thesis is primarily based on publications 1 and 2.

Prof. Yong EL, Dr. Li J, Dr. Xu HE and Dr. Melcher K conceived the project and supervised research.

Ng LM (contributed key data in publications 1 and 2) and Soon FF (contributed mostly in publications 3-5) performed most of the research work, with contributions from all authors.

Dr Zhou XE solved crystal structures.

CHAPTER 1

LITERATURE REVIEW

1.1 Introduction

"There are things known and there are things unknown, and in between are the doors of perception."
— Aldous Huxley

We are constantly surrounded by signals, for example, traffic signals, notifications, advertisements and feelings of pain or hunger. However, we are only aware of these signals if we perceive them. We would not know or respond if we do not perceive them, even if the signals have been there. Thus, in the process of conveying a signal, perception of the signal is as important as existence of the signal itself.

At the cellular level, extracellular signals are often sent to cells through molecules such as hormones. In plants, the hormone abscisic acid (ABA) is produced when environmental condition is harsh, to send signals to the plant cells to adapt as necessary. ABA was discovered in the 1960s and shortly after, much has been established about its chemistry and physiological importance (Weiner et al., 2010). In the following decades, more than 100 mediators involved in ABA signalling have been identified in molecular genetic, biochemical and pharmacological studies (Cutler et al., 2010). However, for almost half a century, a missing piece of puzzle remains in our knowledge of ABA signal transduction. That is, how the ABA signal is perceived.

The identification of ABA receptors, plant proteins that sense the hormone and relay the signal to other mediators in the pathway, has been a daunting task full of controversy and frustrations. Since 2006, several reports claimed to have identified the ABA receptors (McCourt and Creelman, 2008), but none has been substantiated after further investigations. The turnaround came in mid 2009 when at least two separate findings convincingly pointed to the same members belonging to the START-domain superfamily of proteins as the candidate ABA receptors (Ma et al., 2009; Nishimura et al., 2010; Park et al., 2009; Santiago et al., 2009b). The 14 members of this group of proteins are named Pyrabactin Resistance 1 (PYR1) and PYR1-like (PYL1–PYL13) (Park et al., 2009) or Regulatory Component of ABA Receptor (RCAR1–RCAR14) (Ma et al., 2009). For simplicity, this group of Arabidopsis START-domain proteins are referred to as PYL(s) in this thesis. The discovery of PYLs as the likely ABA receptors shed light into uncovering how plant cells perceive and relay the ABA signal, a knowledge that has valuable agricultural and economic implications.

This literature review focuses on the field of ABA signalling up till the initial discovery of the PYL proteins as the likely ABA receptors, highlighting the gaps that were to be addressed by the study presented in this thesis.

1.2 Physiological role of ABA in abiotic stress tolerance

ABA is a vital phytohormone that confers abiotic stress tolerance in plants (Zhu, 2002). Under stressful environmental conditions such as water shortage, salinity and temperature extremes, the ABA content in plants rises significantly, stimulating stress-tolerant effects that help them to cope and survive in the adverse conditions (Figure 1). It has been demonstrated that mutant plants engineered with enhanced sensitivity to ABA do better than their wild type counterparts in drought conditions (Saez et al., 2006). Under drought or osmotic stress, ABA promotes stomata closure to prevent water loss through transpiration and the accumulation of osmocompatible solutes to retain water (Cutler et al., 2010; Kim et al., 2010). It has also been shown that ABA is required for tolerance to freezing, by the induction of dehydration tolerance genes (Xiong et al., 2001).

The role of ABA as a negative plant growth regulator has been long established (Milborrow, 1974). The action of ABA in the induction and maintenance of seed dormancy is attributed to its potent effects in the inhibition of seed germination (Lopez-Molina et al., 2001). ABA also inhibits the growth and development of whole plants or plant parts and counteracts the effects of growth-stimulating hormones such as gibberellins (Cutler et al., 2010). The inhibitory effects of ABA on germination and growth help plants surpass the stress conditions and germinate only when the conditions are favourable for growth.

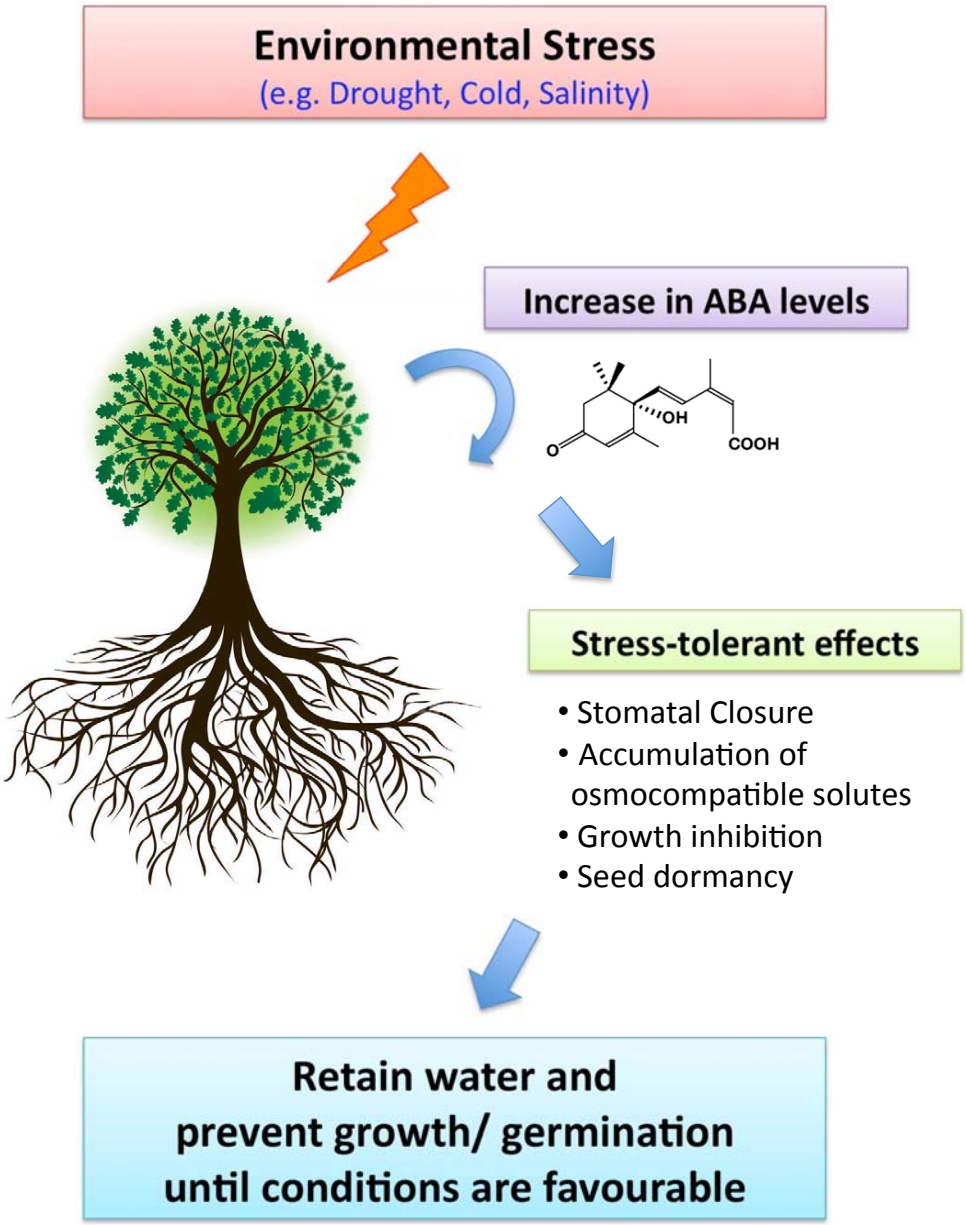

Figure 1. ABA confers abiotic stress tolerance in plants.

Overview of the ABA-mediated physiological responses that enable plants to adapt and survive in harsh environmental conditions.

1.3 Biosynthesis and transport of ABA

Stress signals induce the expression of enzymes responsible for ABA biosynthesis. Most of the ABA biosynthesis genes have been identified and cloned, which includes zeathanxin epoxidase (ZEP), 9-cis-epoxycarotenoid dioxygenase (NCED) and abscisic aldehyde oxidase (AAO3) (Xiong et al., 2001; Xiong et al., 2002). ABA is synthesized from C_{40} carotenoids through several enzymatic steps (Figure 2) (Nambara and Marion-Poll, 2005). Zeaxanthin, formed from the hydroxylation of β-carotene, is converted to violaxanthin by ZEP. This is followed by the synthesis and oxidative cleavage of neoxanthin into xanthoxin, the C_{15} precursor of ABA. The production of xanthoxin catalyzed by NCED is thought to be the key regulatory step in ABA biosynthesis. Xanthoxin is then converted into abscisic aldehyde which is oxidized into ABA.

The endogenous concentration of ABA is determined by the balance between ABA biosynthesis and catabolism, as well as the rate of ABA transport to the site of action. However, the mode of intercellular movement of ABA has been previously unclear. Although ABA can diffuse passively across biological membranes, recent evidence suggest that active transporters are involved in shuttling ABA in and out of cells. One such transporter, AtABCG25, was identified in a genetic screen of mutants with altered ABA sensitivity (Kuromori et al., 2010). AtABCG25 is an ATP-binding cassette (ABC) transporter expressed mainly in vascular tissues where ABA is predominantly synthesized.

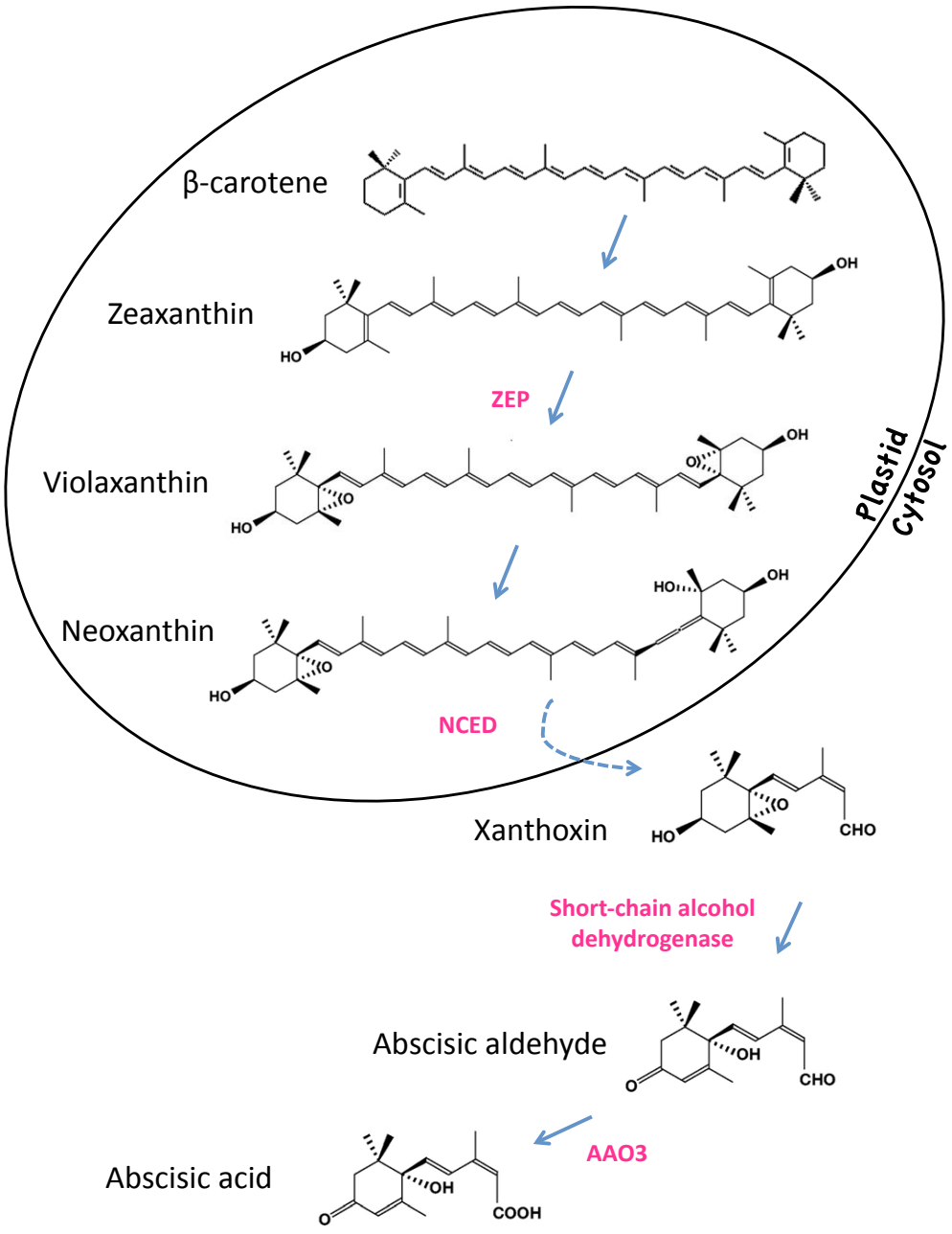

Figure 2. ABA biosynthetic pathway.

ABA is derived from C_{40} epoxycarotenoid precursors through oxidative cleavage reactions in the plastid. The C_{15} intermediate, xanthoxin, is exported to the cytosol where it is converted to ABA through a two-step reaction via abscisic aldehyde. The ABA biosynthetic enzymes, zeathanxin epoxidase (ZEP), 9-cis-epoxycarotenoid dioxygenase (NCED), short-chain alcohol dehydrogenase and abscisic aldehyde oxidase (AAO3), are shown in pink.

In AtABCG25-expressing membrane vesicles derived from insect cells, ATP-dependent efflux of ABA was detected, suggesting the role of AtABCG25 as an ABA exporter. Simultaneously, another ABC transporter, AtABCG40, was identified to be an ABA importer (Kang et al., 2010). ABA uptake was increased in cells overexpressing AtABCG40 and decreased in cells with defective AtABCG40. More recently, another ABA importer, ABA-importing transporter 1 (AIT1), has been identified (Kanno et al., 2012), additionally demonstrating the involvement of ABA transporters in the intercellular transmission of ABA. Thus, a simple model of ABA translocation has been proposed (Umezawa et al., 2010). In this model, ABA synthesized in vascular cells are actively transported by ABA exporters into the extracellular apoplastic space, after which uptake into the sites of action, such as guard cells, occur through active ABA importers.

1.4 Catabolism of ABA

When stress signals are alleviated, ABA is metabolized into inactive products. ABA catabolism occurs largely through two types of reaction, hydroxylation and conjugation. ABA can be hydroxylated on one of the three methyl groups (C-7', C-8' and C-9') of the ring structure (Figure 3). Of these, 8'-hydroxylation is thought to be the predominant ABA catabolic pathway (Cutler and Krochko, 1999). Accordingly, the products of the 8'-hydroxylation pathway, phaseic acid (PA) and dihydrophaseic acid (DPA) are the most abundant ABA catabolites. While 8'-hydroxy ABA contains substantial biological activity, spontaneous cyclization to form PA causes

significant reduction in activity (Zou et al., 1995). PA is further catabolized to the biologically inactive DPA.

Endogenous ABA levels in Arabidopsis decreases under high humidity conditions, primarily by ABA catabolism through the 8'-hydroxylation pathway (Okamoto et al., 2009). ABA 8'-hydroxylation is catalyzed by ABA 8'-hydroxylase, a cytochrome P450 encoded by CYP707A family of genes (Kushiro et al., 2004; Saito et al., 2004). Transcript levels of the 4 members of CYP707A family, CYP707A1–CYP707A4, are increased under drought stress and strongly induced upon rehydration (Kushiro et al., 2004), with the highest induction observed in CYP707A3 (Umezawa et al., 2006). Recent findings indicated that CYP707A3 functions in vascular tissues to reduce systemic ABA levels whereas CYP707A1 catabolizes local ABA pools inside guard cells in response to high humidity (Okamoto et al., 2009).

In addition to hydroxylation, ABA and its hydroxylated catabolites can be conjugated to glucose. The major glucose conjugate of ABA, ABA glucosyl ester (ABA–GE), is biologically inactive and may function as a storage form of releasable ABA (Dietz et al., 2000). In Arabidopsis, dehydration induces the activation of AtBG1, a β-glucosidase that hydrolyzes ABA–GE, leading to an increase in the active ABA pool (Lee et al., 2006). In plant leaves, ABA–GE is stored in the vacuole and apoplastic space (Dietz et al., 2000) whereas AtBG1 is localized to the endoplasmic reticulum (ER) (Lee et al., 2006). With its limited membrane permeability, it remains unclear how ABA–GE translocates from its storage site to the ER where it is hydrolyzed.

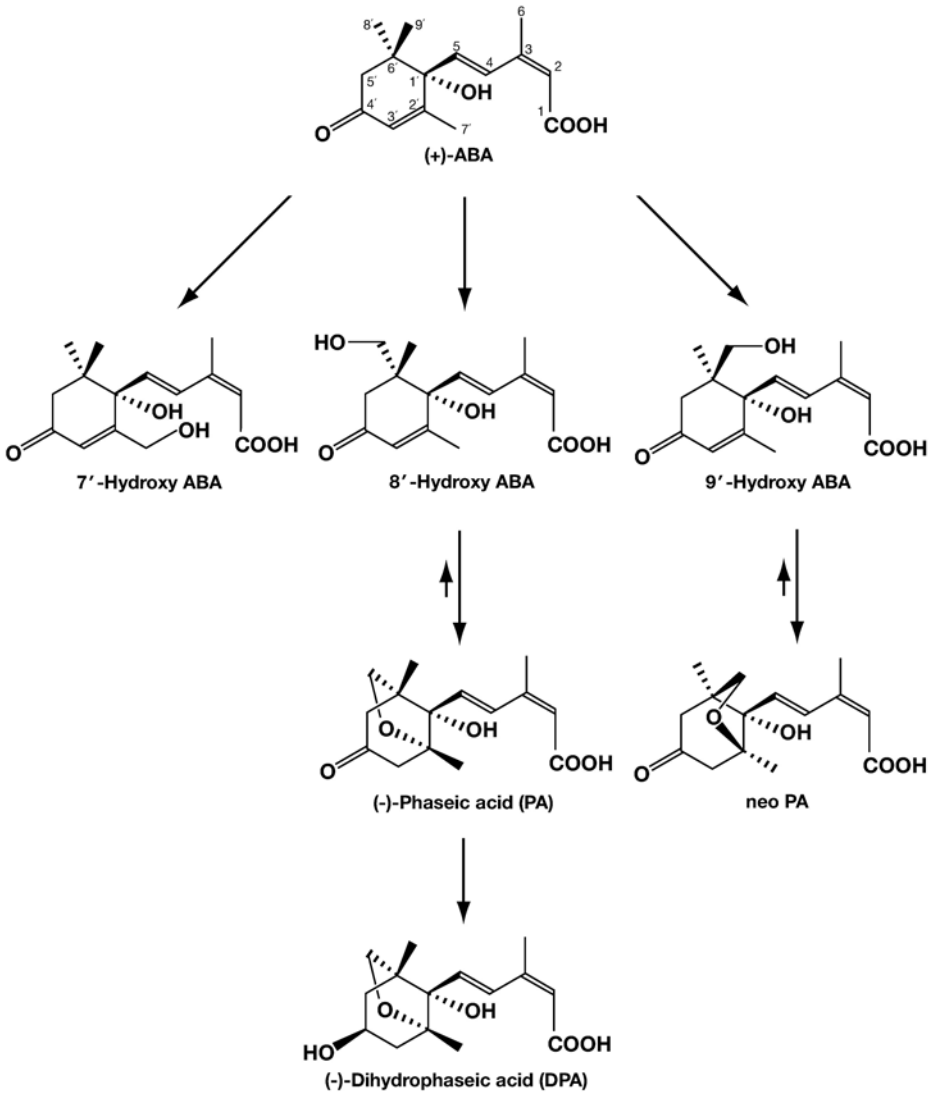

Figure 3. ABA catabolic pathways.

Three catabolic pathways via C-7', C-8' and C-9' hydroxylation are shown. Figure is adapted from *Annu. Rev. Plant Biol. 56:165–85* (Nambara and Marion-Poll, 2005).

1.5 Chemical features of ABA

The natural and biologically active isomer of ABA is the *S*-(+)-2-*cis*-4-*trans*-ABA, also commonly known as *S*-ABA, (+)-ABA or *S*-(+)-ABA. The molecular structure consist of a cyclohexene ring with a monomethyl group, a dimethyl group, a ketone group, a hydroxyl group and a hydrocarbon side chain conjugated to the carboxylic acid group (Figure 4). The 2-*cis*-4-*trans* side chain geometry is reversibly isomerized by light to form the 2-*trans*-4-*trans* inactive isomer (Cutler et al., 2010). Studies using ABA analogues lacking the 7', 8' or 9' methyl groups showed that the 7'- methyl group is critical to bioactivity (Walker-Simmons et al., 1994). A flip of the cyclohexene ring around the chiral carbon produces unnatural the *R*-(–)-enantiomer which has weak biological activity (Lin et al., 2005).

Specific ABA analogues, which are structural variants of the natural *S*-(+)-ABA, have been used to identify ABA-responsive genes and some are potential plant growth regulators (Asami et al., 1998; Huang et al., 2007). For instance, PBI-51, an acetylenic ABA analogue, has ABA antagonistic effects in *Brassica napus* and *Vicia faba* (Wilen et al., 1993; Yamazaki et al., 2003) while it is a weak ABA agonist in Arabidopsis (Nishimura et al., 2004). The use of PBI-51 to screen for ABA-related mutants has led to the isolation of novel ABA hypersensitive mutants (Nishimura et al., 2004). In addition, pyrabactin, a selective ABA agonist that does not structurally resemble ABA (Figure 4), has been employed in the isolation of PYR1 which led to the

discovery of the PYL family of proteins as ABA receptors (Park et al., 2009). This landmark study will be reviewed in further detail in section 1.6.6.1.

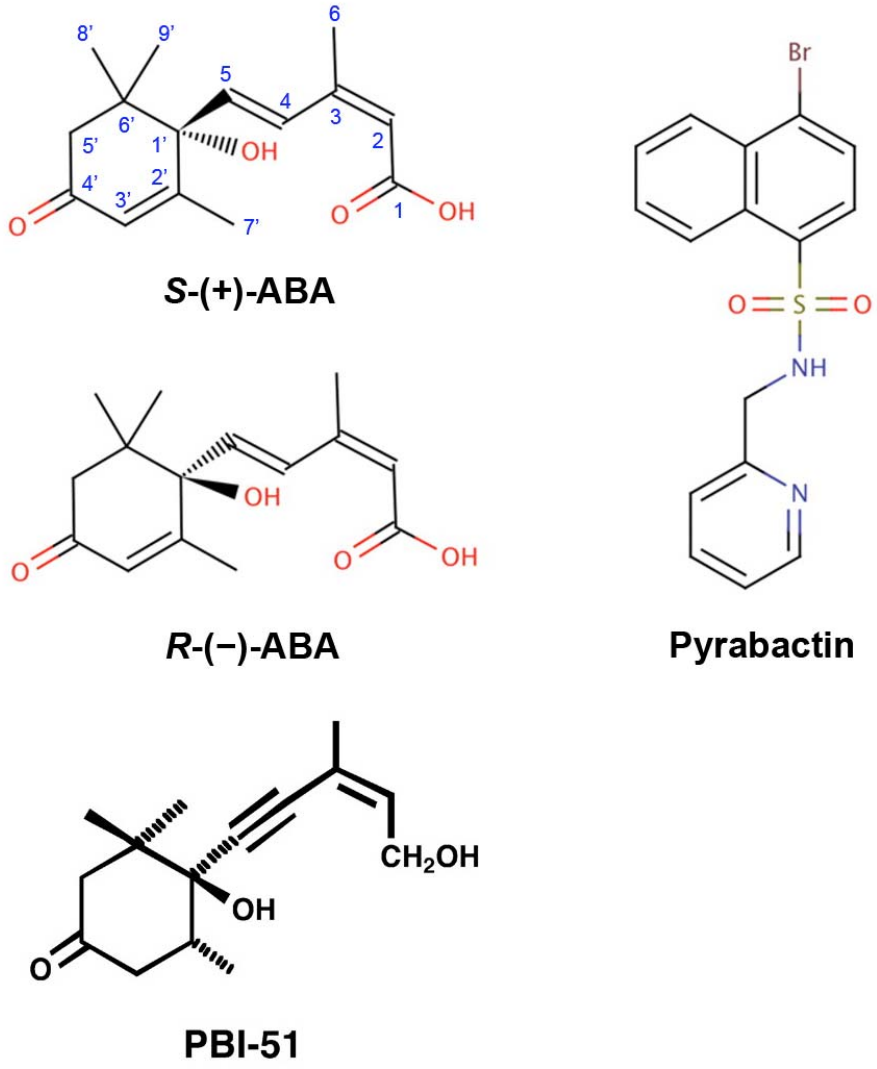

Figure 4. Chemical structures of ABA stereoisomers, structural analogue and pyrabactin.

The *S*- and *R*- stereoisomers of ABA differ by a flip around the chiral carbon (C-1'). PBI-51 is a structural analogue of ABA, while pyrabactin, which does not structurally resemble ABA, is a selective ABA agonist. Functional groups of ABA and pyrabactin are shown in colours. Nomenclature for the naming of carbon atom positions is shown for the *S*-(+)-ABA structure.

1.6 Components and model of the core ABA signalling pathway

1.6.1 PP2Cs negatively regulate ABA signalling

Reversible protein phosphorylation mediated by protein kinases and protein phosphatases is a major mechanism of cellular signal transduction across organisms. PP2Cs are a group of Mg^{2+}/Mn^{2+}-dependent Ser/Thr phosphatases. In plants, PP2Cs represent a major phosphatase family. Of the 112 phosphatases encoded in the Arabidopsis genome, 76 are PP2Cs, which genetically clustered into 10 groups (A-J) with the exception of 6 genes that could not be clustered (Figure 5) (Schweighofer et al., 2004). At least 6 of the 9 members of group A PP2Cs have been shown to be involved in ABA signalling, of which ABI1, ABI2 and HAB1 have been best characterized.

The isolation and characterization of Arabidopsis ABA-insensitive mutants have led to identification of members of group A PP2Cs as negative regulators of ABA signalling. Dominant mutations *abi1-1* (ABI1 G180D) and *abi2-1* (ABI2 G168D) resulting in reduced ABA responsiveness have been isolated in genetic screens of mutagenized Arabidopsis seeds (Leung et al., 1994; Leung et al., 1997; Meyer et al., 1994; Rodriguez et al., 1998a). Both mutants display reduced ABA-induced effects on seed dormancy, seedling growth, drought tolerance and stomatal regulation. The *ABI1* and *ABI2* genes encode homologous PP2C proteins and are transcriptionally upregulated by ABA treatment. Subsequently, HAB1 was identified based on its sequence homology to ABI1 and ABI2 (Rodriguez et al., 1998b).

Group	AGI code	Gene name
A	At4g26080	ABI1
	At5g57050	ABI2
	At1g72770	HAB1
	At1g17550	HAB2
	At5g51760	AHG1
	At3g11410	PP2CA
	At5g59220	HAI1
	At1g07430	HAI2
	At2g29380	HAI3
B	At1g67820	
	At2g40180	PP2C5
	At1g07160	
	At2g30020	
	At3g27140	
	At4g08260	
C	At3g16560	
	At2g46920	POL
	At2g35350	PLL1
	At5g02400	PLL2
	At3g09400	PLL3
	At2g28890	PLL4
	At1g07630	PLL5
D	At5g02760	
	At3g17090	
	At3g12620	
	At3g55050	
	At4g38520	
	At3g51370	
	At5g66080	
	At4g33920	
	At5g06750	
E	At1g03590	
	At1g16220	
	At1g79630	
	At5g01700	
	At3g02750	
	At5g36250	
	At5g26010	
	At4g32950	
	At3g16800	
	At3g05640	
	At5g27930	
	At2g20050	
	At3g06270	

Group A PP2C:

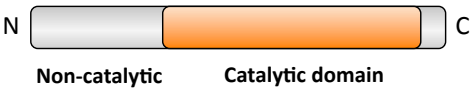

Group	AGI code	Gene name
F	At3g23360	
	At2g34740	
	At1g78200	
	At1g22280	PAPP2C
	At1g34750	
	At3g15260	
	At2g20630	PIA1
	At4g28400	
	At1g43900	
	At5g53140	
	At4g31750	WIN2
	At5g24940	
	At5g10740	
G	At3g62260	
	At1g48040	
	At3g17250	
	At2g25620	DBP1
	At2g33700	
	At3g51470	
H	At1g09160	
	At1g47380	
	At1g68410	
I	At2g25070	
	At4g31860	
J	At3g63320	
	At3g63340	
Unclassified	At4g11040	
	At1g18030	
	At1g75010	
	At4g27800	TAP38
	At2g40860	
	At5g19280	KAPP

Figure 5. Classification of Arabidopsis PP2Cs.

Classification is based on genetic clustering data from *TRENDS in Plant Science. 9:236-243* (Schweighofer et al., 2004). The general domain structure of group A PP2C, which comprises of an N-terminal non-catalytic region and a C-terminal PP2C catalytic domain, is shown beside the group A cluster. AGI: Arabidopsis Genome Initiative.

Consistent with the phenotypic effects observed in the *abi1-1* and *abi2-1* mutations, the corresponding mutation in HAB1 (G246D) resulted in strong ABA insensitivity (Robert et al., 2006). The *abi1-1*, *abi2-1* and HAB1 G246D mutations correspond to substitution of a conserved glycine residue with aspartate in the phosphatase catalytic centre, causing a dramatic reduction in the phosphatase activity towards phospho-casein, used as a heterologous substrate. However, owing to the dominant nature of the mutation, it was uncertain whether these PP2Cs are involved in ABA signalling or the mutation introduces unspecific phenotypes that are not related to the original function of the wild type proteins.

It was the additional isolation of recessive loss-of-function mutations in the catalytic regions of ABI1, ABI2 and HAB1 resulting in ABA hypersensitive phenotypes that provided critical evidence that these PP2Cs negatively regulate ABA signalling (Gosti et al., 1999; Merlot et al., 2001; Saez et al., 2004). This concept was further demonstrated by double or triple PP2C knockout mutants displaying enhanced hypersensitivity to ABA (Rubio et al., 2009; Saez et al., 2006). Consistently, the constitutive expression of HAB1 (35S:HAB1) in Arabidopsis led to reduced ABA sensitivity, supporting its role as inhibitor of ABA signalling (Saez et al., 2004).

Based on the negative regulatory roles of the group A PP2Cs, it remained enigmatic how the *abi1-1* and *abi2-1* mutations and the corresponding G246D mutation in HAB1 induce dominant ABA insensitive phenotypes. Interestingly, the abi1-1 mutant protein was able to inhibit ABA signal

transduction as effectively as the wild type protein, shown in an ABA-inducible transcription assay in plant protoplasts (Sheen, 1998). More recent studies have revealed the hypermorphic nature of this type of mutation (Moes et al., 2008; Robert et al., 2006), but do not fully explain how such mutation interferes with ABA signal transduction. Elucidation of the molecular basis of how PP2Cs negatively regulate ABA signalling is required.

1.6.2 SnRK2s mediate the ABA response

The identification of PP2Cs has indicated that protein phosphorylation events are important in ABA signalling. In line with this concept, the SnRK2 family was identified as ABA-activated protein kinases (Mustilli et al., 2002; Yoshida et al., 2002). SnRK2 belong to the SnRK group of protein kinases that are closely related to the yeast Snf1 and mammalian AMPK kinases. The Arabidopsis genome contains 38 SnRKs, which are classified into 3 groups, namely SnRK1 (1.1–1.3), SnRK2 (2.1–2.10) and SnRK3 (3.1–3.25) (Hrabak et al., 2003) (Figure 6a). The SnRK1 group shares the highest degree of homology with Snf1 and AMPK. Like its yeast and mammalian counterpart, SnRK1 is best known for its role as a key metabolic regulator (Polge and Thomas, 2007). In contrast, SnRK2 and SnRK3 are unique to plants and are thought to be involved in abiotic stress signalling (Coello et al., 2011).

There are 10 SnRK2 members in Arabidopsis, designated as SRK2I–SRK2J (Yoshida et al., 2002) or SnRK2.1–SnRK2.10 (Hrabak et al., 2003), and are

divided into 3 subclasses, I, II and III (Figure 6a). All SnRK2 members, except SnRK2.9, can be activated by osmotic stress as shown in Arabidopsis protoplast system (Boudsocq et al., 2004). Consistently, Arabidopsis decuple mutant lacking all 10 SnRK2s grew poorly under osmotic stress (Fujii et al., 2011), revealing the importance of SnRK2s in osmotic stress signalling. However, not all SnRK2 members can be activated by ABA, suggesting that osmotic stress signalling consists of ABA-dependent and ABA-independent pathways. While SnRK2 subclass I members are not activated by ABA, subclass II members, represented by SnRK2.7 and SnRK2.8, are weakly activated by ABA. In contrast, the members of the subclass III are strongly activated by ABA (Boudsocq et al., 2004).

Subclass III of the Arabidopsis SnRK2 family contains 3 kinases, namely SnRK2.2/SRK2D, SnRK2.3/SRK2I and SnRK2.6/SRK2E/OST1. This subclass of ABA-responsive kinases has been identified as the main positive regulators of ABA signalling. The physiological role of SnRK2.6 has been initially determined in guard cells. Loss-of-function mutations in SnRK2.6 disrupted ABA-induced stomata closure in Arabidopsis (Mustilli et al., 2002; Yoshida et al., 2002). On the other hand, a snrk2.2 snrk2.3 double mutant showed strong ABA insensitivity in seed germination and root growth inhibition (Fujii et al., 2007). Consequently, triple mutants lacking SnRK2.2, SnRK2.3 and SnRK2.6 resulted in impairment in almost all ABA responses, indicating the centrality of these kinases to ABA signalling (Fujii and Zhu, 2009; Fujita et al., 2009; Nakashima et al., 2009a).

SnRK2s contain a well-conserved kinase catalytic domain and a C-terminal regulatory region that encompasses 2 domains. Domain I, which is also known as SnRK2 box, is conserved within all SnRK2s. Domain II is a highly acidic region that is only conserved among the ABA-responsive members, and thus is also known as the ABA box (Belin et al., 2006; Yoshida et al., 2006) (Figure 6b).

Many reports have demonstrated that phosphorylation is important for the activation of SnRK2s. Active recombinant SnRK2.6 is autophosphorylated and several phosphorylation sites have been identified, in which phosphorylation of S175 in the activation loop is critical for its kinase activity (Belin et al., 2006). Active SnRK2s are able to directly phosphorylate targets such as ion channels and transcription factors to elicit the ABA response (reviewed in sections 1.6.3 and 1.6.4).

The group A PP2Cs ABI1, ABI2 and HAB1 have been shown to directly bind to and dephosphorylate SnRK2.6 (Vlad et al., 2009) and the ABA box domain of SnRK2.6 is important for such interaction (Yoshida et al., 2006). Altogether, these findings suggest that group A PP2Cs negatively regulate ABA signalling by repressing the class III SnRK2s, which are positive transducers of the ABA response. However, how ABA accumulation leads to SnRK2 activation had been unknown.

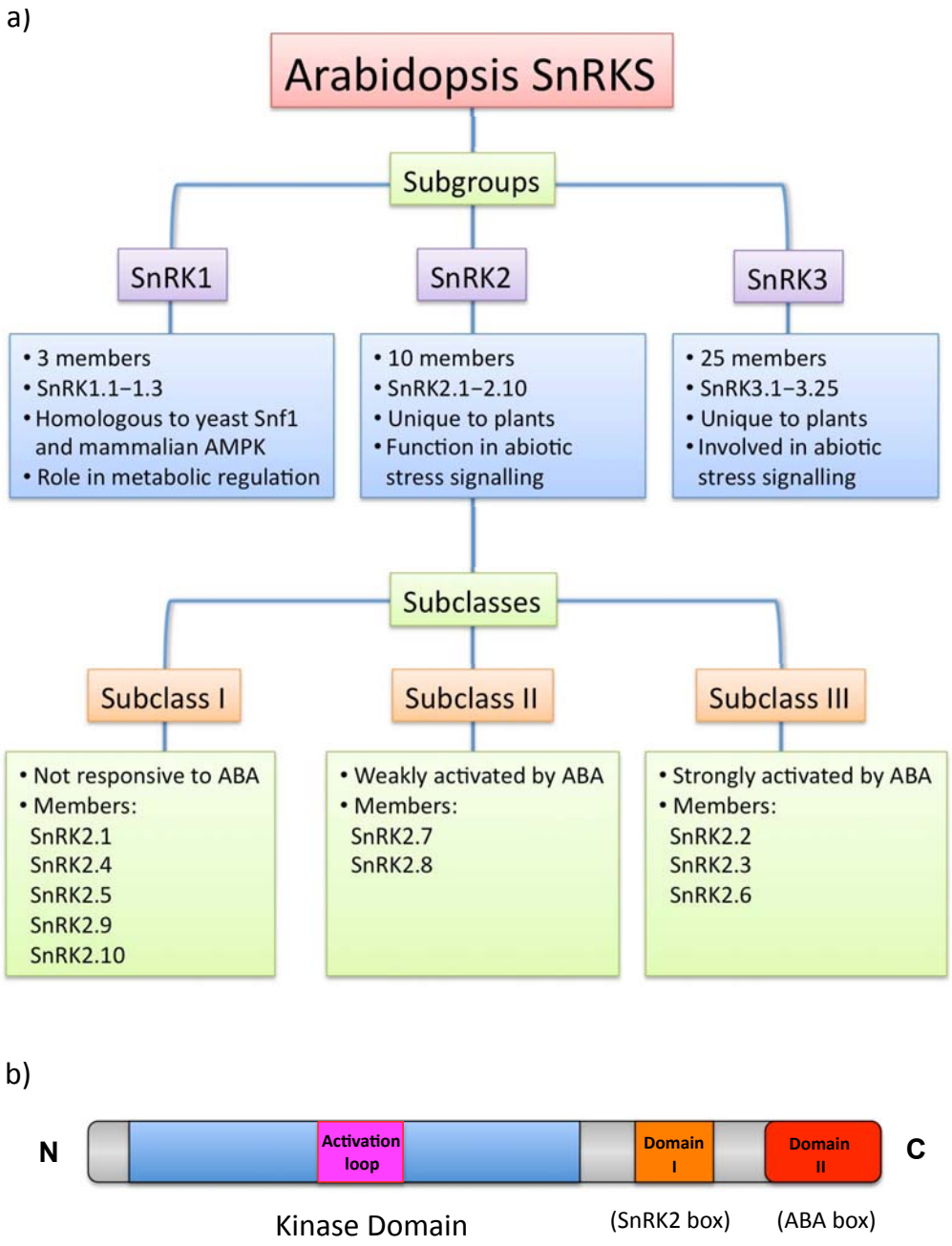

Figure 6. Classification and domain structure of Arabidopsis SnRK2.

a) Diagram showing the classification of Arabidopsis SnRK groups and subclasses of the SnRK2s. **b)** Domain structure of Arabidopsis SnRK2.

1.6.3 ABA regulation of ion channels

ABA-induced stomata closure appears to act through ion channels on guard cell membranes. One of these is the slow-type anion channel, SLAC1, shown to be essential in stomata closure in response to in response to various factors such as ABA and CO_2 (Negi et al., 2008; Vahisalu et al., 2008). SLAC1 is phosphorylated and activated by SnRK2.6, and this activation can be inhibited by PP2C (Geiger et al., 2009; Lee et al., 2009). In addition, an inward-rectifying potassium channel, KAT1, is also a target of SnRK2.6. ABA-activated SnRK2.6 can phosphorylate Thr306 of KAT1 and such modification reduces KAT1 activity, suggesting that active SnRK2.6 negatively regulates KAT1 by phosphorylation to promote stomata closure (Sato et al., 2009). Therefore, SnRK2s are important regulators of ion channels in mediating ABA-induced stomata closure.

1.6.4 ABA regulation of gene expression

ABA accumulation in plant cells leads to changes in gene expression that generally contributes to drought stress tolerance. Transcriptome studies in rice and Arabidopsis have shown that exposure to ABA and various abiotic stresses result in changes to about 5–10 % of the genome, whereby more than half of these changes were common to drought, salinity and ABA treatments (Nakashima et al., 2009b; Shinozaki et al., 2003). ABA-induced genes code for proteins involved in stress tolerance such as dehydrins, enzymes that

detoxify reactive oxygen species (ROS) and regulatory proteins such as transcription factors, protein phosphatases and kinases. ABA-repressed genes are enriched for those encoding proteins associated with cell growth.

Many *cis*-acting DNA elements have been identified by analysis of the promoters of ABA-responsive genes (Busk and Pages, 1998). These elements, designated as ABA-responsive elements (ABREs), commonly contain the PyACGTGG/TC consensus sequence belonging to the G-box family (CACGTG), which has been implicated in a wide range of gene expression mechanisms in plants (Menkens et al., 1995). ABA-responsive gene expression requires multiple ABREs or the combination of an ABRE with a coupling element (Gomez-Porras et al., 2007; Zhang et al., 2005).

The ABRE-binding (AREB) proteins, or ABRE-binding factors (ABFs) were isolated by using ABRE sequences as bait in yeast one-hybrid screenings (Choi et al., 2000; Uno et al., 2000). The AREB/ABFs encode basic-domain leucine zipper (bZIP) transcription factors and belong to the group A subfamily, which is composed of nine homologues in the Arabidopsis genome that share a highly conserved C-terminal bZIP domain and three additional N-terminal conserved regions designated as C1, C2 and C3 (Jakoby et al., 2002). These nine homologues can be divided into two groups, the ABI5 family (ABI5, EEL, DPBF2/AtbZIP67, DPBF4, and AREB3) which are mainly expressed in seeds and are involved in seed development and maturation (Bensmihen et al., 2005; Bensmihen et al., 2002; Finkelstein and Lynch, 2000; Kim et al., 2002), and the AREB/ABF family (ABF1, AREB1/ABF2,

AREB2/ABF4, and ABF3) that are mainly expressed in vegetative tissues under abiotic stress conditions (Choi et al., 2000; Fujita et al., 2005; Kang et al., 2002; Kim et al., 2004; Uno et al., 2000). While ABF1 is strongly induced by cold but not by osmotic stress (Kim, 2006), AREB1/ABF2, AREB2/ABF4 and ABF3 are induced by dehydration, high salinity and ABA treatment during vegetative growth (Fujita et al., 2005). Overexpression of these factors enhances drought stress tolerance (Fujita et al., 2005; Kang et al., 2002; Kim et al., 2004) and triple mutation causes impaired stress-responsive gene expression (Yoshida et al., 2010), indicating that AREB1, AREB2 and ABF3 are master transcription factors that regulate ABRE-dependent expression of stress-responsive genes.

Several studies suggest that ABA-dependent phosphorylation of AREB/ABFs is needed for their full activation. AREB1 requires ABA for its full activation and its activity is regulated by ABA-dependent multi-site phosphorylation of the conserved domains (Furihata et al., 2006). ABA-activated SnRK2s, including SnRK2.2, SnRK2.3 and SnRK2.6, have been shown to phosphorylate AREB1 (Furihata et al., 2006). Loss of function of SnRK2.2 and SnRK2.3 resulted in reduction in the phosphorylation of ABFs (Fujii et al., 2007). In the triple mutant lacking SnRK2.2, SnRK2.3 and SnRK2.6, ABA-induced gene expression was eliminated (Fujii and Zhu, 2009). These results suggest that SnRK2s are essential for ABA-induction of gene expression through the phosphorylation and activation of ABFs. However, the molecular events leading to ABA-dependent activation of SnRK2s remained unknown. Identification of ABA receptors is an important step to link our

understanding from ABA perception to SnRK2 activation. The search for ABA receptors have started with several controversial candidates, as reviewed below.

1.6.5 Putative ABA receptor candidates

1.6.5.1 Flowering Time Control Protein A (FCA)

The first gene reported to be an ABA receptor is the FCA, an RNA-binding protein which controls flowering time in Arabidopsis (Razem et al., 2006). FCA shares sequence similarity with the barley protein ABAP1, which was reported to bind ABA with high affinity (Razem et al., 2004). However, FCA does not appear to have any function in classical ABA responses such as seed dormancy and stomata regulation, thus its role as an ABA receptor has been questionable (McCourt and Creelman, 2008). When later attempts failed to detect any interaction between ABA and FCA, doubts were raised about the quality of proteins and assay methods used in the earlier studies (Risk et al., 2008). Both the ABAP1 and FCA reports were eventually retracted at the authors' request following findings that the ABA-binding data could not be reproduced.

1.6.5.2 Magnesium chelatase H subunit (CHLH)

The second putative ABA receptor is the CHLH/ABAR/GUN5, the H subunit of the magnesium-protophyrin IX chelatase that is involved in the first step of chlorophyll synthesis (Shen et al., 2006). In addition, CHLH has also been known to play a key role in retrograde signalling between chloroplast and nucleus under stressful conditions (Mochizuki et al., 2001). Reduction of CHLH levels through RNA interference resulted in ABA insensitivity whereas overexpression led to whole plant ABA hypersensitivity, suggesting its role as a positive regulator of the ABA response. Moreover, Arabidopsis CHLH was shown to bind ABA with high affinity, at a K_d of 32 nM (Shen et al., 2006). Despite so, there has been extensive debate about the role of CHLH in ABA signalling. The initial identification of broad bean CHLH as an ABA-binding protein employed an affinity resin that immobilized ABA at its carboxylate (Zhang et al., 2002), which is a potentially problematic approach given that ABA's carboxylate is needed for its bioactivity. Barley's CHLH does not bind ABA and its loss of function did not affect ABA response, suggesting that CHLH is not an ABA receptor in barley (Muller and Hansson, 2009). Another study of Arabidopsis CHLH failed to detect ABA binding by radioligand binding assay (Tsuzuki et al., 2011). Even though CHLH appears to be involved in the crosstalk between ABA signalling and chloroplast-nucleus retrograde signalling (Koussevitzky et al., 2007), ambiguous evidence remains for its function as an ABA receptor and further molecular explanations are required to understand how Arabidopsis CHLH mediates the ABA responses reported by Shen et al., 2006.

1.6.5.3 G-protein-coupled receptor 2 (GCR2)

Mutational studies of the alpha subunit (GPA1) of heterotrimeric G protein, which GPCRs are usually associated with, has implicated Arabidopsis GPA1 in ABA responses (Pandey and Assmann, 2004; Ullah et al., 2002) and these findings has contributed to speculations that GPCRs may be involved in ABA signal transduction. The third ABA receptor candidate, GCR2, has been proposed to be a G-protein-coupled receptor (GPCR) (Liu et al., 2007). Reduction and overexpression of GCR2 resulted in classic ABA insensitive or hypersensitive phenotypes, suggesting that GCR2 is a positive regulator of ABA signalling. However, like the previous ABA receptor candidates, the role of GCR2 in ABA signalling has been controversial. First of all, the identity of GCR2 as a GPCR was questionable and it has been suggested to be a plant homologue of the bacterial lanthionine synthetase rather than a membrane protein (Illingworth et al., 2008; Johnston et al., 2007). Furthermore, earlier findings of the role of GCR2 in ABA signalling have been refuted (Gao et al., 2007; Guo et al., 2008) and subsequent binding assays did not detect ABA binding to GCR2 (Risk et al., 2009).

1.6.5.4 GPCR-type G proteins (GTG1, GTG2)

The speculation that the ABA receptor could be a GPCR has led to the identification of GTG1 and GTG2 as putative ABA receptors (Pandey et al., 2009). In this study, the authors searched the Arabidopsis genome for

candidate GPCRs using bioinformatics and identified this unusual pair of proteins that possess features of both GPCRs and G-proteins. They also reported that *gtg1 gtg2* double mutant is hyposensitive to ABA in seed germination, seedling growth and stomatal closure, but shows wild type response for ABA inhibition of stomatal opening. Direct physical interactions between GPA1 and GTGs were observed, in which the GDP-bound rather than the GTP-bound GPA1 activates ABA-binding to GTG. Radioligand binding assay showed that recombinant GTG1 and GTG2 were able to bind directly to ABA with K_d of 35.8 nM and 41.2 nM respectively. However, only 1 % of the recombinant protein assayed binds ABA and the authors attributed such stoichiometry of binding to non-optimal conditions of protein purification, solubilization and renaturation. Unlike the previous ABA receptor candidates, the GTG data has so far not been refuted, although evidence that link GTGs to the core ABA signalling components such as the PP2Cs ABI1, ABI2 and HAB1, is still lacking.

1.6.6 Discovery of PYLs as the ABA receptors

Since the discovery of ABA, many details of its physiological roles, biosynthesis, metabolism and key components of its signal transduction has been established. Significant gaps in our knowledge of ABA signalling still exist and one of the most important being the identity of the protein receptor that directly bind the hormone and trigger the signalling events leading the ABA responses.

Forward genetics is most commonly used in the identification of hormone receptors, whereby mutants are identified by their hormone insensitive phenotypes. For the case of ABA, inhibition of seed germination by exogenous ABA application has been the most widely used assay in mutant screens. These screens have led to the identification of ABA insensitive mutants (Finkelstein, 1994; Koornneef, 1984), five of which has been extensively characterized. These five mutants are designated as *abi1–abi5* for ABA insensitive and they carry mutations in the genes ABI1–ABI5. The ABI1 and ABI2 genes encode PP2Cs (Leung et al., 1994; Leung et al., 1997; Meyer et al., 1994), while ABI3, ABI4 and ABI5 encode transcription factors involved in seed-specific ABA signalling pathway (Finkelstein and Lynch, 2000; Finkelstein et al., 1998; Parcy et al., 1994). None of these genes identified by the classical forward genetics approach appear to have ABA binding or receptor like properties.

As such, the use of alternative approaches have identified several putative ABA receptors as reviewed above, which reportedly bind ABA with high affinity in the nanomolar range (K_d of FCA, CHLH, GCR2, GTG1 and GTG2 were reported to be 19 nM, 32 nM, 21 nM, 35.8 nM and 41.2 nM respectively). These attempts however have not led to unambiguous identification of convincing ABA receptor candidates that fit into the knowledge accumulated by ABA physiological, genetical and biochemical studies over the years (McCourt and Creelman, 2008).

The discovery of PYLs as candidate ABA receptors has been different from that of the earlier putative ABA receptors. Independent findings from several groups converged upon this novel class of ABA binding proteins, which fit elegantly in a model that connected the core components of the ABA signal transduction pathway. Here, four of the landmark studies that contributed to the discovery of the PYLs are reviewed.

1.6.6.1 Chemical genetic screen using pyrabactin

Genetic redundancy has been a major issue hindering the identification of ABA receptors by classical reverse genetics. To overcome this problem, Park et al., 2009 used a synthetic seed germination inhibitor, named pyrabactin, as a selective agonist of ABA. Pyrabactin's effects on global gene transcription correlated highly with that of ABA in seeds, but the correlation is weaker in seedlings, indicating that pyrabactin is a highly selective ABA agonist that mediates a subset of ABA's activities. Forward genetic screens for mutants resistant to pyrabactin identified the Pyrabactin Resistance 1 (PYR1) locus. By sequence analysis, 13 other PYR1-like (PYL) genes were identified and designated PYL1 through PYL13 (Figure 7). Using yeast two-hybrid assay, the authors detected interactions between multiple PP2Cs and several PYL members in the presence of ABA. They also demonstrated that PYR1 inhibits HAB1's phosphatase activity in the presence of ABA, with an IC_{50} of 125 nM ABA. The binding of ABA to PYR1 has also been detected by heteronuclear single quantum coherence (HSQC) nuclear magnetic resonance (NMR)

experiments, which probe chemical shifts of protein amide–NH bonds in response to ligands. Collectively, these data suggest that PYLs are ABA receptors that upon ABA binding, inhibits PP2Cs by direct interaction.

1.6.6.2 Identification of PYLs as PP2C interactors

To identify the link between ABA perception and PP2Cs, Ma et al., 2009 used yeast two-hybrid to screen for Arabidopsis proteins interacting with ABI2. Using this approach, this group discovered an ABI2-interacting protein and named it Regulatory Component of ABA Response 1 (RCAR1). Subsequently, 13 structurally similar proteins were identified and named RCAR2 through RCAR14 (Figure 7). The 14 RCAR members discovered in this study turned out to be the same as the 14 PYL members identified by Park et al., 2009. By isothermal titration calorimetry (ITC), the interaction between RCAR1 and *S*-ABA was determined with an apparent K_d of ~0.66 μM. The binding affinity was about 10-fold higher in the presence of ABI2, suggesting the formation of a stable receptor–ABA–PP2C complex. RCAR1 was shown to interact with and inhibit the phosphatase activity of ABI1 and ABI2 in the presence of ABA, consistent with the PYL binding and inhibition of PP2C activity demonstrated by Park et al., 2009.

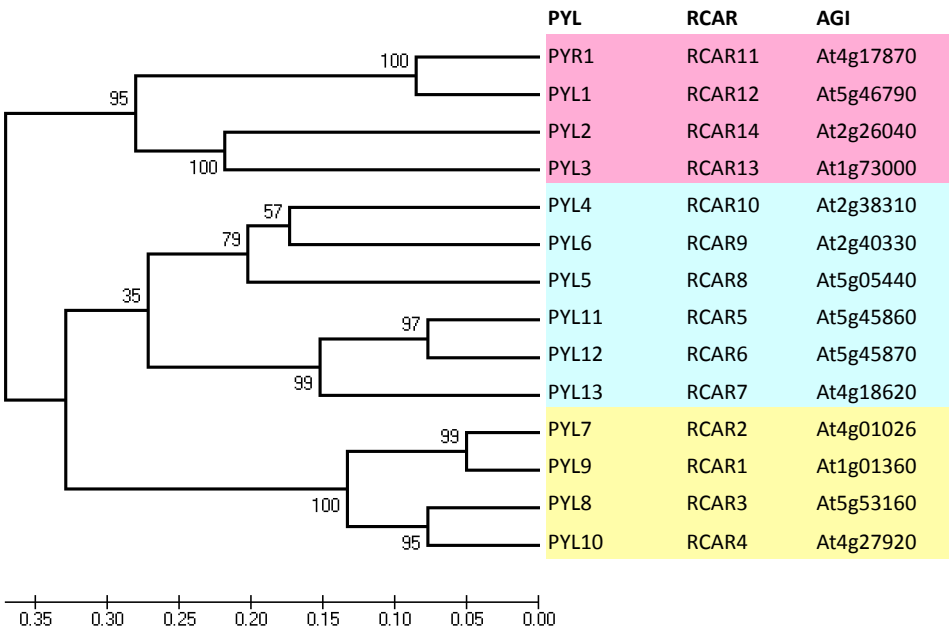

Figure 7. Phylogenetic tree of the 14 members of the Arabidopsis PYL/RCAR family.

The members can be grouped into 3 subfamilies highlighted in pink, cyan and yellow respectively. Amino acid sequences of the 14 PYL proteins are aligned with ClustalW algorithm and Neighbour-joining method was used to construct phylogenetic tree using MEGA software (Tamura et al., 2011). 1000 bootstrap replicates were performed. Bootstrap values and phylogenetic distance scale are shown. The corresponding RCAR designation and AGI code is shown for each PYL.

In a similar approach, Santiago et al., 2009b identified PYL5, PYL6 and PYL8 in a yeast two-hybrid screen for HAB1 interacting proteins. Consistent with the findings of Park et al., 2009 and Ma et al., 2009, members of the PYL family inhibited the phosphatase activities of ABI1, ABI2 and HAB1 in an ABA-dependent manner. By ITC, the apparent K_d of *S*-ABA binding to PYL5 in the absence and presence of HAB1 was determined to be 1.1 μM and 38 nM respectively, supporting the formation of a stable trimeric complex as suggested by Ma et al., 2009. In addition, Santiago et al., 2009b observed that while certain PYL members such as PYR1 and PYL4 only interact with PP2Cs in the presence of ABA, the interaction of PYL5, PYL6 and PYL8 with HAB1 does not require ABA, although ABA enhances the binding affinity of PYL5 to HAB1. This finding suggests that differential roles between PYL members exist whereby a subset of the PYL proteins constitutively inhibits PP2Cs.

Finally, in another independent study, Nishimura et al., 2010 screened for ABI1-interacting proteins *in planta* by coimmunoprecipitation followed by mass spectrometry and identified 9 of the 14 PYL members. Co-immunoprecipitation experiments showed that ABA induces interaction between PYR1 and ABI1 *in vivo* within 5 minutes of ABA treatment.

In summary, these findings collectively identified a group of highly similar proteins in Arabidopsis in which their ABA-binding properties relate to the interaction and inhibition of the PP2Cs that negatively regulate the ABA response.

1.6.6.3 Helix-grip fold receptors

The 14 PYL members in Arabidopsis belong to the Bet v 1-fold/ START-domain superfamily of proteins (Park et al., 2009). The proteins in this superfamily contain the helix-grip fold motif characterized by the presence of a central 7-stranded β-sheet surrounded by N- and C-termini α-helices, with the long C-terminal α-helix packing tightly against the β-sheet (Iyer et al., 2001). The helix-grip fold creates a large ligand-binding pocket that can bind hydrophobic ligands such as hormones and lipids (Iyer et al., 2001; Radauer et al., 2008).

The Bet v 1 is a major allergen in the pollen of white birch (*Betula verrucosa*). Members of the Bet v 1-superfamily include plant pathogenesis-related proteins (class PR-10) that function in microbial defence and abiotic stress tolerance (Liu and Ekramoddoullah, 2006). Some Bet v 1-fold proteins have also been shown to bind cytokinin and brassinosteroid hormones *in vitro* (Fernandes et al., 2008; Markovic-Housley et al., 2003; Pasternak et al., 2006), thus it is not surprising that the PYL proteins can bind ABA. The Bet v 1-fold proteins have been classed together with the steroidogenic acute regulatory (StAR)-related lipid transfer (START)-domain proteins (Iyer et al., 2001; Ponting and Aravind, 1999). START domain is an evolutionary conserved motif of approximately 210 amino acids. A subclass of mammalian START domain (STARD) proteins has been shown to bind specifically to cholesterol (Lavigne et al., 2010). In plants, START domain proteins have

been implicated in both biotic and abiotic stresses (Cao et al., 2009; Fu et al., 2009; Yu et al., 2008).

1.6.7 Model of the core ABA signalling pathway

With the new findings that PYLs bind ABA and inhibit PP2Cs, a model of the core ABA signaling pathway has been proposed, which links ABA recognition to transcriptional activation of ABA responsive genes (Figure 8). In this model, the ABA response under basal condition is kept silent by the PP2Cs that negatively regulate ABA response, including ABI1, ABI2 and HAB1. These phosphatases act by inhibiting the SnRK2s, including SnRK2.2, SnRK2.3 and SnRK2.6 that are positive regulators of the ABA signalling pathway. High levels of ABA induce PYLs, which are the proposed ABA receptors, to bind to and inhibit PP2Cs. This relieves the PP2C inhibition of SnRK2s, allowing the kinases to autophosphorylate and activate downstream effectors such as ion channels and ABF transcription factors resulting in the activation of ABA responses.

This concept has been elegantly demonstrated by *in vitro* reconstitution of the core ABA signalling pathway. Coexpression of a set of the core ABA signalling components, PYL, PP2C, SnRK2 and ABF2 transcription factor, in plant protoplast is sufficient and necessary to induce the expression of ABA-responsive reporter gene upon treatment with ABA (Fujii et al., 2009). In another study, *in vitro* reconstitution analyses performed with PYR1, ABI1

and SnRK2 showed that PYR1 inhibited the ABI1-mediated suppression of SnRK2 activity in an ABA-dependent manner (Umezawa et al., 2009), supporting the current model of the core ABA signalling pathway.

Prior to mid 2009, the precise mode of ABA–PYL interaction and the molecular mechanisms underlying the signal transduction process remained to be elucidated and had emerged as a focus in abiotic stress signalling research.

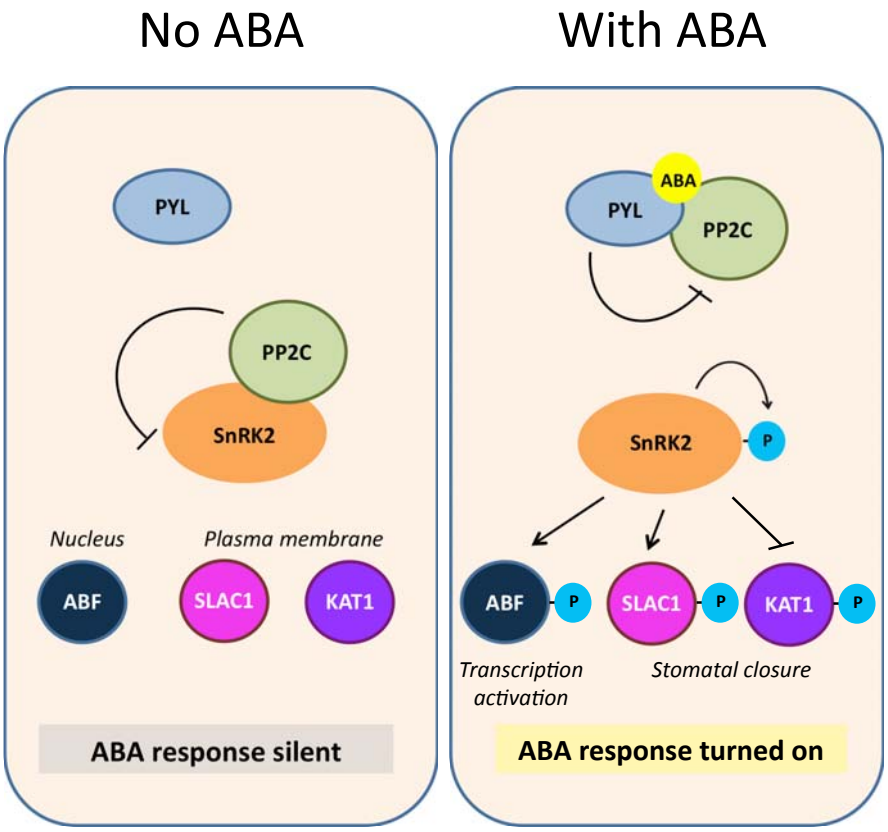

Figure 8. Model of the core ABA signalling pathway.

In the absence of ABA, PP2Cs inhibit SnRK2s, keeping the ABA response silent. ABA accumulation, induced by stress signals, activates PYLs to inhibit PP2Cs. SnRK2s can then become activated by autophosphorylation. Active SnRK2s mediate the ABA response by phosphorylation of downstream targets such as ABF transcription factors or the SLAC1 and KAT1 ion channels.

1.7 Aims, objectives and significance of the study

The discovery of PYLs as potentially the bona fide ABA receptors that have been long sought after has provided significant advancement in the field of abiotic stress signalling. Several groups have independently demonstrated the ability of PYLs to bind ABA and inhibit PP2Cs, through unknown mechanisms. The observation that ABA binding to PYL5 and PYL9 (RCAR1) is enhanced by more than 10-fold in the presence of a PP2C (Ma et al., 2009; Santiago et al., 2009b) has led to an important but currently unresolved question: does ABA bind to a PYL–PP2C coreceptor or does ABA bind to PYL first followed by secondary interaction with PP2C that stabilizes the ligand binding?

Using X-ray crystallography approach, this study seeks to address the following aims:

- To provide structural evidence for the role of the PYL family as the bona fide ABA receptors;
- To elucidate the structural mechanisms of how ligand binding by PYL is transduced to its immediate downstream effector (i.e. inhibition of PP2Cs);
- To identify the mechanistic basis of selective receptor responses towards pyrabactin.

The objectives of the experiments are to determine the crystal structures of PYLs in ligand-free, ABA-bound and PYL–ABA–PP2C complex forms. To do so, all members of the PYL family will be expressed as recombinant proteins initially in small scale to check for their expression levels and solubility. Soluble recombinant PYL proteins will be biochemically characterized for their ABA-dependent interaction and inhibition of representative PP2Cs, and expressed in large scale for crystallization. Analysis of the crystal structures will provide evidence for the role of PYLs as ABA receptors and insights into the mode of ABA binding and PP2C inhibition.

Pyrabactin has been identified as a selective ABA agonist that activates only a subset of PYL members (Park et al., 2009). Thus, we seek to biochemically characterize PYL members for their pyrabactin-dependent activation, as well as to determine whether these receptors can be antagonized by pyrabactin. Our aim is to understand the molecular basis of how ABA receptors can be selectively activated or antagonized. To address this, our objectives are to determine and compare crystal structures of PYL–pyrabactin complexes representative of pyrabactin-activated and pyrabactin-repressed conformations. These findings can be a basis for future design of specific ABA receptor agonists and antagonists useful for dissecting ABA biology as well as for agricultural applications.

This study addresses the long-standing uncertainty in the identity of the ABA receptors. Our results will provide mechanistic explanations that link the newly discovered ABA receptors with well-established components of the

early steps in ABA signalling. This knowledge shall pave the way to further elucidation of the ABA signalling cascade, fuelling advancements in the field of abiotic stress signalling.

The understanding of how ABA is perceived holds promises in improving drought hardiness in plants through specific control of ABA receptors by ligand design and/or receptor engineering. Given that agriculture consumes about 80 % of the world's fresh water resource and that drought-induced crop loss is predicted to increase with global climate change, development in water efficiency and stress tolerance in plants will have valuable agricultural and economic impact worldwide.

Also, the elucidation of how signalling components co-regulate in plants may lead to new discoveries in biomedical research related to human health and diseases. This intriguing notion stems from the fact that homologues of the components of the core ABA signalling pathway exist across kingdoms. The human homologues of these proteins have been implicated in various conditions including cancers, cardiovascular and metabolic disorders. However, how these proteins are regulated has not been fully known. Thus our mechanistic findings of ABA signal transduction in plants may also serve as a framework for future novel discoveries of analogous intracellular signalling mechanisms in humans.

CHAPTER 2

MATERIALS AND METHODS

2.1 Plasmid construction

The full ORFs of all 14 members of the PYL family and that of the PP2Cs HAB1, ABI1 and ABI2 were obtained as cDNA plasmids from collaborator Dr Zhu Jiankang. The DNA sequences coding for the protein regions to be expressed (listed in Table 2, page 54) were amplified by PCR and cloned into *E. coli* expression vectors which contain 6xHis-GST (H6GST) or 6xHis-SUMO (H6SUMO) sequences for the expression of N-terminus H6GST- or H6SUMO- tagged recombinant proteins. Proteins to be expressed with H6GST tag were cloned into the pET24a vector (Novagen) modified to contain a H6-tag (MKKGHHHHHHG) at the N terminus and a thrombin protease site between GST and the protein of interest. Proteins to be expressed with H6SUMO tag were cloned into the pSUMO vector (LifeSensors). PP2C proteins to be biotinylated for PYL-PP2C interaction assays were cloned into pETDuet1 (Novagen) derivative vector to be expressed as either H6-thioredoxin-avitag-PP2C or avitag-MBP-PP2C in which the 14 amino acid avitag functions as a defined *in vivo* biotinylation site in *E. coli* (Smith et al., 1998). The H6-thioredoxin-avitag- fusion construct contains H6-thioredoxin-thrombin cleavage site- avitag fusion sequences in the MCS-1 and the *E. coli* biotin-ligase gene *BirA* in MCS-2. The avitag-MBP- fusion construct contains avitag-MBP followed by a six residue linker (NAAAEF) fused to the N-terminal of the protein to be expressed in the MCS-1 and *BirA* in the MCS2.

2.2 Protein expression and purification

2.2.1 Small scale expression of tagged recombinant proteins

H6GST-, H6SUMO- and biotinylated MBP-tagged recombinant proteins were expressed in BL21 (DE3) cells transformed with the expression plasmids. 50 ml bacterial cultures were grown at 16 °C to an OD_{600} of ~1.0 and induced with 0.1 mM IPTG for 16 hr. For biotinylated MBP-tagged protein, 40 μM of biotin was added upon induction. Cells were harvested by centrifugation and resuspension in 2 ml of extract buffer (H6SUMO-tagged proteins: 25 mM Tris pH 7.5, 150 mM NaCl, 25 mM imidzole and 10 % glycerol. H6GST- and biotin-MBP proteins: 20 mM Tris, pH 8.0, 200 mM NaCl, and 10 % glycerol.) All buffers used in the purification of PP2Cs contain additional 5 mM $MgCl_2$. Lysis was performed using FastPrep-24 (MP Biomedicals) with 3 cycles of 20 s homogenization at speed 6, with 2 mins of rest in between each cycle. Lysate supernatant were incubated with affinity beads (Ni-NTA agarose, glutathione sepharose and amylose resin for H6SUMO-, H6GST- and biotin-MBP- tagged proteins respectively) in 4 °C for 1 hr with constant rotation. Proteins bound to the beads were washed 3 times with extract buffer and eluted with 300 μl of elution buffer (H6SUMO-tagged proteins: 25 mM Tris pH 7.5, 150 mM NaCl, 500 mM imidzole and 10 % glycerol. H6GST- tagged proteins: 25 mM Tris pH 8.0, 100 mM NaCl, 20 mM reduced glutathione and 10 % glycerol. Biotin-MBP-tagged proteins: 50 mM Tris pH 8.0, 150 mM NaCl, 10 mM maltose and 10 % glycerol). Final protein concentrations were measured using standard Bradford assay or Qubit protein assay with the Qubit fluorometer

(Invitrogen). Proteins were aliquoted, flash frozen in liquid nitrogen and stored in -80 °C until used. The H6SUMO-tagged proteins were dialysed overnight at 4 °C in extract buffer without imidazole before storage.

For the purification of biotin-PP2C from H6-thioredoxin-biotin-PP2C, cells grown in the presence of 40 μM biotin were harvested, resuspended in 100 ml extract buffer (20 mM Tris pH 8.0, 200 mM NaCl, 5 mM $MgCl_2$ and 10 % glycerol) and passed three times through a French press with pressure set at 1000 Pa. The lysate supernatant was loaded on a 50 ml Nickel HP column. The column was washed with 10 % elute buffer (20 mM Tris pH 8.0, 200 mM NaCl, 500 mM imidazole, 5 mM $MgCl_2$ and 10 % glycerol) before eluting the H6-thioredoxin-biotin-PP2C in 100 % elute buffer. The fusion protein was dialyzed in extract buffer overnight and cleaved with thrombin to release the H6-thioredoxin tag. After cleavage, the biotin-PP2C was purified over monomeric avidin columns (Pierce) according to the manufacturer's instructions.

2.2.2 Large scale purification of untagged proteins

H6GST- and H6SUMO-tagged proteins were expressed in BL21(DE3) cells transformed with the expression plasmid. 6 L of bacterial culture were grown at 16 °C to an OD_{600} of ~1.0 and induced with 0.1 mM IPTG for 16 hr. Cells were harvested, resuspended in 100 ml extract buffer (20 mM Tris pH 8.0, 200 mM NaCl, and 10 % glycerol) and passed three times through a French press with pressure set at 1000 Pa. The lysate was centrifuged at 16,000 rpm in a

Sorvall SS34 rotor for 30 min, and the supernatant was loaded on a 50 ml Nickel HP column. The column was washed with 10 % buffer B (20 mM Tris pH 8.0, 200 mM NaCl, 500 mM imidazole, and 10 % glycerol) for 600 ml and eluted in two steps with 50 % buffer B for 200 ml, then 100 % buffer B for 100 ml. The eluted H6GST-proteins were dialyzed in extract buffer and cleaved overnight with thrombin at a protease/protein ratio of 1:250 in the cold room. H6SUMO-tagged proteins were cleaved overnight with Ulp1 SUMO protease at a protease/protein ratio of 1:1000 in the cold room. The cleaved H6GST or H6SUMO tags were removed by passing through a Nickel HP column, and the untagged protein was further purified by chromatography through a HiLoad 26/60 Superdex 200 gel filtration column in 25 mM Tris pH 8.0, 200 mM ammonium acetate, 1 mM dithiotreitol and 1 mM EDTA. All buffers used in the purification of PP2Cs contain additional 5 mM $MgCl_2$.

2.3 Protein crystallization

High throughout crystallization trials of each protein or complex were set up using commercial screens (Hampton Research) with a Phoenix robot (Art Robbins Instruments). Sitting drop vapour diffusion crystallization experiments were set up in 96-well intelli-plates (Rigaku) with 75 μl of condition solution in the reservoir and 0.2 μl of the protein, typically ~ 5 to 15 mg/ml, added to an equal volume of the crystallization condition in the sitting drop well. Crystals were optimized by setting up hanging drop grid screens in 24-well VDX plates (Hampton Research), varying the conditions that produced crystals in the initial screens. The conditions that produced crystals

in the initial screens and the optimized conditions that gave high resolution structures used in this study are listed in Table 1.

Table 1. List of crystallization conditions.

Protein/ Complex	Initial condition	Optimized condition
PYL1	0.1 M Ammonium sulfate 0.1 M Na-HEPES pH 7.5 10 % PEG 4000	0.1 M Ammonium sulfate 0.1 M Na-HEPES pH 7.5 10 % PEG 4000 30 % Glycerol
PYL2	0.056 M Sodium phosphate monobasic monohydrate 1.344 M Potassium phosphate dibasic pH 8.2	0.056 M Sodium phosphate monobasic monohydrate 1.344 M Potassium phosphate dibasic pH 8.2 5 % Butanediol (20 % Glycerol)
PYL2–ABA	0.1 M HEPES pH 7.5 2.0 M Ammonium sulfate	0.1 M HEPES pH 7.5 2.0 M Ammonium sulfate 20 % Sorbitol (30 % Sorbitol)
ABI2	0.2 M Sodium formate 14 % PEG 3350	0.2 M Sodium formate 18 % PEG 8000 10 % Sucrose (29.5 % Sucrose)
PYL2–ABA–HAB1	0.2 M Ammonium sulfate 0.1 M BIS-TRIS pH 6.5 25 % PEG 3350	0.2 M Ammonium sulfate 0.1 M BIS-TRIS pH 6.5 15 % PEG 3350 (35 % PEG 3350)
PYL2–ABA–ABI2	0.1 M HEPES pH 7.5 4 % PEG 8000	0.1 M HEPES pH 7.0 6 % PEG 8000 10 % Sucrose (39 % Sucrose)
PYL2–pyrabactin	2.0 M Ammonium sulfate 0.1 M HEPES pH 7.5	2.0 M Ammonium sulfate 0.1 M HEPES pH 7.5 10 % Glycerol (20 % Glycerol)
PYL1–pyrabactin–ABI1	0.2 M Ammonium sulfate 0.1 M BIS-TRIS pH 5.5 25 % PEG 3350	0.2 M Ammonium sulfate 0.1 M BIS-TRIS pH 5.5 22 % PEG 3350 (35 % PEG 3350)
PYL2 A93F–pyrabactin	0.2 M Ammonium acetate pH 7.1 20 % PEG 3350	0.2 M Ammonium acetate pH 8.1 22 % PEG 3350 (40 % PEG 3350)
PYL2 A93F–pyrabactin–ABI2	0.1 M HEPES pH 7.5 42 % PEG 200	0.1 M HEPES pH 7.5 10 % PEG 8000 10 % Sucrose (35 % Sucrose)
PYL2 A93F–pyrabactin–HAB1	0.2 M Ammonium sulfate 0.1 M TRIS pH 8.5 25 % PEG 3350	0.2 M Ammonium sulfate 0.1 M TRIS pH 7.5 23 % PEG 3350 10 % Ethylene glycol

Crystals grown in the optimized conditions were serially transferred to well buffer with increasing concentrations of cryo-protectant (final concentration shown in bracket) prior to flash freezing in liquid nitrogen.

2.4 Data collection and structure determination

Datasets were collected with MAR300 and MAR225 CCD detectors (MAR Research) at the ID-D and ID-F lines of sector-21 (LS-CAT) at the Advanced Photon Source at Argonne National Laboratory (USA). The observed reflections were reduced, merged, and scaled with DENZO and SCALEPACK in the HKL2000 package (Otwinowski et al., 2003). All structures were solved by Dr Zhou XE as briefly described below.

The first PYL structure, apo PYL2, was solved by molecular replacement using the known structure of Bet V I, a birch pollen allergen that contains a START domain (PDB code: 1bv1), as a starting model. The model for HAB1 in the PYL2-ABA-HAB1 complex was built using the structure of PPM1B, a human PP2C that shares 38 % homology with the HAB1 PP2C core domain (PDB code: 2P8E) (Almo et al., 2007). All other structures were solved by molecular replacement using these PYL2 and HAB1 structures or subsequently determined structures as model.

Molecular replacement was performed by using the Collaborative Computational Project 4 (CCP4) program Phaser (McCoy et al., 2007). Program O and Coot were used to manually fit the protein model (Emsley and Cowtan, 2004; Kleywegt and Jones, 1996). Model refinement was performed with CNS and the CCP4 program Refmac5 (Korostelev et al., 2002; Murshudov et al., 1999). The volumes of the ligand binding pocket were calculated with the program Voidoo by using program default parameters and

a probe with a radius of 1.4 Å (Kleywegt and Jones, 1994). Structure figures were prepared by using PyMOL (DeLano Scientific). The statistics of data collection and structure refinement are summarized in Table 3 (page 65) and Table 4 (page 88).

2.5 Assays for the interactions between PYLs and PP2Cs

Interactions between PYLs and PP2Cs were assessed by luminescence-based AlphaScreen technology (Perkin Elmer) as illustrated in Figure 9. Biotinylated PP2Cs were attached to streptavidin-coated donor beads, and H6-tagged PYL proteins were attached to nickel-chelated acceptor beads. The donor and acceptor beads were brought into proximity by the interactions between PYLs and PP2Cs, which were measured with and without *S*-(+)- or *R*-(−)-abscisic acid, or pyrabactin. When excited by a laser beam of 680 nm, the donor beam emits singlet oxygen that activates thioxene derivatives in the acceptor beads, which releases photons of 520–620 nm as the binding signal. The experiments were conducted with 100 nM of PP2Cs and 100 nM of PYL proteins in the presence of 5 μg/ml donor and acceptor beads in a buffer of 50 mM MOPS, pH 7.4, 50 mM NaF, 50 mM CHAPS, and 0.1 mg/ml bovine serum albumin. The binding signals were measured as photon counts in a 384-well microplate using an Envision 2104 plate reader (PerkinElmer). The results were based on an average of three experiments with standard errors typically less than 10 % of the measurements.

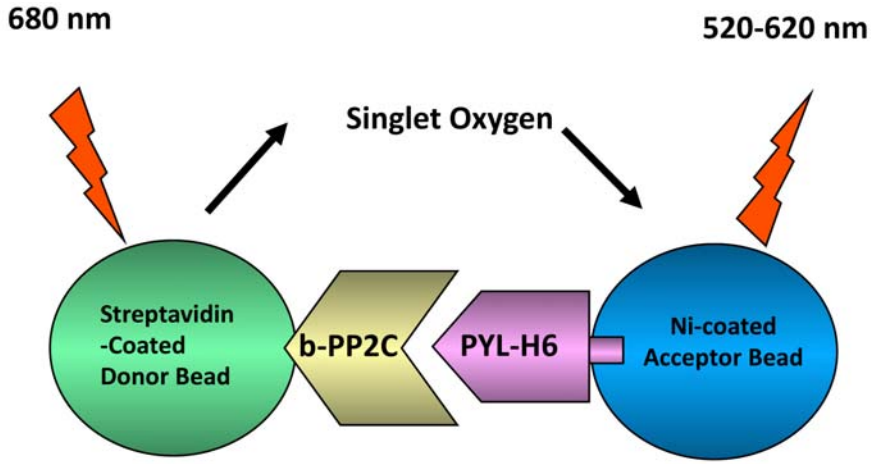

Figure 9. Schematic representation of the Amplified Luminescent Proximity Homogenous Assay (ALPHA) Screen.

H6-tagged PYL (PYL-H6) is immobilized on Ni-chelating acceptor beads and biotinylated PP2C (b-PP2C) on streptavidin-coated donor beads. Donor beads contain a photosensitizer that upon activation at 680 nm converts ambient oxygen to singlet oxygen. If acceptor beads are brought into close proximity of the donor beads by PP2C–PYL interaction, energy is transferred from singlet oxygen to thioxene derivatives in the acceptor beads resulting in light emission at 520–620 nm.

2.6 Assays of PP2C phosphatase activity

Recombinant PP2Cs and PYLs (concentrations vary in each experiment and are indicated in Figure legends) were pre-incubated in 50 mM imidazole, pH 7.2, 5 mM $MgCl_2$, 0.1 % β-mercaptoethanol and 0.5 µg/ml BSA for 30 min at room temperature. Reactions were started by addition of 100 µM a phosphopeptide corresponding to amino acids 170–180 of SnRK2.6 (HSQPKpSTVGTP). This peptide is phosphorylated at a single residue corresponding to Ser175 in SnRK2.6, whose phosphorylation is required for SnRK2.6 kinase activity (Mustilli et al., 2002). Phosphate release from pS175 from the phosphopeptide was determined by colorimetric assay (BioVision).

2.7 Radio-ligand binding assay

2 μM H6GST-PYL2 were incubated with 250 μg of Ytrium silicate copper-chelating scintillation proximity assay (SPA) beads (GE Healthcare) in a buffer of 50 mM MOPS, pH 7.4, 50 mM NaF, 50 mM CHAPS, and 0.1 mg/ml bovine serum albumin for 40 mins shaking on ice. H6GST-PYL2 bound to SPA was separated from free H6GST-PYL2 by centrifugation at 5200 g for 30 s. Bead pellets were washed with 1 ml of the same buffer, then resuspended in 50 μl of the buffer supplemented with 45 nM ^{3}H-labelled ABA (GE Healthcare; mixture of *S*-/*R*- and *cis*-/*trans*-isomers), 1 μM unlabelled *S*-ABA and 10 μM HAB1 and incubated shaking for 1 hour at room temperature. ^{3}H-ABA-PYL2 binding brings the radioactive ABA into the immediate proximity of the scintillant embedded in the SPA beads resulting in the generation of light, which was quantified in a liquid scintillation counter.

2.8 Mutagenesis

Primers for site-directed mutagenesis were designed using the QuikChange primer design program (Agilent Technologies). Mutagenesis PCR was performed using Finnzymes Phusion High-Fidelity DNA polymerase. Initial reaction was set up in 1x Phusion High-Fidelity buffer, 10 mM dNTP, 0.5 units of the polymerase, 25 ng of template plasmid and 10 μM of primer, with the forward primer and reverse primer in separate reactions of 25 μl volume. This is to prevent the forward and reverse primers from preferentially annealing to each other rather than to the target template sequence, as the

primer pairs are completely complementary to each other. The first round of amplification was performed with the following steps: Initial denaturation at 98 °C for 30 s, 5 cycles of denaturation, annealing and extension at 98 °C for 10 s, 55 °C for 30 s and 72 °C for 2 min respectively and a final extension at 72 °C for 5 min. After the 5 cycles of reaction, daughter strands containing the target mutation dominate in the reaction. The 2 reactions containing the forward and reverse primers separately were then combined and added with an additional 0.4 unit of the polymerase and subjected to the same amplification program as the initial step but with 12 cycles instead. At the end of the reaction, 2 µl of DpnI enzyme was mixed with 15 µl of the reaction and incubated at 37 °C for 2 hr to digest the dam methylated parental DNA. The digested product containing intact nascent mutant DNA was transformed into OmniMAX cells (Invitrogen) for clonal plasmid preparation. Mutations and all plasmid constructs were confirmed by sequencing prior to protein expression. Expression and purification of mutant proteins followed the same method as for the wild type proteins described above.

CHAPTER 3

RESULTS

3.1 Preparation of recombinant proteins

3.1.1 Amino acid sequence analysis

For biochemical characterization of the ABA signalling proteins, we designed and generated recombinant H6-tagged PYL proteins and biotin-labelled PP2C proteins. To determine the protein regions to be expressed, full-length amino acid sequences of all 14 members of the PYL family were aligned to identify conserved regions, which may indicate the existence of important structural domains (Figure 10). Based on the sequence alignment, recombinant PYLs with N- and C- terminal truncations were designed to remove terminal flexible regions that may possibly pose problems in crystallization, while preserving regions containing conserved amino acids and hydrophobic residues, which could constitute to secondary structures. A mutation of C34A was introduced into PYL5 to avoid potential non-specific disulfide bond formation, which could result in protein aggregation.

Of the 9 Arabidopsis group A PP2Cs, the 3 best characterized PP2Cs involved in ABA signalling, ABI1, ABI2 and HAB1 were used in this study. Full-length amino acid sequences of the 9 group A PP2Cs were aligned to identify conserved regions (Figure 11). For each of the 3 PP2Cs in this study, the highly conserved C-terminal region containing the PP2C catalytic domain was expressed. The expressed regions of each PYL and PP2C protein and their corresponding theoretical isoelectric focusing point (PI) and molecular weight (MW) are listed in Table 2.

Figure 10. Amino acid sequence alignment of PYLs.

Multiple sequence alignment was performed using ClustalW2 (Larkin et al., 2007) with EMBL-EBI online program (Goujon et al., 2010). Identical sequences, conserved substitutions and semi-conserved substitutions are denoted by symbols "*", ":" and "." respectively. Regions to be expressed are coloured whereas N- and C- terminal regions to be truncated are in grey.

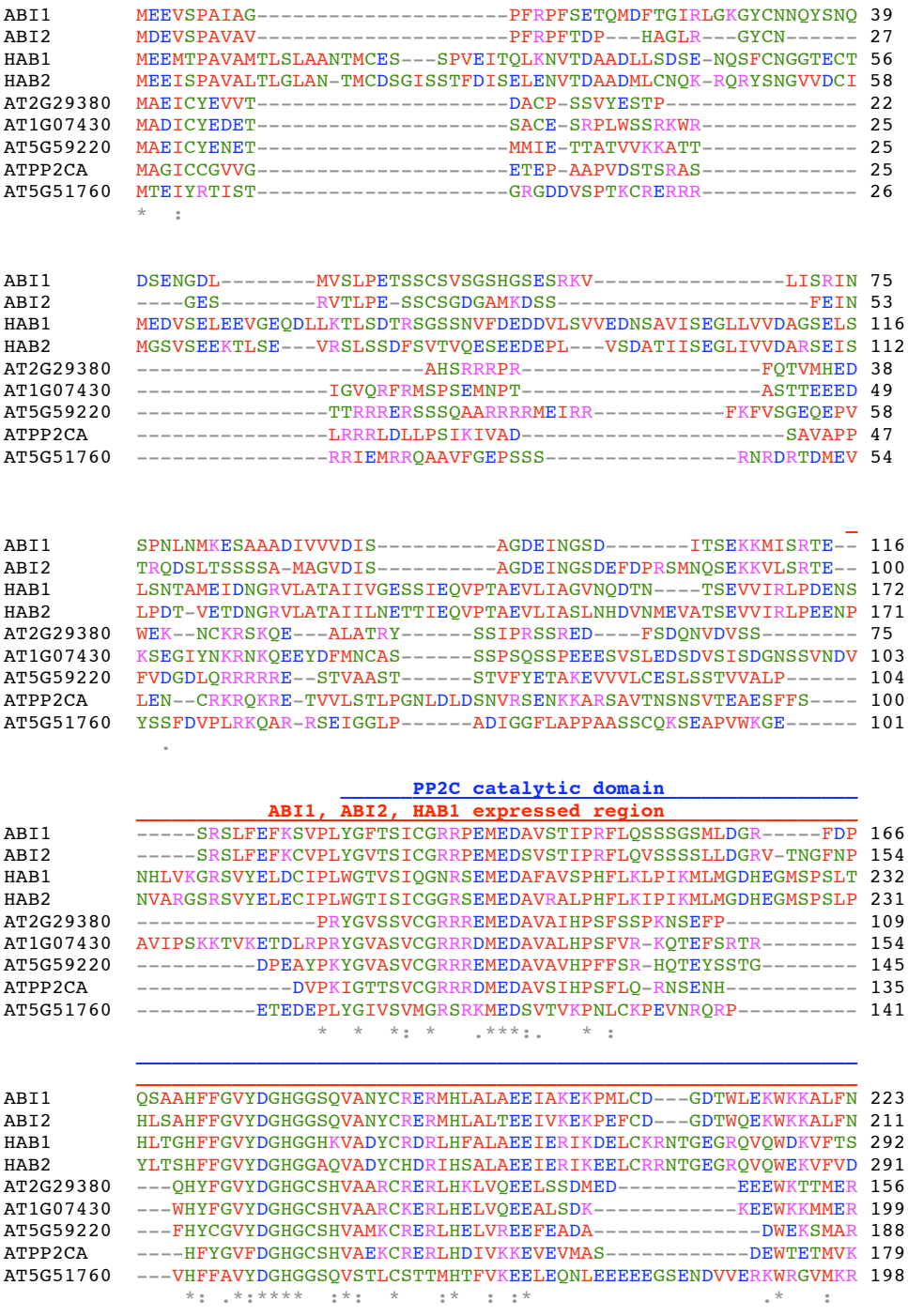

Figure 11. Continued on next page.

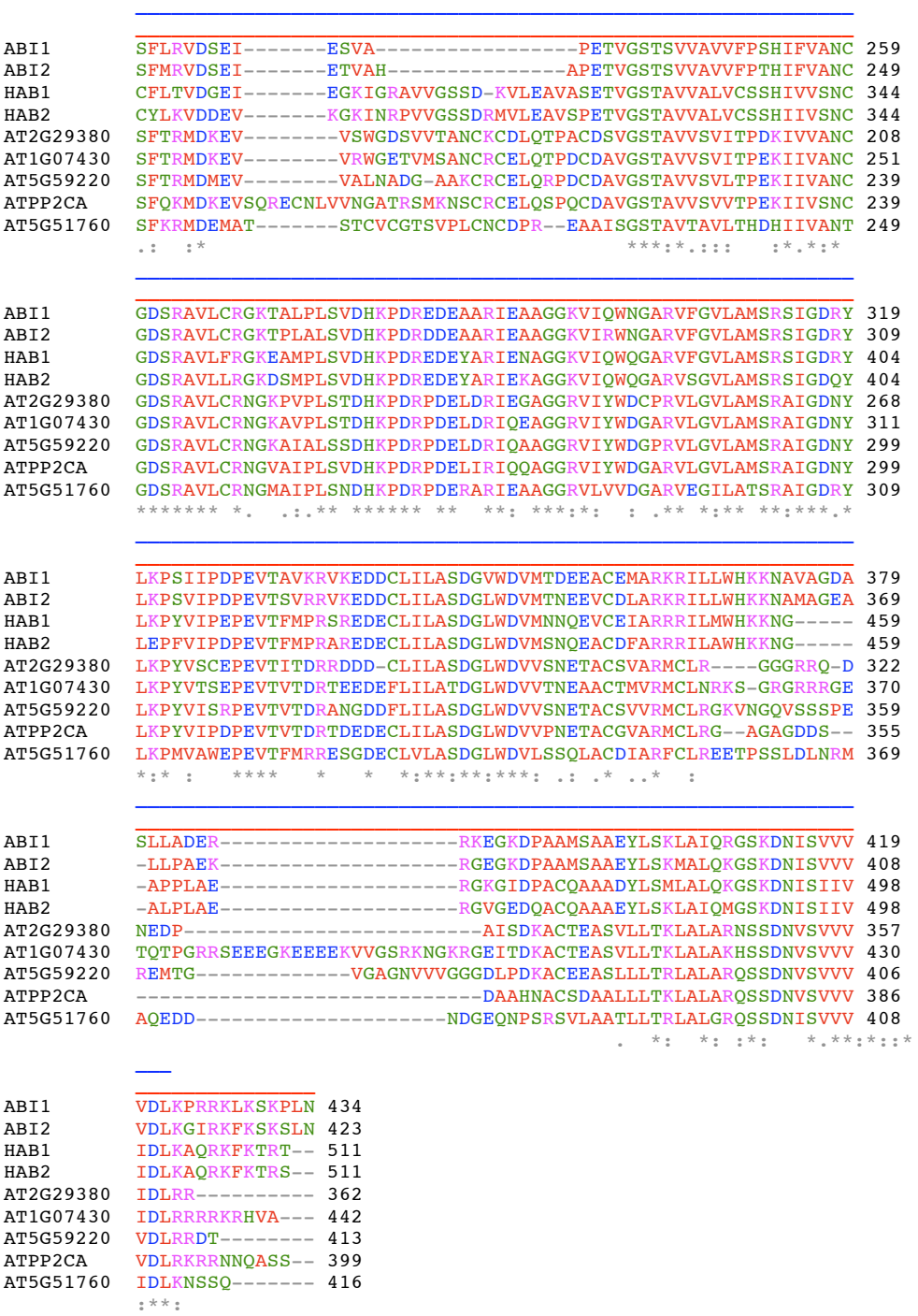

Figure 11. **Amino acid sequence alignment of group A PP2Cs.**

Multiple sequence alignment was performed using ClustalW2 (Larkin et al., 2007) with EMBL-EBI online program (Goujon et al., 2010). Identical sequences, conserved substitutions and semi-conserved substitutions are denoted by symbols "*", ":" and "." respectively. ABI1, ABI2 and HAB1 regions expressed in this study are indicated by red line on top of the sequences. Blue line indicates the conserved PP2C catalytic domain.

Table 2. List of proteins in the study, their expressed regions and calculated properties.

Protein		Expressed region		
		Amino acid positions	PI	MW (Da)
PYL (RCAR)	PYR1 (RCAR11)	9–182	6.08	20045.3
	PYL1 (RCAR12)	36–211	5.49	20506.6
	PYL2 (RCAR14)	14–188	5.84	19878.1
	PYL3 (RCAR13)	29–209	9.17	20556.1
	PYL4 (RCAR10)	17–201	5.94	20252.4
	PYL5 (RCAR8)	29–203 (C34A)	6.04	19716
	PYL6 (RCAR9)	31–215	5.65	20624.9
	PYL7 (RCAR2)	11–189	6.16	20301.8
	PYL8 (RCAR3)	7–184	6.26	20453.9
	PYL9 (RCAR1)	9–187	6.25	20267.8
	PYL10 (RCAR4)	5–178	6.07	19738.1
	PYL11 (RCAR5)	4–161	4.78	17500.4
	PYL12 (RCAR6)	4–159	4.61	17329.3
	PYL13 (RCAR7)	4–164	9.12	17836.2
PP2C	ABI1	117–434	7.57	35059.14
	ABI2	101–423	8.06	35673.86
	HAB1	172–511	6.60	37714.22

3.1.2 Small scale expression of recombinant proteins

Each PYL protein, except PYL8 due to unavailability of the cDNA source at that point of time, was expressed as H6GST- and H6SUMO- fusion proteins with PYL regions indicated in Table 2. The recombinant proteins were expressed in *E. coli* and purified by standard glutathione sepharose or Ni-NTA agarose affinity chromatography and analysed by SDS-PAGE to determine their relative expression levels and solubility and to prepare these proteins for biochemical assays. PYR1 and PYLs 1–6 yielded relatively high levels of soluble proteins when expressed with both H6GST- and H6SUMO- tags, whereas PYLs 7–13, with the exception of H6GST-PYL10, expressed poorly with both tags (Figure 12). These observations are consistent with the expression and purification of recombinant PYLs reported in another study (Hao et al., 2011). Therefore, subsequent crystallization experiments and biochemicals analyses were focused on the more soluble PYR1 and PYL1–PYL6 proteins.

Biotinylated recombinant PP2Cs with MBP tags were expressed in *E. coli* and purified by amylose affinity chromatography for biochemical assays (Figure 13).

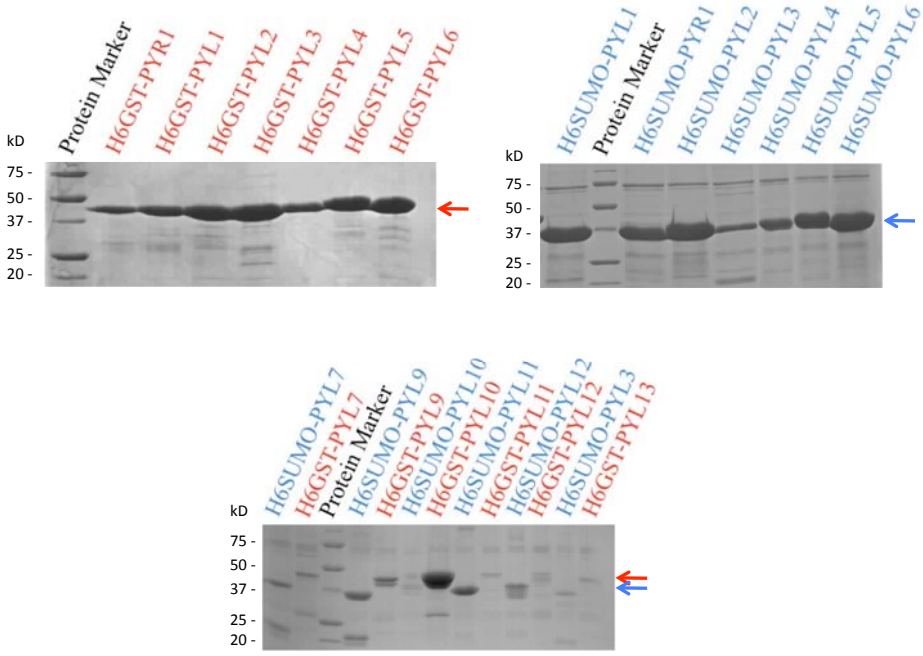

Figure 12. **Small scale expression of recombinant PYLs.**

Elute fractions of recombinant H6GST- (red label) and H6SUMO- (blue label) PYLs purification. Red and blue arrows indicate the approximate sizes of H6GST-PYL (~40-45 kD) and H6SUMO-PYL (~37-40 kD) respectively.

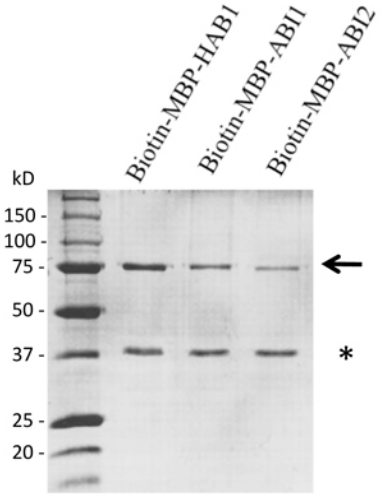

Figure 13. **Small scale expression of recombinant PP2Cs.**

Elute fractions of biotin-MBP-PP2Cs purification. Arrow indicates the approximate sizes of the recombinant PP2Cs (~80 kD). An additional band of truncated product of ~37 kD, marked by asterisk (*) is also observed.

3.2 ABA-dependent interactions of PYLs with PP2Cs

To assess the ABA-mediated interaction of PYLs with PP2Cs, H6 tagged-PYR1 and PYLs 1−6 were tested in AlphaScreen protein-protein interaction assay (illustrated in Materials and Methods, Figure 9) with biotinylated recombinant PP2Cs in the presence and absence of (+)-ABA or (−)-ABA. While the PYL members tested interacted with the ABA-signalling PP2Cs ABI1, ABI2 and HAB1, each PYL showed differential PP2C interaction depending on the absence or presence of ABA, the particular ABA stereoisomer used, and the PP2C probed (Figure 14). These observations suggest that functional variations may exist between different PYL members in PP2C binding and signalling.

PYL2 interacted with HAB1 in an ABA-dependent manner, with a marked preference for the naturally occurring (+)-stereoisomer (Figure 15a). Consistently, PYL2 also inhibited HAB1 phosphatase activity with an IC_{50} of 0.15 μM with (+)-ABA and 1.7 μM with (−)-ABA (Figure 15b). This 11-fold difference in stereoisomer selectivity is comparable to the 19-fold difference shown for PYL5 in another study (Santiago et al., 2009b).

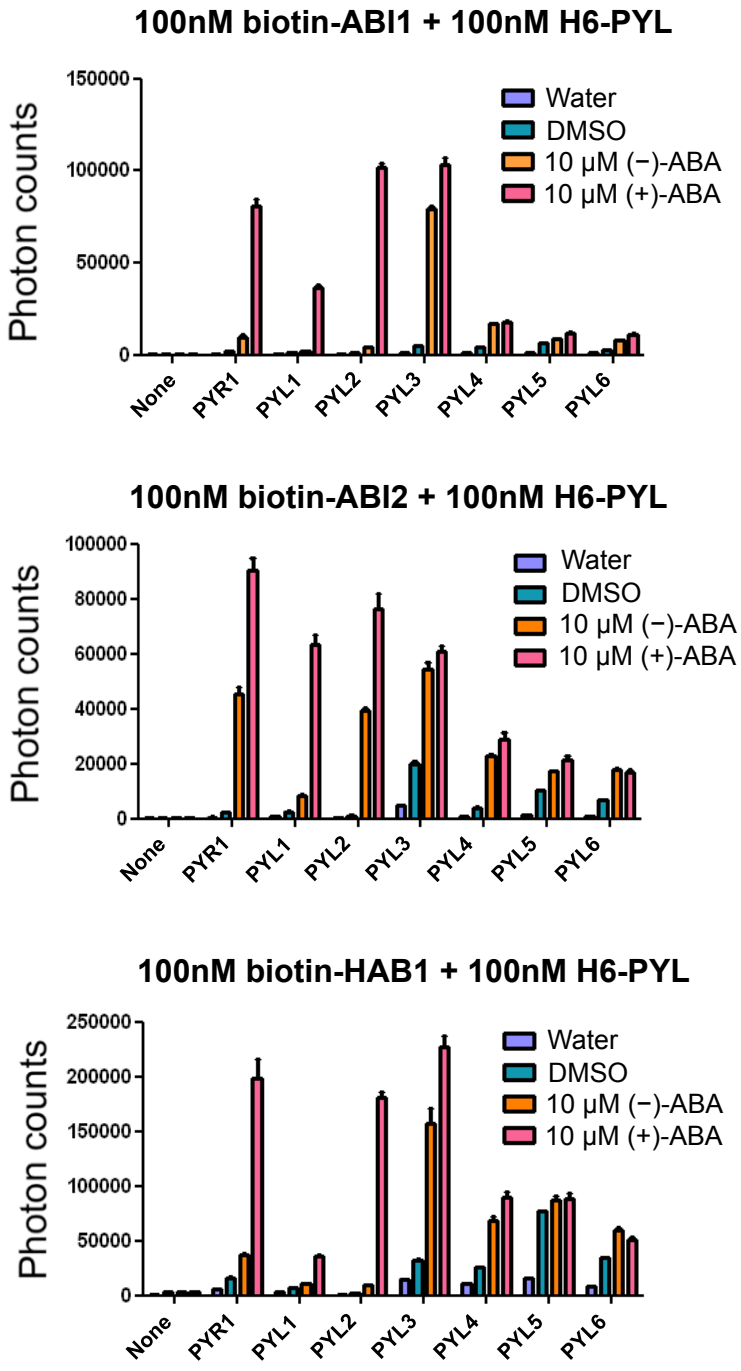

Figure 14. **AlphaScreen assay of PYL proteins interactions with PP2Cs.**

Recombinant H6-tagged PYL proteins were incubated with recombinant biotinylated PP2Cs ABI1 (top), ABI2 (middle), and HAB1 (bottom) in the presence and absence of 10 µM (+)-ABA or (−)-ABA. The interaction signals are shown as photon counts (n=3, error bars=SD).

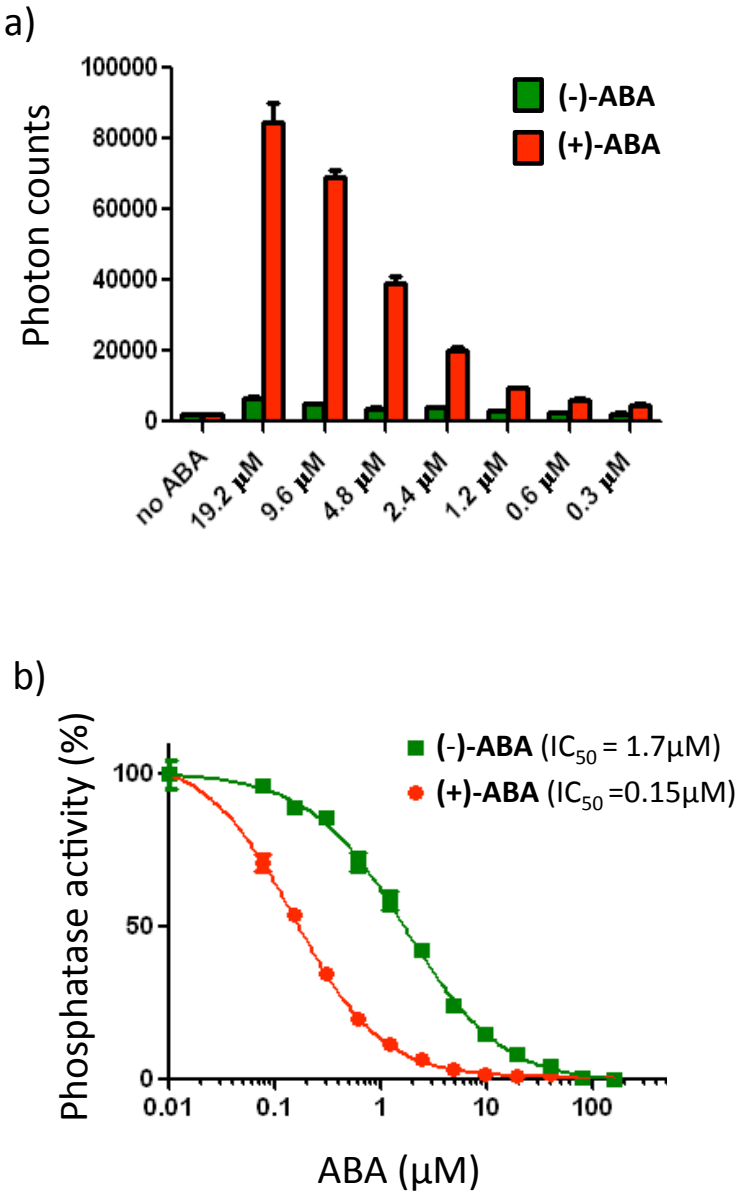

Figure 15. PYL2 binds to and inhibits HAB1 in an ABA-dependent manner.

a) ABA-dependent interaction of PYL2 with HAB1. AlphaScreens assay of interaction of 100 nM of recombinant H6-tagged PYL2 with 100 nM of biotinylated recombinant HAB1 at the indicated concentrations of (+)- and (−)-ABA. The relative strengths of interactions are shown as photon counts (n=3, error bars=SD). **b)** ABA-dependent inhibition of HAB1 phosphatase activity by PYL2. Reactions contain 100 nM of biotin-HAB1 and 500 nM of PYL2 with the indicated concentrations of (+)- and (−)-ABA (n=3, error bars=SD). The IC_{50} values were derived from curve fitting based on a competitive inhibitor model for the binding of ABA-bound PYL2 to HAB1 (R^2=0.998 for (+)-ABA and 0.997 for (−)-ABA).

3.3 Large scale purification and crystallization of PYLs

To prepare proteins for crystallization, H6GST-PYL2 was expressed from 6 L of *E. coli* and purified using standard nickel affinity chromatography in the initial large scale PYL preparation attempt. A total of 665 mg of H6GST-PYL2 was obtained from pooled elute fractions with relatively good purity as seen in SDS-PAGE analysis (Figure 16a). Thrombin was added to pooled elute in a 1:250 protease to protein ratio to cleave off the H6GST tag after which the cleaved tag was removed by nickel affinity column. Proteolytic cleavage was highly inefficient and most of the fusion protein remained uncleaved (Figure 16b). Less than 20 mg of untagged PYL2 protein was recovered and further purified by size exclusion chromatography (SEC). The peak volume in SEC profile suggested that PYL2 eluted as a monomer (Figure 16d). Pooling of peak SEC fractions yielded 7.6 mg of purified PYL2 (Figure 16c), which was concentrated to 6.6 mg/ml for crystallization.

The thrombin proteolytic cleavage of H6GST-PYL2 was highly inefficient, possibly due to presence of secondary structure at the N-terminal of PYL hindering the cleavage site. The inefficient proteolytic cleavage was also observed in the purification of PYR1 with H6GST-tag, which produced similar yields as PYL2. Therefore in the next round of large scale PYL preparation, PYL1 was purified from H6SUMO-tagged protein. Nickel affinity chromatography eluted 146 mg of H6SUMO-PYL1 protein (Figure 17a), which cleaved efficiently in a 1:1000 protease to protein ratio (Figure 17b). SEC peak volume gave a calculated molecular weight of 31 kD, which

may suggest that PYL1 eluted in a monomer/dimer equilibrium (Figure 17d). SEC peak fractions yielded 47 mg of purified PYL1 (Figure 17c), which was concentrated to 9 mg/ml for crystallization.

Subsequently, PYL3–PYL6 and all future large scale preparations of PYL proteins were performed with H6SUMO-tagged proteins.

High throughput crystallization screens were set up for apo PYR1 and PYL1–PYL6 by vapor diffusion method in 96-well sitting drop format using 5 commercial screens from Hampton Research (Index HT, CrystalScreen HT, MemFac HT, PEGIon HT and PEGRx HT) as initial trials. Of these members, PYL1, PYL2 and PYL5 were able to crystallize, but only PYL1 and PYL2 formed large crystals with and good surface in a number of conditions. Crystallization conditions were optimized for PYL1 and PYL2 to obtain better crystals for diffraction (Figure 18). PYL–ABA complexes were prepared by adding 5 times molar excess of (+)-ABA to PYL1 and PYL2 and initial crystallization screens were carried out as above. Only PYL2 produced crystals in the presence of ABA (Figure 18).

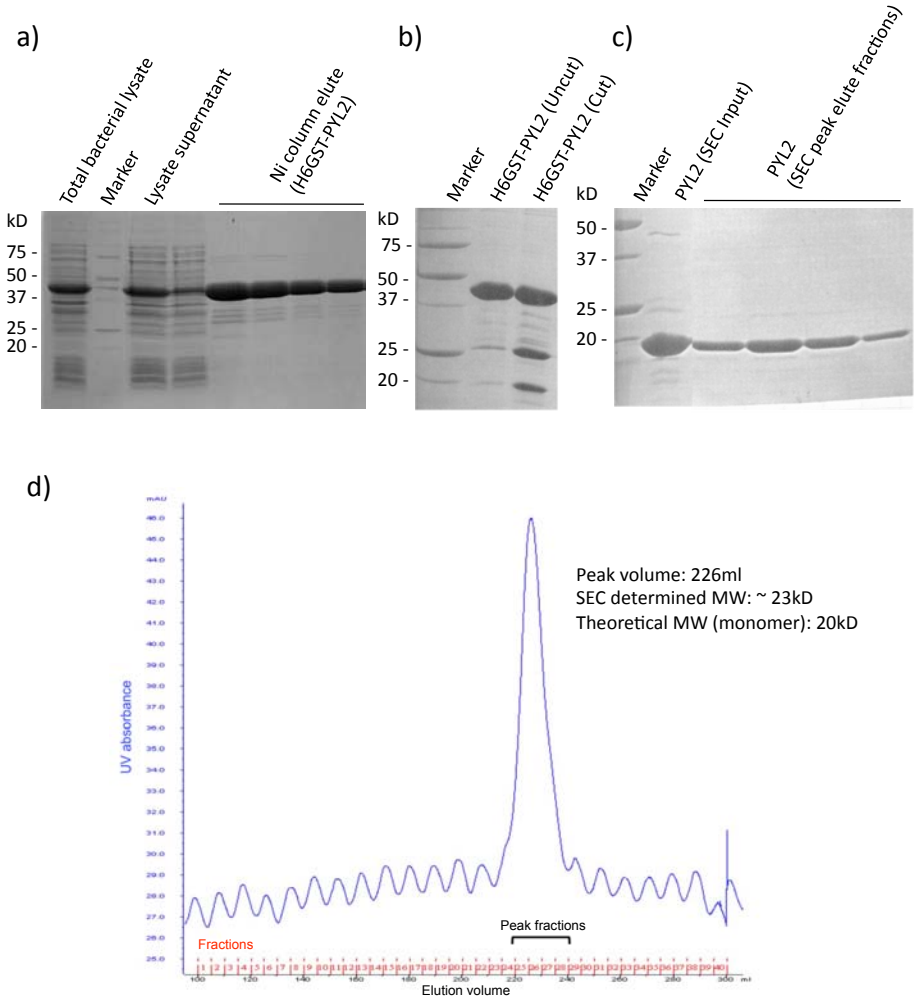

Figure 16. **Large scale purification of PYL2.**

SDS-PAGE of **a)** purification of H6GST-PYL2 by nickel affinity chromatography; **b)** proteolytic cleavage of H6GST tag by thrombin digestion; **c)** size exclusion chromatography (SEC) of untagged PYL2. **d)** SEC profile. The theoretical molecular weights (MW) of H6GST-PYL2, H6GST tag and untagged PYL2 are 45 kD, 25 kD and 20 kD respectively.

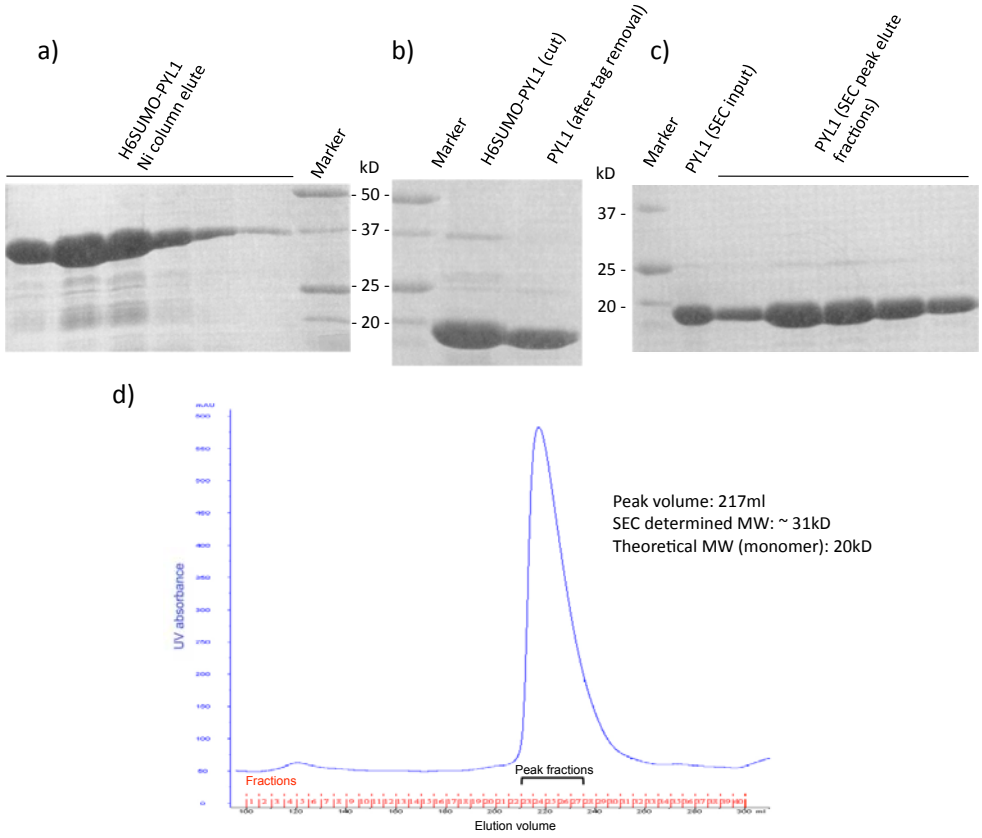

Figure 17. **Large scale purification of PYL1.**

SDS-PAGE of **a)** purification of H6SUMO-PYL1 by nickel affinity chromatography; **b)** proteolytic cleavage of H6SUMO tag by Ulp1 SUMO protease; **c)** size exclusion chromatography (SEC) of untagged PYL1. **d)** SEC profile. The theoretical molecular weight (MW) of H6SUMO is 12 kD, but it migrates at about 15–18 kD.

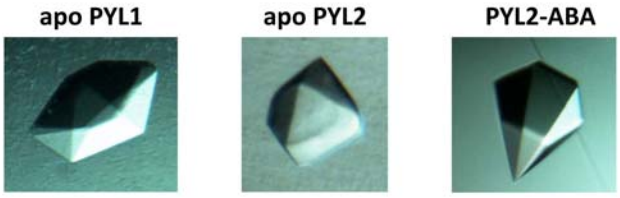

Figure 18. **Crystals of the apo and ABA-complexed PYL receptors.**

3.4 Molecular features of PYL–ABA interaction

To provide structural evidence for PYLs as ABA receptors and to identify the molecular mechanisms of ABA recognition, high resolution crystal structures of ligand-free PYL1 and PYL2 and that of ABA-bound PYL2 were determined at 2.40 Å, 1.95 Å and 1.85 Å respectively, with the statistics of structure refinement shown in Table 3.

3.4.1 Overall structures of apo PYL1 and PYL2

The structures of PYL1 and PYL2 exhibit the characteristic helix-grip fold of START domain proteins, marked by the existence of a central β-sheet surrounded by N- and C-terminal α-helices (Iyer et al., 2001) (Figure 19). The distinct features of the receptors are the presence of a long C-terminal α-helix, 3 shorter helices, a 7-stranded anti-parallel β-sheet and a large pocket of 543 $Å^3$ between the C-terminal helix and the β-sheet. PYL1 and PYL2 share 51% amino acid sequence identity and their overall structures are highly similar. The major differences observed between the PYL1 and PYL2 receptors are the relative positions of their N-terminal helices and the loop structure between β-strands 6 and 7, which is not resolved in the PYL1 structure. In contrast, their C-terminal α-helices, central β-sheets and ligand binding pockets overlap closely with each other (Figure 19c).

Table 3. Statistics of structure refinement for apo PYLs, ABI2 and ABA-bound complexes.

	PYL1 apo	**PYL2 apo**	**PYL2–ABA**	**ABI2 apo**	**PYL2–ABA–HAB1**	**PYL2–ABA–ABI2**
PDB code	3KAY	3KAZ	3KB0	3UJK	3KB3	3UJL
Data collection						
Space group	$P6_5$	$C222_1$	$P6_122$	$P3_221$	$P2_12_12_1$	$P2_12_12_1$
Resolution (Å)	30-2.40	30-1.85	30-1.95	30-1.90	30-1.95	30-2.50
Cell dimensions						
a, *b*, *c* (Å)	126.76, 126.76, 61.41	62.19, 104.91, 185.41	61.27, 61.27, 255.10	89.67, 89.67, 91.87	60.32, 64.46, 143.90	61.43, 98.58, 132.84
α, β, γ (°)	90, 90, 120	90, 90, 90	90, 90, 120	90, 90, 90	90, 90, 90	90, 90, 90
Total /Unique reflections	499298 /22235	570933 /49882	852408 /21765	374836 /34099	511848 /41807	71996 /25223
Completeness (%)	100.0 (100.0)	95.4 (94.9)	99.8 (100.0)	100.0 (100.0)	93.9 (64.9)	87.7 (86.8)
I/σ	47.6 (4.0)	26.4 (3.3)	49.1 (4.5)	46.2 (4.5)	38.4 (2.5)	13.9 (2.1)
Redundancy	22.5 (21.5)	11.4 (11.9)	39.2 (33.5)	11.0 (11.0)	12.2 (6.5)	2.9 (2.7)
R_{sym}	0.079 (0.685)	0.085 (0.816)	0.100 (0.889)	0.053 (0.583)	0.093 (0.689)	0.076 (0.464)
Refinement						
Resolution (Å)	30-2.40	30-1.85	30-1.95	30-1.90	30-1.95	30-2.50
No. reflections	18156	46102	20100	31421	38149	23335
No. residues	354	531	177	301	498	459
No. solvent molecules	170	321	128	131	324	69
No. of non-H atoms	2988	4508	1534	2450	4013	2652
R_{cryst}	20.80%	20.60%	19.00%	16.50%	20.70%	21.40%
R_{free}	24.30%	23.70%	22.90%	19.60%	24.80%	24.20%
RMSD Bonds (Å)	0.021	0.024	0.027	0.006	0.023	0.022
RMSD Angles (°)	1.68	1.84	2.02	1.25	1.84	1.71
Average B factor ($Å^2$)	60.51	36.46	35.45	59.3	38.72	48.3

Notes:

RMSD is the root-mean-square deviation from ideal geometry of protein.
Values in parentheses are for highest-resolution shell.
One crystal was used for each structure.

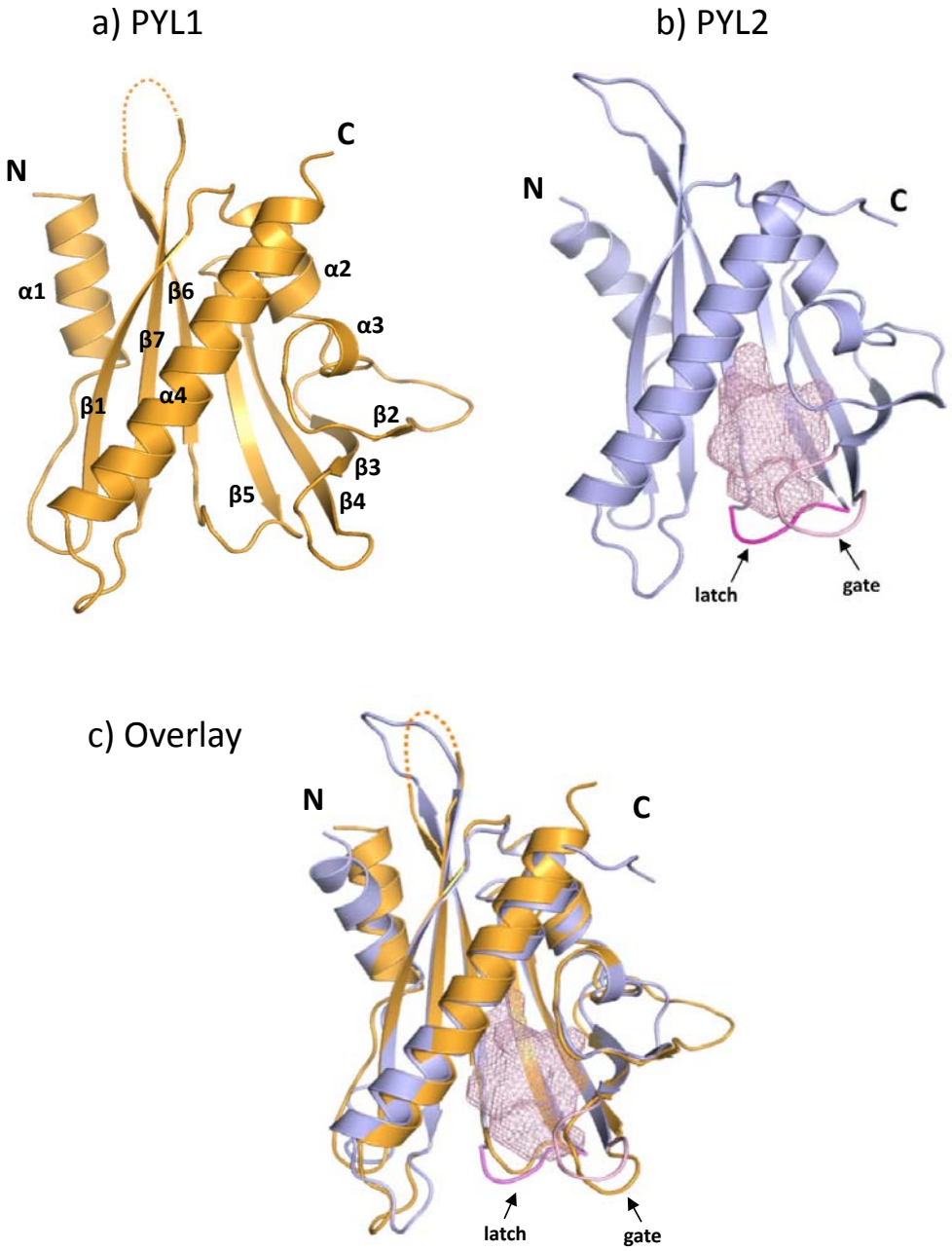

Figure 19. **Structures of the apo ABA receptors.**

a) Structure of PYL1 with labelled positions of the 4 α-helices and 7 anti-parallel β-strands. The unresolved loop region is shown in dotted line. **b)** Structure of PYL2 with the empty ligand binding pocket shown as mesh, flanked by the gate (pink) and latch (magenta) loops. **c)** Overlay of the apo PYL1 (orange) and PYL2 (grey) receptors.

3.4.2 Structure of ABA-bound PYL2

The (+)-ABA-bound PYL2 crystallized as a monomeric receptor-ligand complex with 1:1 stoichiometry. The overall structure of the ligand-bound receptor resembles that of the apo receptor (Figure 20). ABA is clearly defined in the receptor pocket by a high resolution electron density map (Figure 21a). Analysis of the ligand-bound pocket revealed a network of intermolecular interactions between ABA and receptor pocket residues (Figure 21b). The carboxylate group of ABA forms a charged interaction with the side chain of receptor residue K64 and a network of water-mediated hydrogen bonds with residues E98, N173 and E147. The hydroxyl and ketone groups of the ABA also make direct or water-mediated polar interactions with the receptor, while its cyclohexene ring and hydrocarbon chain form many non-polar interactions in the mainly hydrophobic pocket. Involvement of the receptor pocket residues in ABA interaction was functionally validated by biochemical assays. Expectedly, mutations of these pocket residues reduced the ability of PYL2 in ABA binding and ABA-induced HAB1 interaction and phosphatase inhibition (Figure 22).

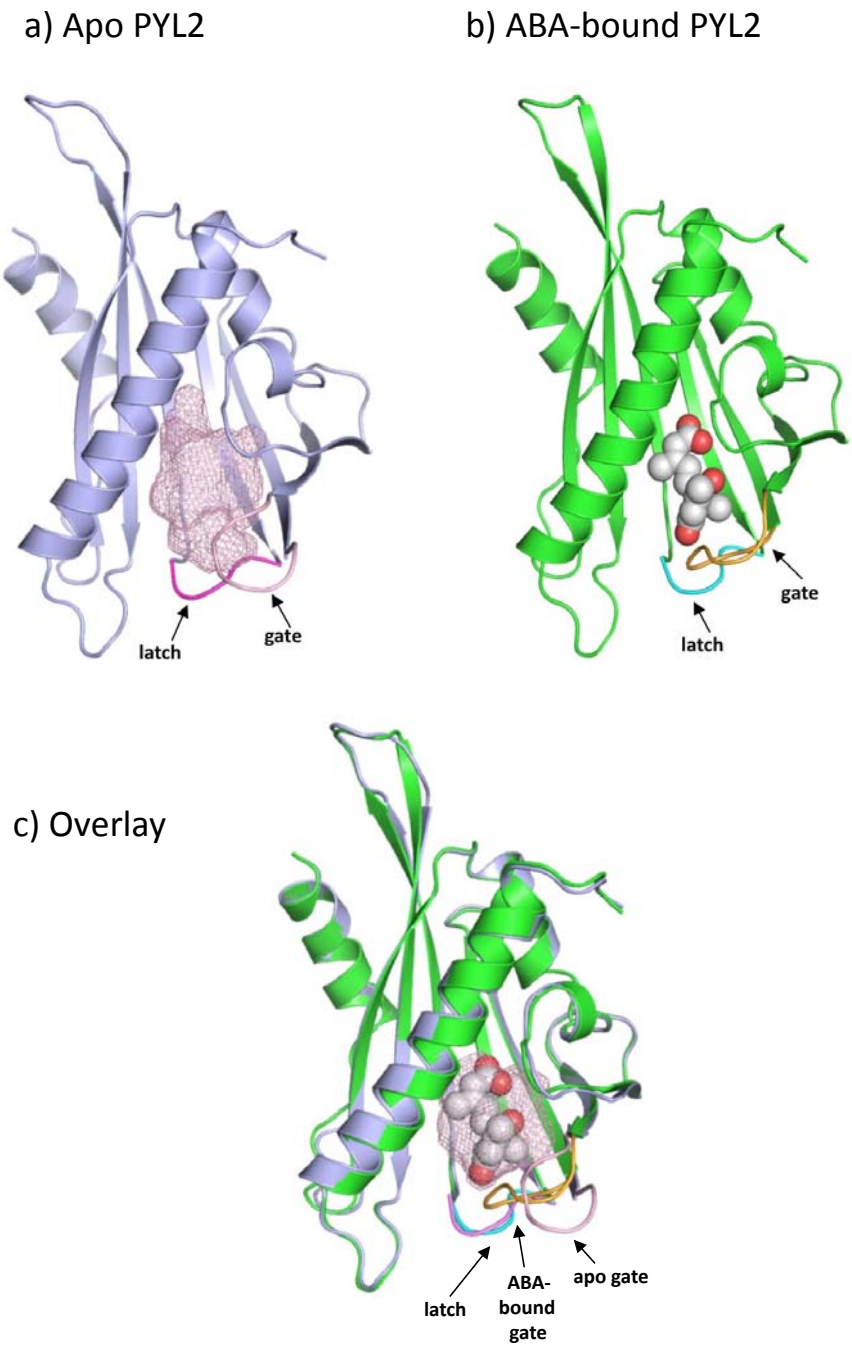

Figure 20. **Structures of the ligand-free and ABA-bound PYL2.**

a) Structure of PYL2 with the empty ligand binding pocket shown as mesh, flanked by the gate (pink) and latch (magenta) loops. **b)** Structure of the ABA-bound PYL2 with ABA shown as a ball model. The gate (orange) and latch (cyan) loops are indicated by arrows. **c)** Overlay of the apo (grey) and ABA-bound (green) PYL2 structures. The latch (magenta for apo and cyan for ABA-bound) and the conformational change in the gate (pink for apo and orange for ABA-bound) are indicated by arrows.

a)

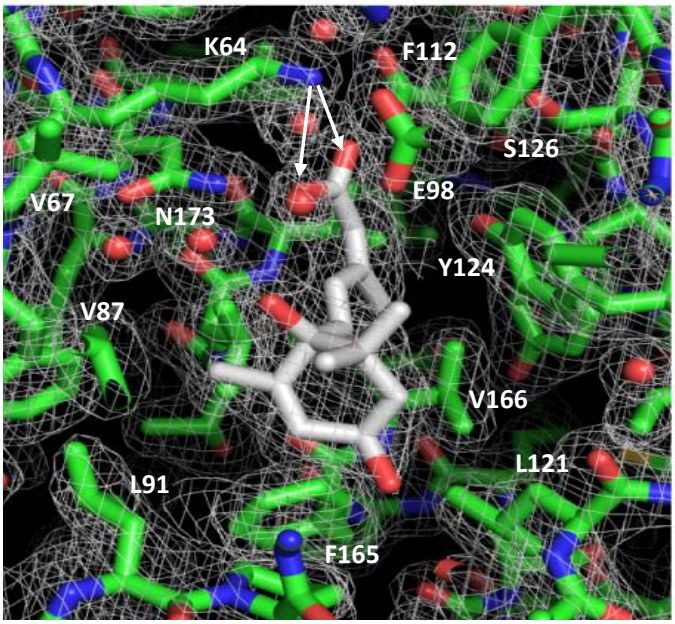

b)

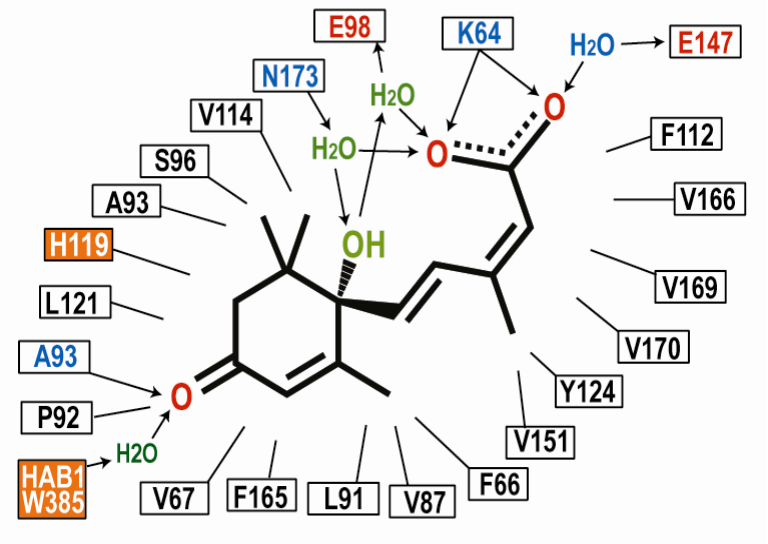

Figure 21. **Intermolecular interactions in the ABA-bound PYL2 pocket.**

a) A 2 F_o–F_c electron density map of ABA and surrounding PYL2 pocket residues contoured at 1.0 σ. The charged interaction between the ABA acid group and K64 is indicated by two arrows. **b)** Schematic presentation of the interactions between PYL2 pocket residues and the bound ABA. Charged interactions and hydrogen bonds are indicated by arrows, hydrophobic interactions by solid lines with H-bond donors in blue and acceptors in red. The two orange-boxed residues, PYL2 H119 and HAB1 W385, contact ABA only upon formation of the trimeric PYL2–ABA–HAB1 complex.

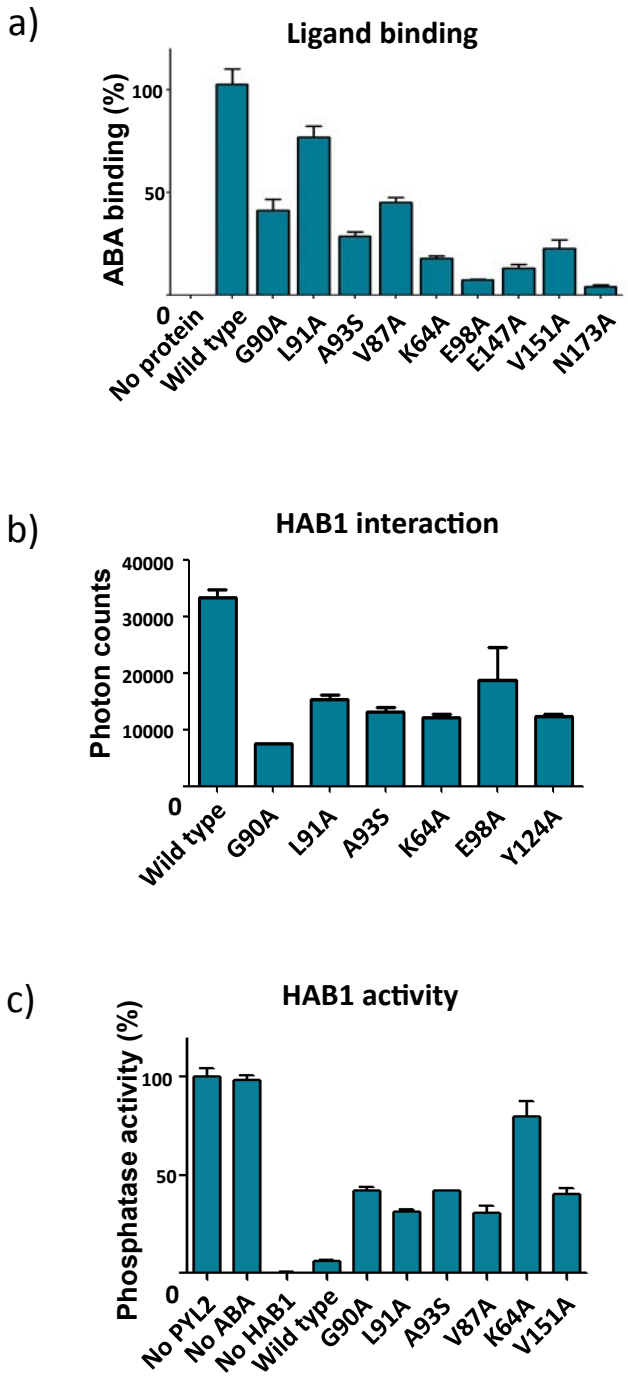

Figure 22. **Mutational analysis of the ABA-binding pocket.**

Mutations in key ligand binding pocket residues of PYL2 reduces **a)** ABA binding as determined by scintillation proximity assay with ^{3}H-labelled ABA (n=3, error bars=SD), **b)** HAB1 interaction determined by AlphaScreen assays (n=3, error bars=SD) and **c)** inhibition of HAB1 determined by phosphatase activity assays containing 100 nM of recombinant HAB1 and 500 nM of recombinant wild type or mutant PYL2 in the presence of 10 μM (+)-ABA (n=3, error bars=SD).

3.4.3 Basis for stereoselectivity

The ABA-bound PYL2 structure reveals the basis for its preference for the natural (+)-stereoisomer. In the ABA-bound pocket, the monomethyl group of the ABA cyclohexene ring occupies a narrow region formed by residues F66, V87, L91, P92, F165 and V169, while the dimethyl group fits into a larger region formed by A93, S96 and V114 (Figure 23b). In case of the (–)-isomer, the cyclohexene ring will be flipped such that the positions of the monomethyl and dimethyl groups are interchanged (Figure 23a) and this would cause stereo collision between the dimethyl group and the narrow pocket that accommodates the monomethyl group. Therefore, the size and shape of the receptor's pocket that accommodates the cyclohexene ring, together with the network of specific hormone-receptor interactions, contribute to its stereoselectivity.

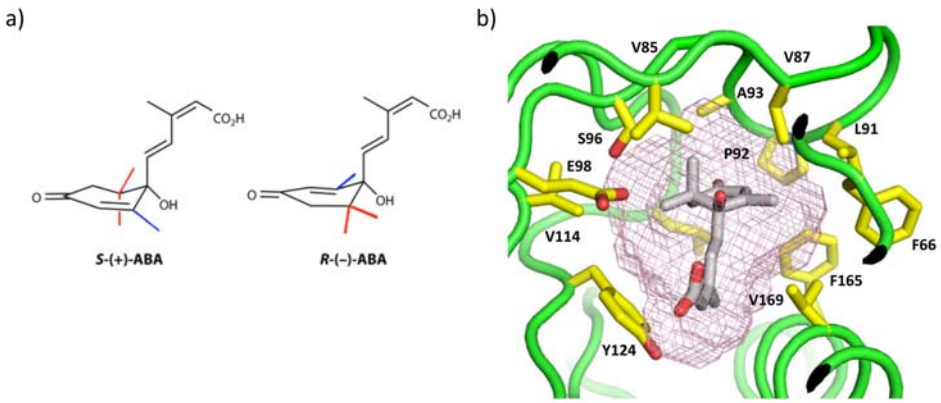

Figure 23. Stereoselectivity of the ligand binding pocket.

a) Chemical structures of the *S*-(+)- and *R*-(–)-ABA stereoisomers. Rotation around the chiral center results in a swap of the relative positions of the monomethyl (blue) and dimethyl (red) groups on the ring. **b)** The pocket topology of PYL2 surrounding the mono-methyl and the dimethyl groups of ABA shown with key PYL2 residues and the ligand binding pocket (mesh).

3.4.4 Conformational changes upon ABA binding

Conformational differences between the ABA-bound and unbound PYL2 structures reveal the involvement of 2 loop regions in hormone binding and signal transduction. These 2 loops, namely the gate (residues 89–93: SGLPA) and latch (residues 119–121: HRL) loops, guard the entrance of the ligand binding pocket. The most striking difference between the ligand-free and ligand-bound PYL2 structures is the conformational change of the gate loop upon ABA-binding (Figure 20), which closes the ABA-bound pocket and seals the bound ABA molecule from the exposure to the solvent (Figure 24a). While the backbone of the latch loop stays fairly rigid, the side chain of the E118 residue preceding the latch motif, which points into the ligand-free pocket, rotates ~150° outwards upon ABA-binding. This creates space for the closure of the gate loop onto the latch. In the closed conformation, the gate and latch residues form intramolecular interactions (Figure 24b), creating a new interface for PP2C interaction.

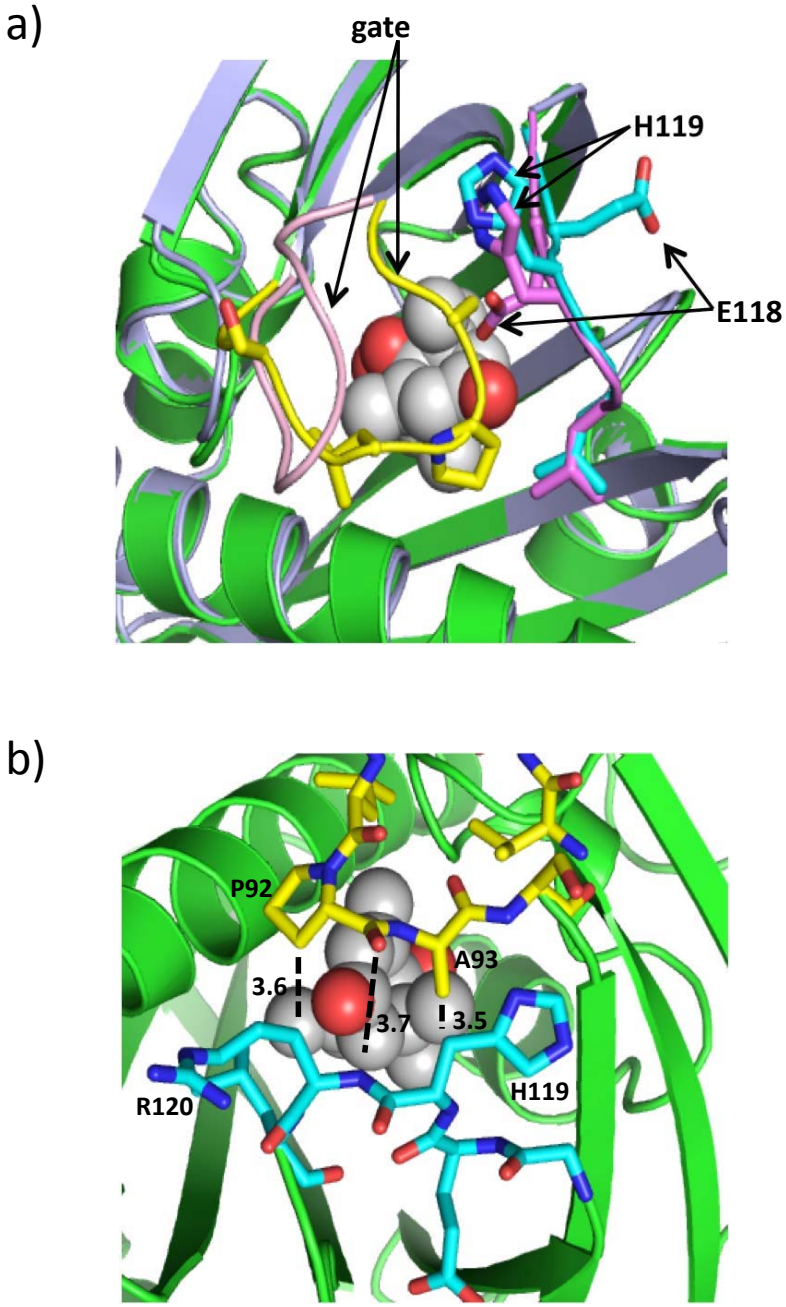

Figure 24. **A gate and latch mechanism in ligand-binding.**

a) Conformational differences between apo PYL2 (grey molecule, pink gate, magenta latch) and ABA-bound PYL2 (green molecule, yellow gate, cyan latch). **b)** Interactions between gate (yellow) and latch (cyan) residues in the ABA-PYL2 structure. Distances between residues are indicated in Å.

3.5 Mechanism of ABA-induced PYL binding and inhibition of PP2C

To unravel the mechanism of PP2C inhibition by the PYL proteins, each of the ABA-signalling PP2Cs ABI1, ABI2 and HAB1 was subjected to crystallization trials as apo proteins as well as in ternary complexes with PYL2–ABA. Because of the high binding affinity of PYL2 to HAB1 in the presence of (+)-ABA, the PYL2–ABA–HAB1 complex was stable and formed crystals readily (Figure 25). A 1.95 Å resolution structure was determined and used for initial analysis and publication. In contrast, the apo PP2Cs did not form highly diffracting crystals as easily. Of the three PP2Cs tested, only ABI2 was able to form crystals that diffracted to high resolution after extensive crystallization trials. The structures of the apo ABI2 and the PYL2–ABA–ABI2 complex, determined at 1.90 Å and 2.50 Å respectively, were obtained at a later time and supported our initial analysis based on the PYL2–ABA–HAB1 structure. The statistics of structure refinement are shown in Table 3.

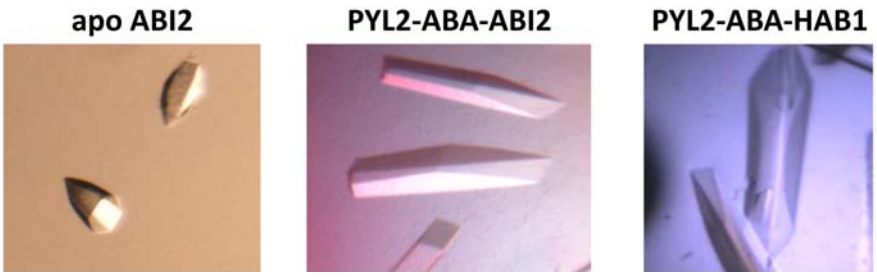

Figure 25. Crystals of the apo PP2C and in complexes with the ABA-bound PYL2 receptor.

3.5.1 Overall structure of apo PP2C

The catalytic domain of ABI2 adopts a typical PP2C fold (Das et al., 1996), containing two five-stranded β-sheets that are sandwiched by two pairs of anti-parallel α-helices (Figure 26). The active site is located at the top edge of the two central β-sheets and contains three Mg^{2+} ions.

3.5.2 Structures of the PYL2–ABA–PP2C complexes

The overall structures of PYL2–ABA–ABI2 and PYL2–ABA–HAB1 are almost identical and both revealed monomeric complexes with 1:1:1 receptor–ligand–PP2C stoichiometry (Figure 27). The PP2C in the apo structure and in both complexes are superimposable (Figure 26), indicating that PP2Cs have a fairly rigid fold and do not undergo obvious conformational changes in their interaction with PYL protein.

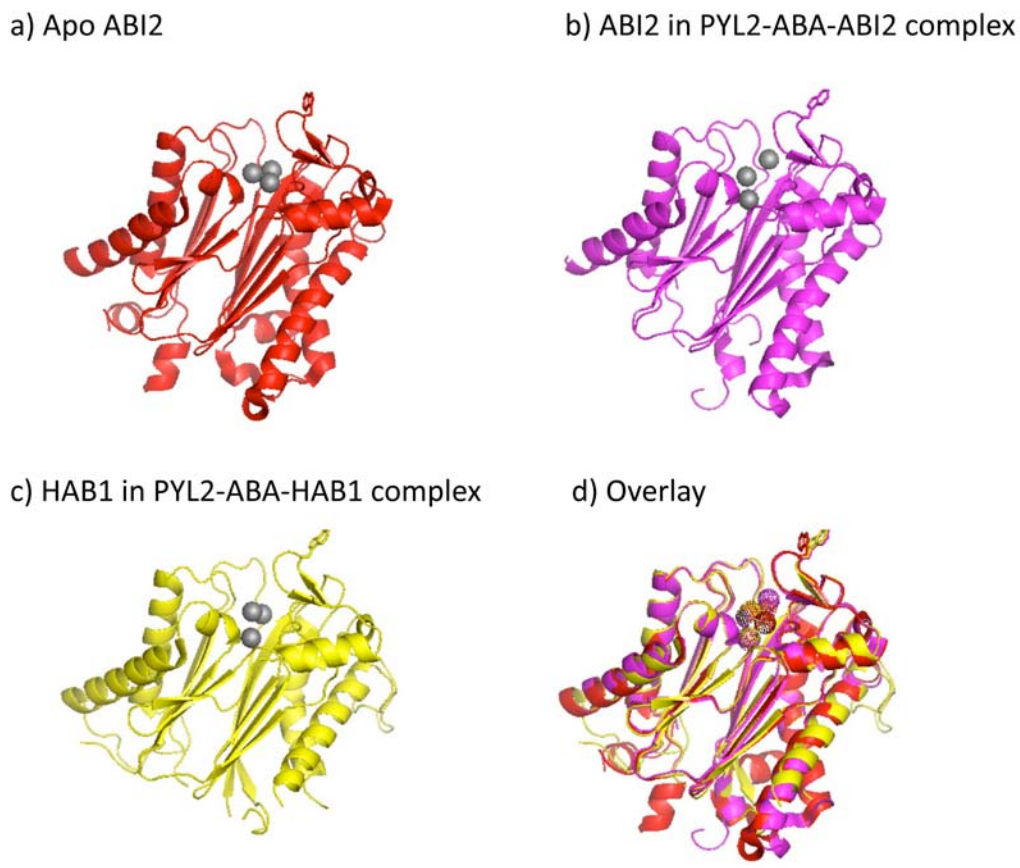

Figure 26. **Structures of the PP2Cs.**

a) ABI2 in apo form, **b)** ABI2 in the PYL2–ABA–ABI2 complex, **c)** HAB1 in the PYL2–ABA–HAB1 complex and **d)** overlay of these PP2C structure with apo ABI2 in red, ABI2 in the PYL2–ABA–ABI2 complex in magenta and HAB1 in the ternary complex in yellow. Magnesium ions are shown as spheres and the side chains of the conserved PYL2-interacting tryptophan residues are shown as sticks.

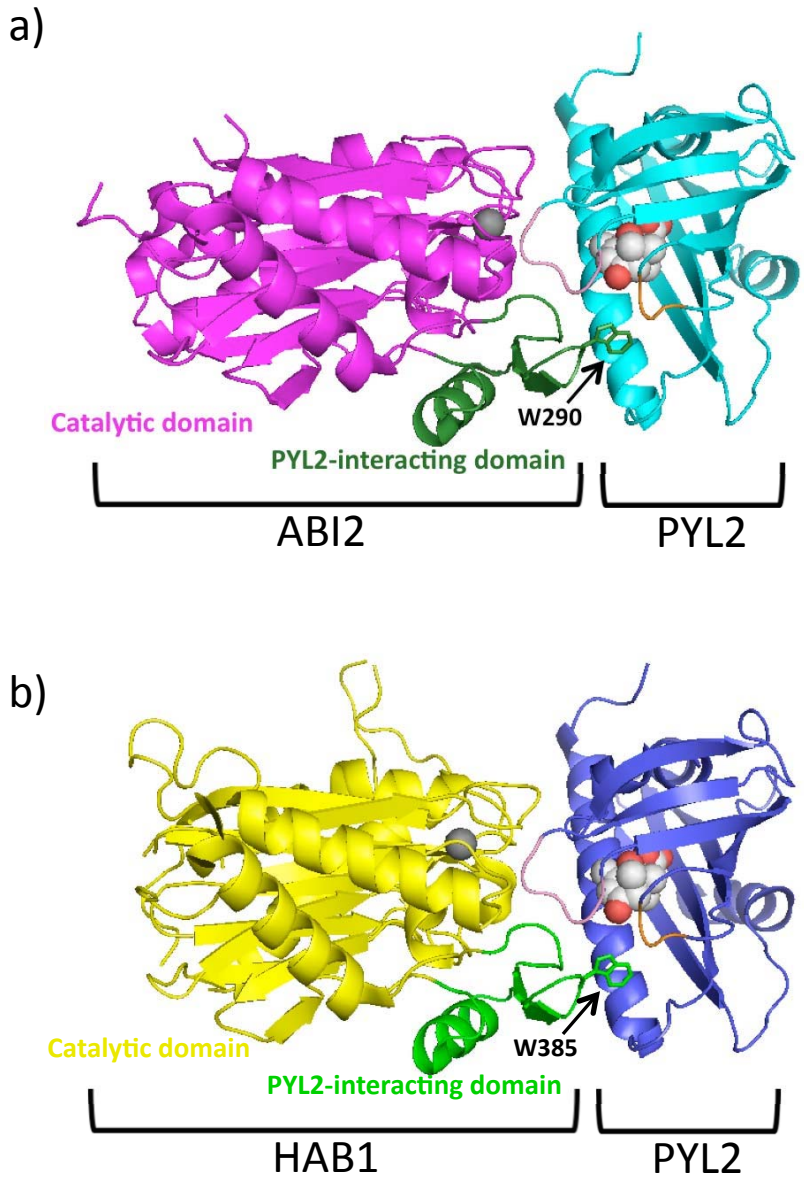

Figure 27. **Structures of the PYL2–ABA–PP2C complexes.**

a) Structure of the PYL2–ABA–ABI2 complex. The ABI2 catalytic domain is coloured in magenta, its PYL2-interatcing domain in dark green showing the side chain of its conserved PYL-interacting tryptophan. PYL2 is shown in cyan with ABA as ball. Gate and latch loops are coloured pink and orange respectively. **b)** Structure of the PYL2–ABA–HAB1 complex with HAB1 catalytic domain in yellow and its PYL-interacting domain in green. PYL2 is shown in blue. Magnesium ions in the PP2Cs are shown as grey spheres.

3.5.3 A gate-latch-lock mechanism of signalling by ABA receptors

Both ABI2 and HAB1 interact with PYL2 at the receptor's closed gate-latch interface, revealing the importance of the closure of the gate loop upon ABA binding to form the interface for PP2C interaction. On the other hand, ABA-bound PYL2 interaction with the PP2C sterically blocks the PP2C catalytic site, which explains the mechanistic basis of ABA-induced PYL inhibition of PP2Cs.

Analysis of the PYL2–ABA–HAB1 ternary interaction interface revealed a number of insightful features. Most strikingly, the indole ring of W385 of HAB1 inserts into the ABA-bound PYL2 pocket, making a water-mediated hydrogen bond with the ketone group of ABA (Figure 28a,b). This observation implies that HAB1 serves as a co-receptor that senses the binding of ABA into the PYL receptors. The gate and latch loops of the receptor undergo movements in response to HAB1 interaction. Most drastically, the side chain of H119, which faces outwards of the pocket in both apo and ABA-bound PYL2 structures, points into the pocket and makes contacts with the dimethyl group of ABA's cyclohexene ring in the HAB1-bound structure (Figure 28c). Correspondingly, the cyclohexene ring of ABA apparently shifts ~1.3 Å, positioning its ketone group for the water-mediated interaction with the W385 of HAB1. In this configuration, the W385 of HAB1 functions as a molecular lock to stabilize the interaction interface, keeping the gate and latch in closed position. This could explain the higher ABA binding affinities of PYLs observed in the presence of PP2Cs (Ma et al., 2009; Santiago et al.,

2009b). The intermolecular interactions between ABA-bound PYL2 and HAB1 are illustrated in Figure 29. The functional importance of the receptor gate has been validated by mutagenesis data (Figure 22). In addition, mutations of latch residues H119A and R120A compromised ABA-dependent PP2C interaction and phosphatase inhibition (Figure 30a,b), supporting the role of the latch loop in PP2C regulation. To further validate our structural observations, we screened a number of HAB1 mutants for their phosphatase activities in the absence and presence of PYL2 (Figure 30c). Notably, a triple mutation at the W385 region (Q384A/W385A/Q386A) resulted in loss of regulation by PYL2, as indicated by the comparable levels of phosphatase activity in the absence and presence of PYL2. Similarly, G246D mutation abolished its regulation by PYL2. The G246D mutation in HAB1 corresponds to the abi1-1 and abi2-1 mutations that have been well documented to cause dominant ABA-insensitivity (Robert et al., 2006), but the mechanisms have been previously unexplained. In our PYL2–ABA–HAB1 structure, the receptor gate loop packs closely with residues D243 to G246 of HAB1. The distance of G246 to the gate loop is only 2.8–4.0 Å. Thus, mutation to a residue with larger side chain would result in collision with the gate loop, affecting PYL2 regulation, as supported by our phosphatase assay data.

Altogether, we have elucidated the structural mechanisms of ABA binding and signal transduction by the PYL ABA receptor. In summary, ABA binding closes the receptor gate, forming the complementary gate-latch interface for PP2C interaction. PP2C docking further locks the gate and latch interface

through a conserved tryptophan residue. In this configuration, the phosphatase catalytic site is blocked, resulting in inhibition of the phosphatase activity.

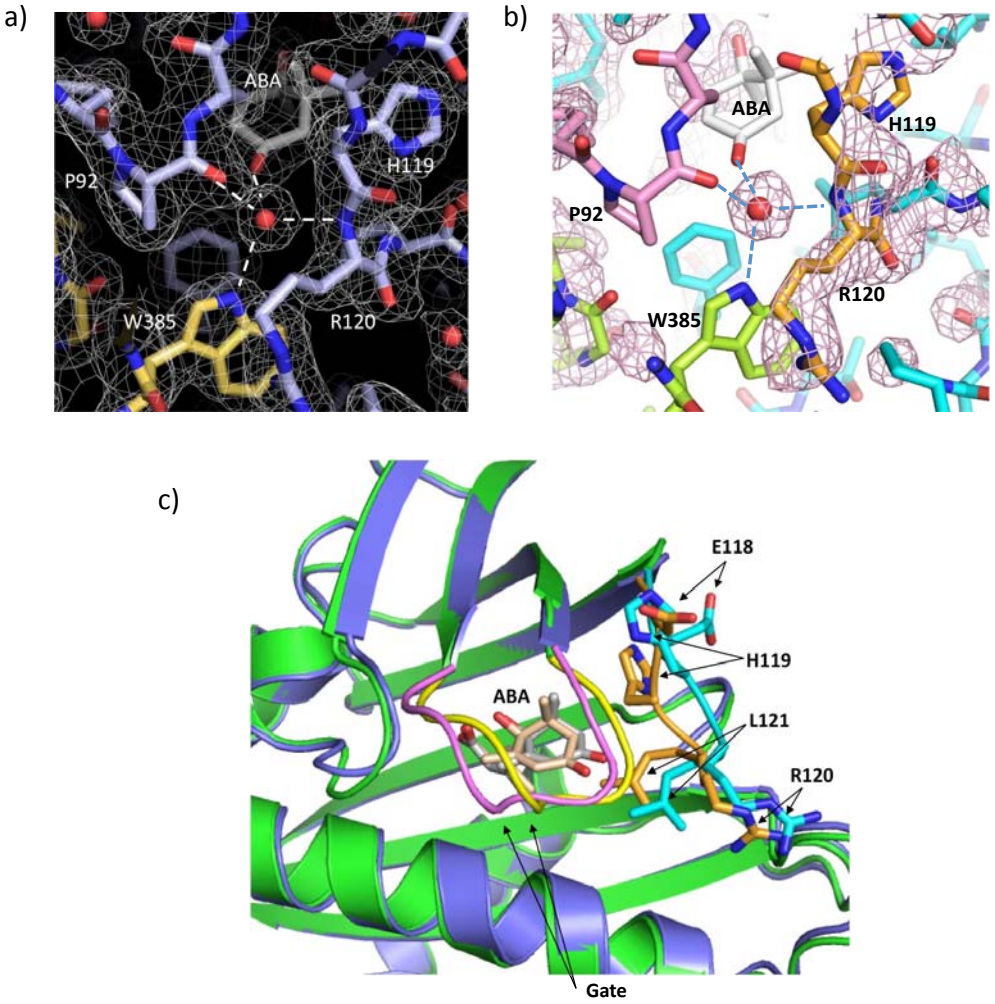

Figure 28. **The HAB1–PYL2 interaction interface.**

Network of water-mediated interactions between key residues and the ketone group of ABA shown by **a)** a refined 2 F_o–F_c electron density map contoured at 1.0 σ, and **b)** and an unbiased F_o–F_c difference density contoured at 1.0 σ. **c)** Conformational changes induced by HAB1 docking. A close-up overlay of PYL2–ABA in the presence (blue) and absence (green) of HAB1. The latch is shown in cyan (-HAB1), and orange (+HAB1), the gate in yellow (-HAB1) and pink (+HAB1) and ABA in grey (-HAB1) and light pink (+HAB1).

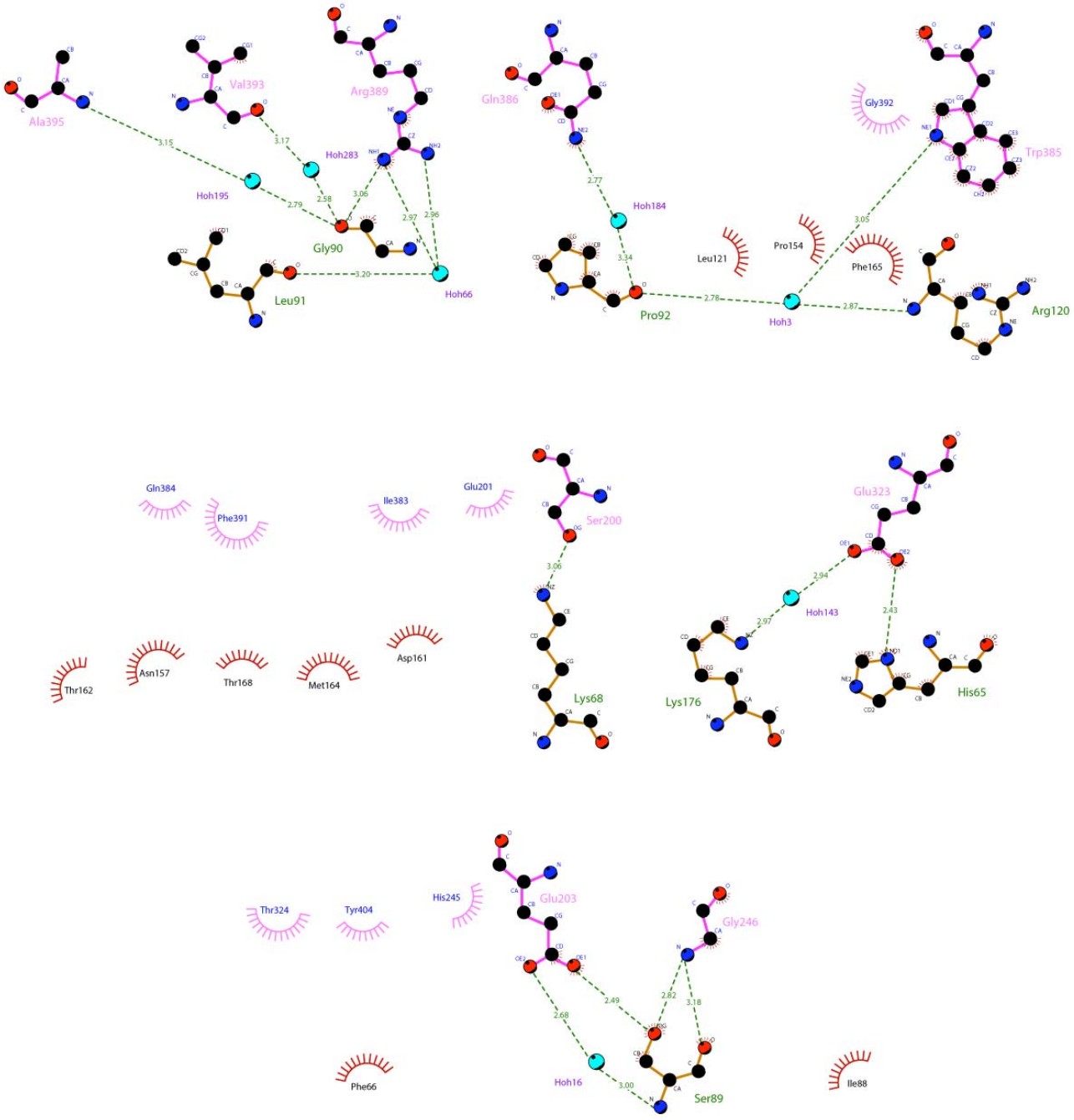

Figure 29. DimPlot analysis of interactions in the PYL2–HAB1 interface.

Interactions were mapped using DimPlot program in LigPlot software (Wallace et al., 1995) with cutoff distances for hydrogen bonds set at 2.70 Å for hydrogen-acceptor distances and 3.35 Å for donor-acceptor distances and 2.9–3.9 Å for non-bonded distances. HAB1 residues involved in polar and hydrophobic interactions are labeled in pink and blue respectively. PYL2 residues involved in polar and hydrophobic interactions are labeled in green and black respectively. Water molecules are labeled in purple and bond distances are indicated and shown by green dashed lines.

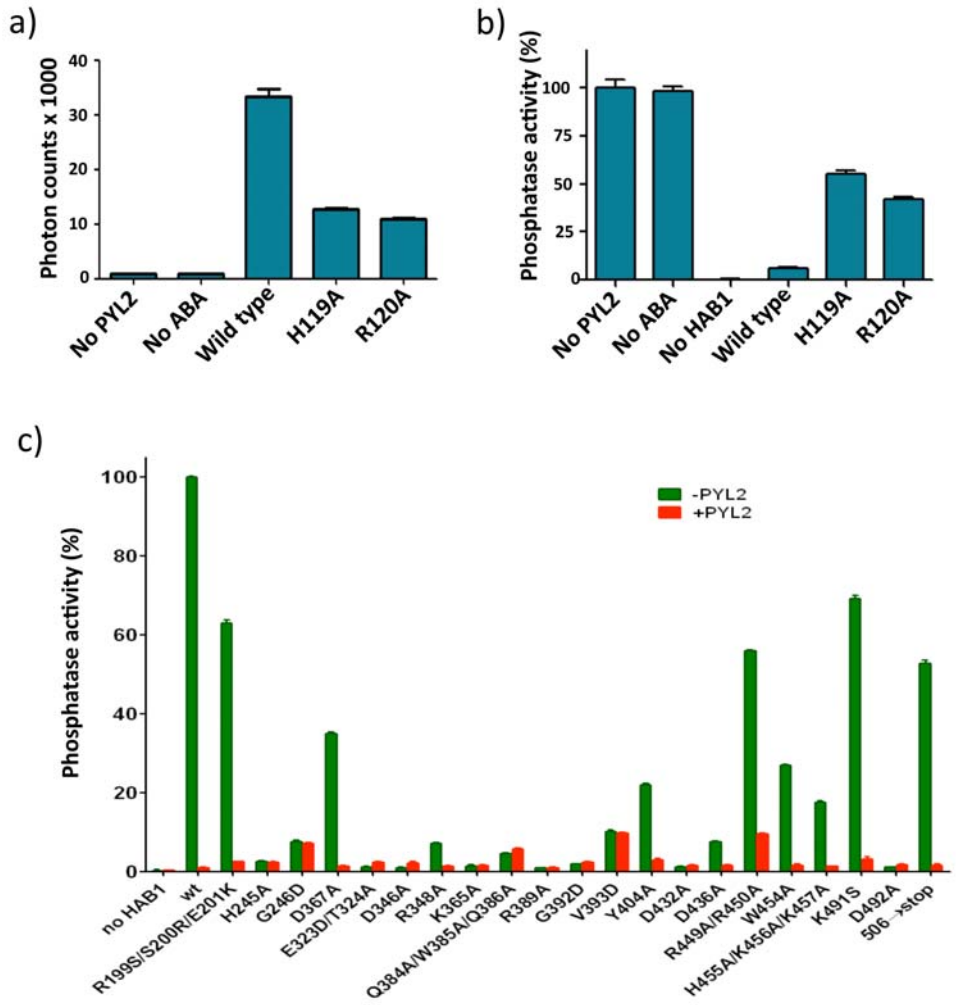

Figure 30. **Mutational analysis of PYL2 and HAB1 interface.**

a) Functional analysis of mutations in PYL2 latch residues in HAB1 interaction as determined by AlphaScreen (n=3, error bars=SD). **b)** Functional analysis of mutations in PYL2 latch residues in HAB1 inhibition determined by phosphatase activity assays containing 100 nM recombinant HAB1 and 500 nM recombinant wild type or mutant PYL2 (n=3, error bars=SD). **c)** Functional analysis of HAB1 mutations by phosphatase activity assays containing 100 nM wild type or mutant recombinant HAB1 in the absence and presence of 500 nM PYL2 (n=3, error bars=SD).

3.6 Selective pyrabactin activation and antagonism of PYLs

Pyrabactin (Figure 4) is a synthetic seed germination inhibitor whose activity correlates with some but not all of the effects of ABA, and is therefore a selective ABA agonist (Park et al., 2009). Agreeably, our data show that while ABA is a pan agonist of PYLs, pyrabactin selectively promotes the interaction of a subset of PYLs with PP2Cs (Figure 31a). Pyrabactin strongly promoted the interaction of PYR1 with all 3 PP2Cs, consistent with its original identification as a selective PYR1 agonist (Park et al., 2009). While pyrabactin promoted the interaction of PYL1, PYL3 and PYL4 to different extents with different PP2Cs, it failed to activate PYL2 to interact with any of the PP2Cs. Consistently, phosphatase activity assay showed selectivity of pyrabactin-induced PYL inhibition of PP2Cs activity (Figure 31b). All of the PYLs tested were able to be activated by ABA to inhibit all 3 PP2Cs, implying that the inability of pyrabactin to induce PYL2 interaction and inhibition of PP2Cs was not due to inactive PYL2 protein (Figure 31b).

Despite having high endogenous levels of ABA under unstressed conditions (Harris et al., 1988; McCourt and Creelman, 2008; Zhang et al., 2001) and that some PYL members can constitutively inhibit PP2Cs even in the absence of ABA (Santiago et al., 2009b), the ABA response in plants is kept silent under basal conditions. These observations suggest that ABA receptors could be inhibited under unstressed conditions, and such speculation prompted us to determine whether PYL2 could be antagonized by pyrabactin. Indeed, increasing concentrations of pyrabactin reversed the ABA-induced PYL2

interaction and inhibition of PP2Cs, establishing that pyrabactin is a selective PYL2 antagonist (Figure 32).

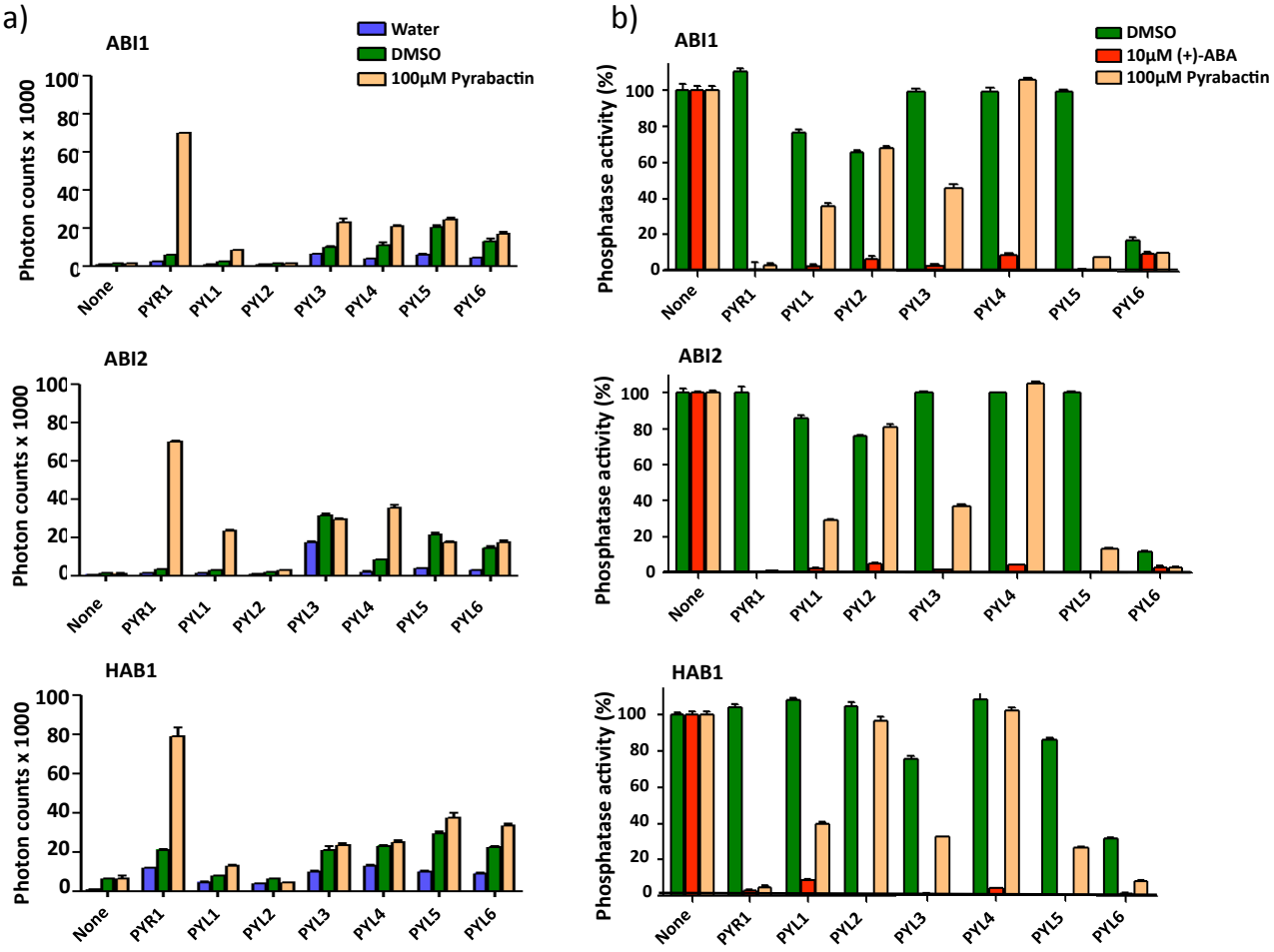

Figure 31. **Selective activation of PYL receptors by pyrabactin.**

a) Receptor interaction with PP2Cs by determined by AlphaScreen (n=3, error bars=SD) and **b)** receptor inhibition of PP2C determined by phosphatase activity assays containing 200 nM of recombinant PP2Cs and 2 µM of recombinant PYLs (n=3, error bars=SD).

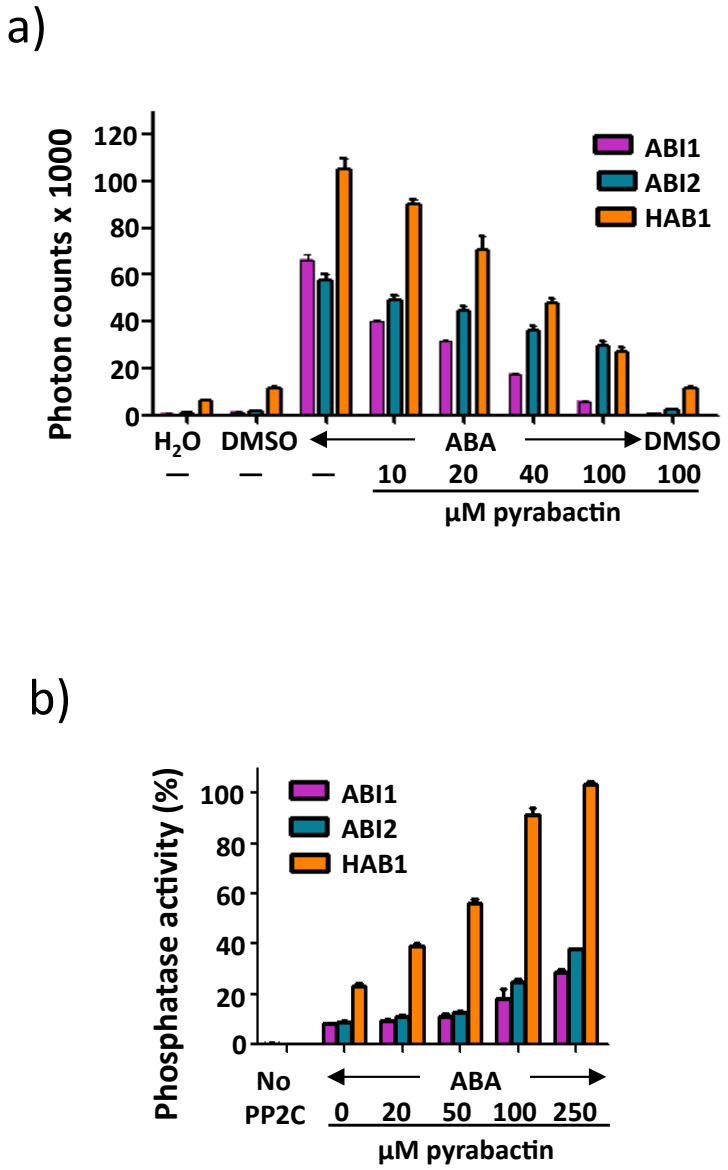

Figure 32. Pyrabactin reverses the ABA-induced activation of PYL2.

a) Pyrabactin inhibits the ABA-induced PYL2 interaction with PP2Cs as determined by Alphascreens interaction assay in the presence or absence of 10 µM (+)-ABA and the indicated concentrations of pyrabactin (n=3, error bars=SD). **b)** Pyrabactin relieves the ABA-mediated PYL2 inhibition of PP2C activity as determined by phosphatase activity assays containing 200 nM recombinant PP2Cs, 600 nM PYL2, 10 µM (+)-ABA and the indicated concentrations of pyrabactin (n=3, error bars=SD).

3.6.1 Mechanism of pyrabactin-mediated receptor activation

Pyrabactin, whose chemical structure does not resemble ABA (Figure 4), acts as an agonist in a subset of PYLs, including PYR1 and PYL1 (Figure 31). To understand how pyrabactin activates ABA receptors, we determined a 2.15 Å crystal structure of a PYL1–pyrabactin–ABI1 ternary complex, representing a pyrabactin-activated ABA receptor complex structure (Figure 33a). The statistics of structure refinement are shown in Table 4. The overall structure of the PYL1–pyrabactin–ABI1 complex resembles that of the PYL2–ABA–HAB1 and PYL2–ABA–ABI2 complexes, with the gate and latch loops in a closed conformation that is further stabilized by the docking of the conserved tryptophan residue W300 from ABI1. In the pyrabactin-activated complex, PYL1 packs against the catalytic site of ABI1, showing a consistent mechanism of phosphatase inhibition as the ABA-activated ternary structure.

Analyses of the receptor pocket revealed that pyrabactin forms a "π"-shaped configuration and interacts with receptor pocket residues in a similar network of polar and hydrophobic interactions as observed in the PYL2–ABA structure (Figure 33b,c). In this configuration, pyrabactin mimics ABA in the ligand-binding mode, with its naphthalene double ring overlapping with the cyclohexene ring of ABA, and its pyridyl nitrogen mimicking the carboxylate group of ABA in its interaction with a conserved lysine residue, K86 of PYL1, corresponding to K64 in PYL2 (Figure 33d). These interactions provide a

common mechanistic basis of ligand-recognition and receptor activation and can be useful for future designs of new ABA agonists.

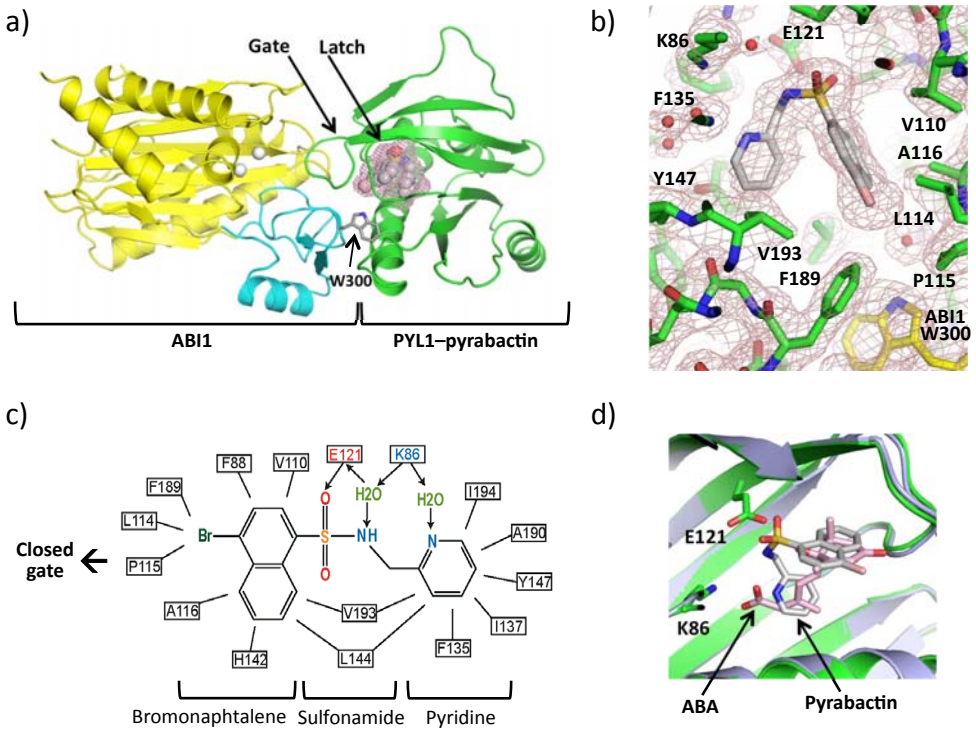

Figure 33. **Structure of the PYL1–pyrabactin–ABI1 complex.**

a) Overall structure of the complex. The ABI1 catalytic domain and PYL1-interacting domain are shown in yellow and cyan respectively. The side chain of its conserved PYL-interacting tryptophan residue is shown as stick representation and magnesium ions as white spheres. PYL1 is shown in green with pyrabactin as ball representation in the PYL1 pocket shown as mesh. **b)** 2 F_0–F_c electron density map of bound pyrabactin and its surrounding residues contoured at 1.0 σ. **c)** Schematic representation of the interactions between pyrabactin and PYL1 binding pocket residues. Charged interactions and hydrogen bonds are indicated by arrows, hydrophobic interactions by solid lines with hydrogen bond donors in blue and acceptors in red. The position of pyrabactin relative to the closed gate is indicated. **d)** Overlay of pyrabactin (grey) with (+)-ABA (pink) in the PYL1 binding pocket.

Table 4. Statistics of structure refinement for pyrabactin-bound complexes.

	PYL2–Pyrb	**PYL1–Pyrb–ABI1**	**PYL2 A93F–Pyrb**	**PYL2 A93F–Pyrb–HAB1**	**PYL2 A93F–Pyrb–ABI2**
PDB code	3NMH	3NMN	3NMP	3NMT	3NMV
Data collection					
Space group	$C222_1$	P1	$C222_1$	$P2_12_12_1$	$P2_12_12_1$
Resolution (Å)	30–1.85	30–2.15	30–2.10	30–2.55	30–2.10
Cell dimensions					
a, *b*, *c* (Å)	62.27, 105.07, 185.08	59.98, 66.71, 72.60	62.08, 105.57, 182.90	62.08, 105.57, 182.90	62.13, 97.59, 134.50
α, β, γ (°)	90, 90, 90	115.8, 95.4, 105.6	90, 90, 90	90, 90, 90	90, 90, 90
Total /Unique reflections	646811 /51071	140047 /50236	291389 /35374	164481 /19661	511848 /41807
Completeness (%)	96.9 (92.8)	97.6 (96.2)	99.9 (99.9)	100.0 (100.0)	100.0 (100.0)
I/σ	32.2 (3.90)	49.1 (4.5)	27.6 (2.9)	15.9 (2.4)	32.4 (3.7)
Redundancy	12.7 (12.8)	13.4 (2.3)	8.2 (8.4)	8.4 (8.6)	14.7 (14.6)
R_{sym}	0.100 (0.706)	0.098 (0.752)	0.093 (0.725)	0.164 (0.793)	0.102 (0.764)
Refinement					
Resolution (Å)	30-1.85	30-2.15	30-2.10	30-2.55	30-2.10
No. reflections	18156	46283	32811	18181	25445
No. residues	528	888	528	472	456
No. solvent molecules	354	101	273	137	172
No. of non-H atoms	4643	7243	4511	3877	3599
R_{cryst}	19.1%	21.2%	23.0%	22.3%	19.4%
R_{free}	23.6%	25.5%	26.9%	26.0%	22.3%
RMSD bonds (Å)	0.018	0.021	0.022	0.018	0.023
RMSD angles (°)	1.71	1.73	1.66	1.44	1.74
Average B factor (Å^2)	32.07	41.41	42.63	41.62	36.0

Notes:

Pyrb: Pyrabactin
RMSD is the root-mean-square deviation from ideal geometry of protein.
Values in parentheses are for highest-resolution shell.
One crystal was used for each structure.

3.6.2 Mechanism of PYL2 antagonism by pyrabactin

To understand the mechanism of PYL2 antagonism by pyrabactin, the structure of PYL2 in complex with pyrabactin was determined at 1.85 Å resolution (Figure 34a), with statistics shown in Table 4. As previous ligand-bound structures, pyrabactin forms a network of polar and hydrophobic interactions with PYL2 pocket residues (Figure 34b). The sulfonamide group of pyrabactin mimics the carboxylate group of ABA, forming interactions with K64 and E98 of PYL2 (Figure 34b,c). The naphthalene ring of pyrabactin forms parallel packing interactions with its pyridine ring the phenol ring of Y124 of PYL2 (Figure 34c).

In contrast, comparison of the pyrabactin-bound pockets of the PYL1 complex and PYL2 structures revealed a flip of ~180° in the orientation of pyrabactin between the two structures (Figure 34d). In this configuration, the gate loop of pyrabactin-bound PYL2 assumes an open conformation similar to the apo PYL2 structure, in contrast to the closed conformation of the active receptor complexes (Figure 34a). These observations indicate that pyrabactin occupies the ligand pocket in PYL2 but assumes a non-productive conformation that does not form the closed-gate conformation necessary for PP2C interaction.

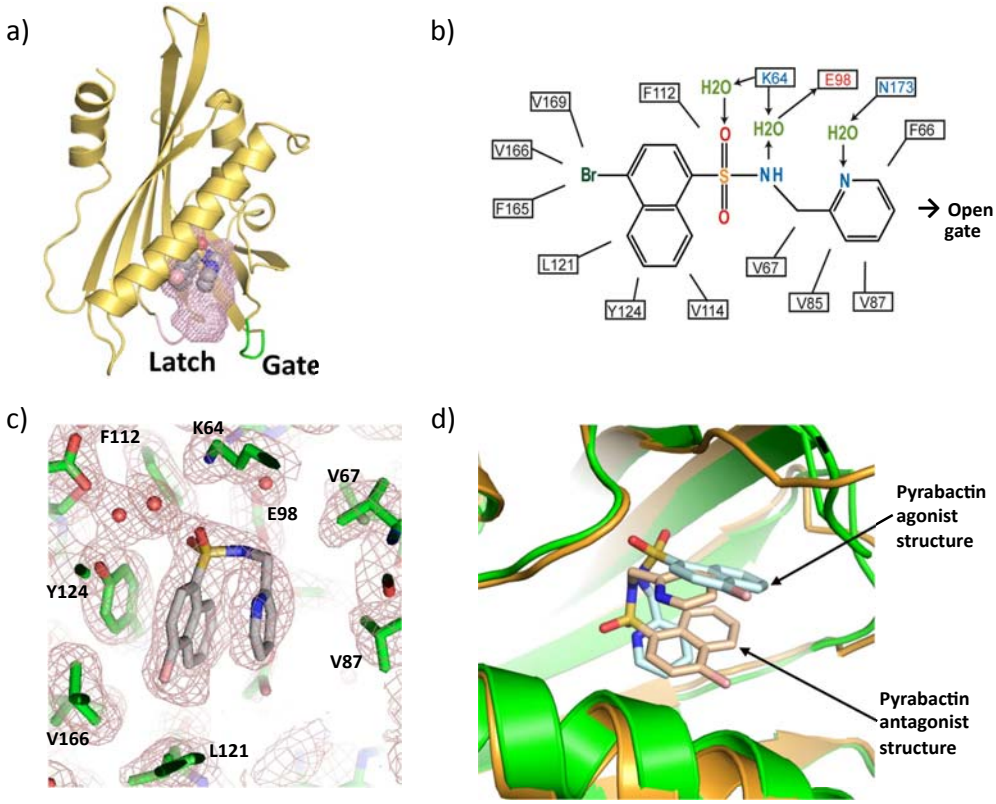

Figure 34. **The PYL2–pyrabactin structure.**

a) Overview of the PYL2–pyrabactin structure with pyrabactin as ball model in the PYL2 pocket shown as mesh. The gate and latch are shown in green and magenta respectively. **b)** Schematic representation of the interactions between pyrabactin and PYL2 binding pocket residues. Charged interactions and hydrogen bonds are indicated by arrows, hydrophobic interactions by solid lines with hydrogen bond donors in blue and acceptors in red. The position of pyrabactin relative to the open gate is indicated. **c)** 2 F_0–F_c electron density map of bound pyrabactin and its surrounding residues contoured at 1.0 σ. **d)** Overlay of pyrabactin in the PYL2 antagonist (brown/ pale brown) and PYL1 agonist (green/ pale cyan) structures.

3.6.3 I137V converts PYL1 to a pyrabactin-inhibited receptor

To further understand the molecular features determining the selective receptor activation, receptor amino acid sequences were analyzed to identify residues responsible for the differential responses towards pyrabactin. It was observed that the V114 pocket residue in PYL2 corresponded to an isoleucine residue, I137 in PYL1. An overlay of the pyrabactin-bound pockets of these receptors suggested that PYL1 I137 clashes with pyrabactin in the antagonist structure, forcing the pyrabactin to flip into the agonist configuration (Figure 35a). Thus we predicted that mutation of PYL1 I137V would allow pyrabactin to adopt the antagonist conformation.

To test this, the I137V mutation was introduced into PYL1 habouring a A190V or V193I mutation. This is because pyrabactin is a weak agonist in wild type PYL1, while single A190V or V193I mutations in the receptor greatly enhanced pyrabactin activity (Figure 35b). Indeed, introduction of I137V into either PYL1 A190V or PYL1 V193I converted the pyrabactin-activated receptor into pyrabactin-antagonized receptor, as demonstrated by the concentration-dependent pyrabactin inhibition of ABA-activated mutant PYL1 receptors (Figure 35c–f).

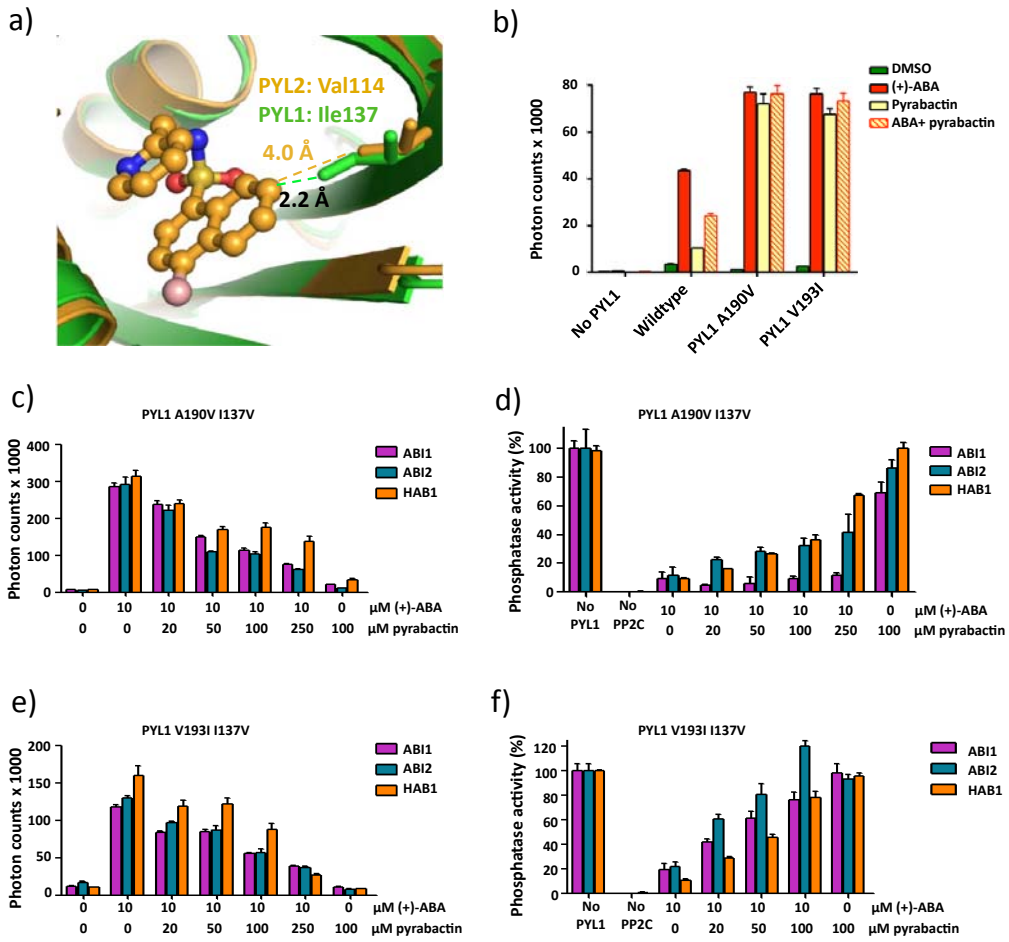

Figure 35. I137V converts PYL1 into a pyrabactin-inhibited receptor.

a) PYL1 I137 clashes with the pyrabactin antagonist structure. Overlay of pyrabactin in the PYL2 ligand binding pocket (brown) with the PYL1 ligand binding pocket (green). I137 and the corresponding residue in PYL2, V114, are represented as stick models. Their distances to pyrabactin in the PYL2 antagonist structure are indicated. **b**) PYL1 A190V and V193I mutations increase the pyrabactin-mediated PYL1–ABI2 interaction. AlphaScreen interaction in the presence or absence of 10 µM (+)-ABA, 100 µM pyrabactin, or 5 µM (+)-ABA + 100 µM pyrabactin (n=3, error bars=SD). (**c,e**) Pyrabactin inhibits the ABA-stimulated interaction between PYL1 I137V and PP2Cs. Alphascreen interactions with PYL1 A190V I137V (c) or V193I I137V (e) (n=3, error bars=SD). (**d,f**) Pyrabactin relieves the ABA-stimulated inhibition of PP2C phosphatase activity by PYL1 A190V I137V (d) or V193I I137V (f). Reactions contained 200 nM recombinant PP2Cs and 600 nM PYL1 A190V I137V or V193I I137V (n=3, error bars=SD).

3.6.4 A93F converts PYL2 to a pyrabactin-activated receptor

The next key question we sought to address is why pyrabactin binding does not activate PYL2. In the structure of the pyrabactin-bound PYL2, the pyridine group of the pyrabactin is positioned at a distance of 11–13 Å from the gate loop that is too far away to make interactions to keep the gate closed (Figure 34a). Therefore, to facilitate the closure of the gate, a mutation of A93F was designed to introduce a bulky residue in the gate loop of PYL2 to bridge the distance between the gate and the pyridine ring of pyrabactin. While pyrabactin did not induce PP2C interaction and inhibition in wild type PYL2, it activated PYL2 A93F to bind and inhibit ABI1 activity (Figure 36), suggesting that the A93F mutation converted PYL2 from a pyrabactin-repressed to pyrabactin-activated receptor.

To further understand how the A93F mutation switched the pyrabactin response of PYL2, the crystal structures of pyrabactin-bound PYL2 A93F, as well as ternary complexes of PYL2 A93F–pyrabactin bound to ABI2 and HAB1 were determined at resolutions of 2.10 Å, 2.10 Å and 2.55 Å respectively. The structures of the PP2C-bound ternary complexes further provided evidence that pyrabactin acts as an agonist in PYL2 A93F. The overall structures of the ternary complexes resemble the active PYL2–ABA–HAB1 and PYL1–pyrabactin–ABI1 structures, with their gate and latch loops in closed conformation and the conserved tryptophan residues of the PP2Cs inserted in the pyrabactin-bound receptor pocket (Figure 37a,b). In these structures, the pyrabactin adopted an intermediate position between

the agonist and antagonist conformations, with both ring systems making interactions with the F93 residue to stabilize the gate in a closed conformation (Figure 37c).

In the pyrabactin–PYL2 A93F structure, the gate loop is unexpectedly in an open conformation, resembling that of the apo wild type PYL2 structure (Figure 37d). The latch however, assumes an active conformation observed in the active ternary complexes, with its H119 side chain flipped into the pocket, making contact with pyrabactin and E118 side chain flipped outside of the pocket to allow closure of the gate onto the latch upon PP2C docking (Figure 37d). In this state, pyrabactin binding poised the mutant receptor to be activated upon PP2C binding, therefore providing the basis of pyrabactin agonism in the A93F mutant receptor.

In summary, we have shown that members of the PYL ABA receptor family can be selectively activated or inhibited by pyrabactin and elucidated the structural basis of such agonism and antagonism. In addition, we have also identified single amino acid residues as molecular determinants of the receptor response towards pyrabactin and demonstrated the ability to switch the selective responses through receptor engineering.

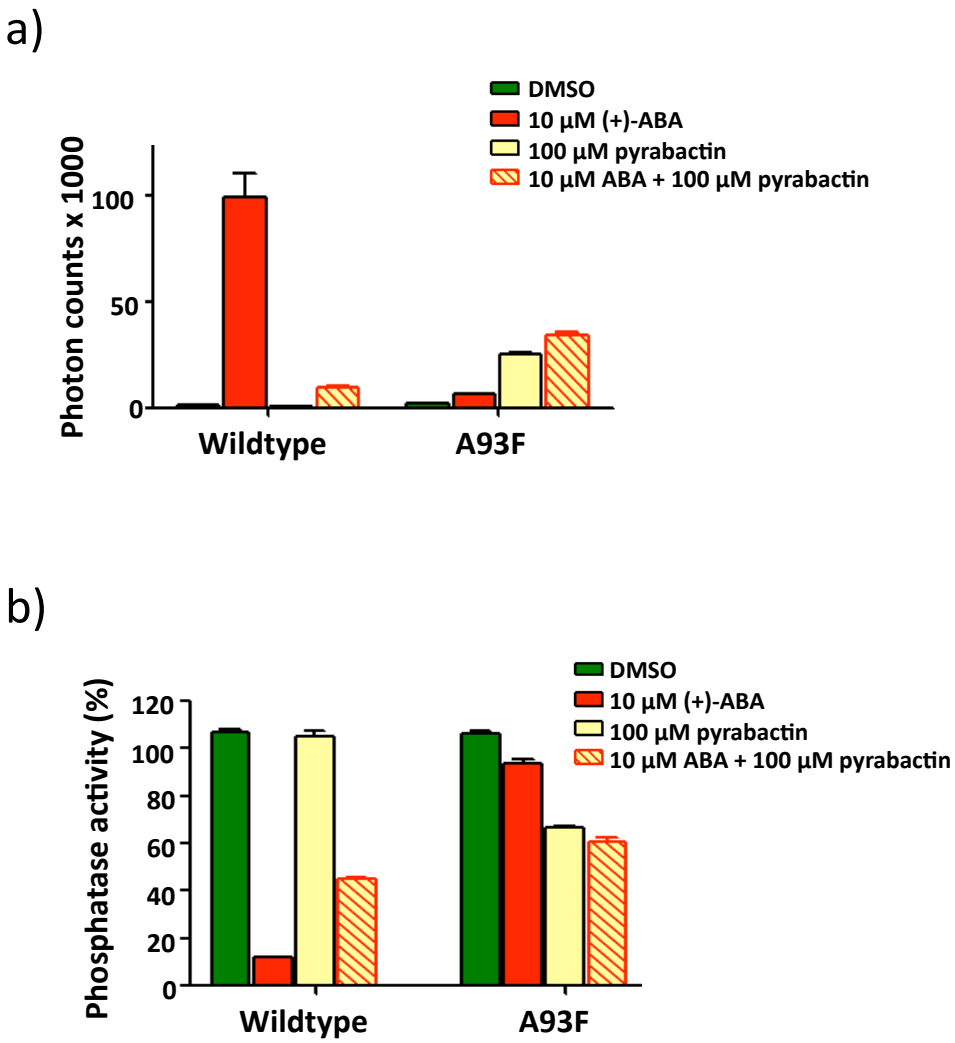

Figure 36. A93F converts PYL2 to a pyrabactin-activated receptor.

PYL2 A93F is activated by pyrabactin to bind and inhibit ABI1 as determined by **a)** AlphaScreen assay (n=3, error bars=SD) and **b)** phosphatase assay containing 200 nM ABI1 and 600 nM wild type or A93F mutant PYL2 (n=3, error bars=SD).

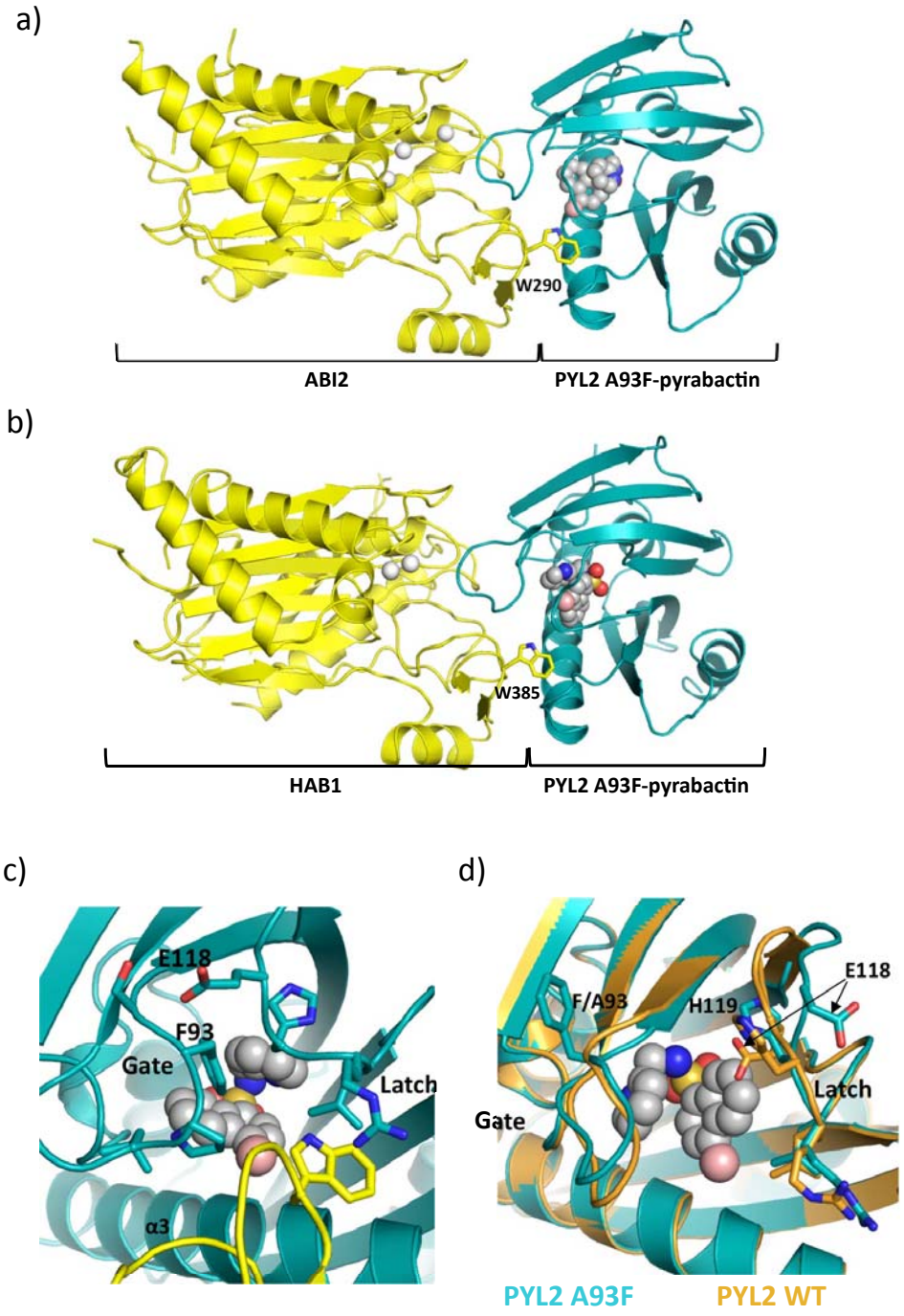

Figure 37. The PYL2 A93F–pyrabactin agonist complex structures.

Overview of the **a)** PYL2 A93F–pyrabactin–ABI2 and **b)** PYL2 A93F–pyrabactin–HAB1 structures. **c)** Close-up view of pyrabactin in the PYL2 A93F–pyrabactin–ABI2 trimeric complex. ABI2 with W290 is shown in yellow. **d)** Structure of pyrabactin in the PYL2 A93F ligand binding pocket (cyan) overlaid with the PYL2 wildtype structure (brown).

CHAPTER 4

DISCUSSION

In this study, we present crystal structures of representative PYLs in apo-forms, ABA-bound form, in complex with ABA and PP2C, as well as the structure of an apo PP2C. These structures provided evidence for the role of PYL proteins in ABA perception and signal transduction, thereby answering the long-standing uncertainty in the identity of ABA receptors. Importantly, our structural findings highlighted a gate-latch-lock mechanism of ABA binding and signalling by the PYLs and PP2Cs, validated by extensive biochemical and mutagenesis data. In this model, the ligand binding pocket of PYL is surrounded by the gate and latch loops, whereby the gate is in an open conformation in the absence of ABA occupancy (Figure 38a). ABA binding results in closure of the gate onto the latch loop, forming the complementary interface for PP2C interaction. The PYL–ABA–PP2C interaction involves docking of a conserved PP2C tryptophan residue, which further locks the receptor gate and latch in a stable, closed position (Figure 38b). The involvement of PP2C in modifying the PYL–ABA contact surface and forming a water-mediated contact with ABA suggested that PP2Cs can function as co-receptors to facilitate the interaction of PYL proteins with ABA, and established that these proteins together are bona fide ABA receptors that transduce plant stress signals.

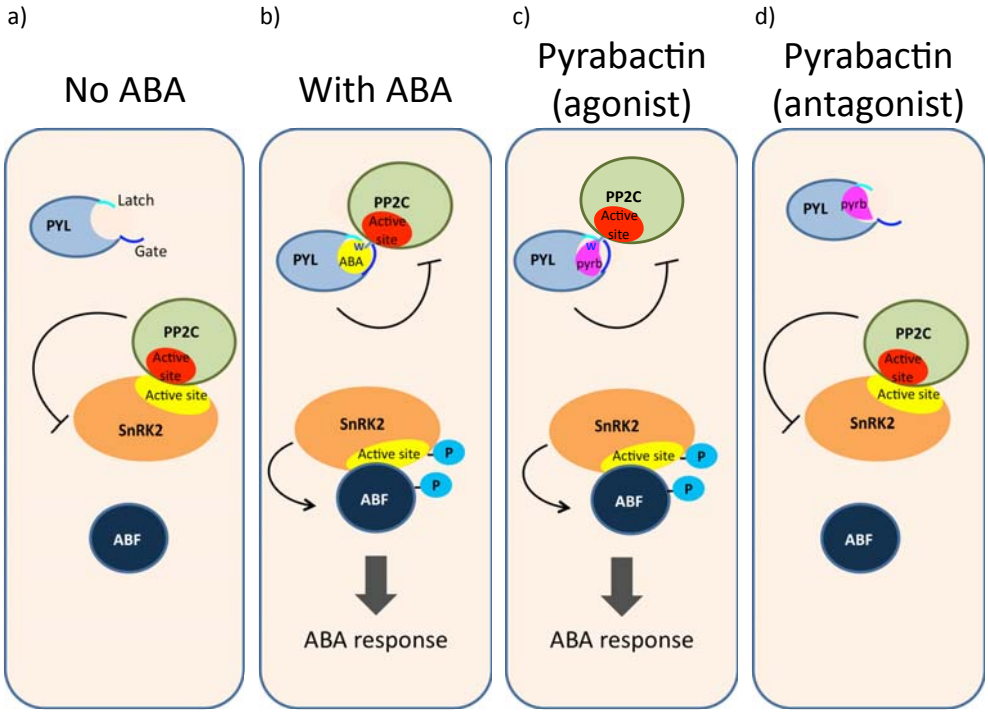

Figure 38. Cartoon summary of the gate-latch-lock mechanism of ligand perception and signal transduction by the PYL ABA receptors.

a) In the absence of ABA, the PYL gate loop is in an open conformation, hindering PP2C interaction. The active PP2C inhibits SnRK2 by dephosphorylating and blocking the kinase active site. **b)** The PYL gate is closed upon ABA binding, allowing it to inhibit PP2C by blocking the phosphatase active site. Upon PP2C binding, a conserved PP2C tryptophan residue (denoted by "W") further locks the gate and latch in a closed position, stabilizing the PYL–ABA–PP2C complex interaction. This releases the SnRK2 from PP2C inhibition, allowing it to achieve full kinase activity by autophosphorylation. The active SnRK2 relays the ABA signal by phosphorylation of downstream effectors, such as the ABF transcription factor. **c)** In the agonist conformation, pyrabactin (pyrb) mimics ABA in its interaction with the receptor pocket, inducing closure of the PYL gate to promote PP2C inhibition. **d)** Pyrabactin acts as an antagonist in certain PYL members, where it occupies the receptor pocket in an orientation that does not induce closure of the PYL gate, thus hindering PP2C interaction.

Our analyses have been further supported by *in vitro* as well as *in vivo* data provided by our collaborators, demonstrating that mutation of key residues that form the gate and latch compromised the receptor activity (Melcher et al., 2009). Functional studies of PYL2 with mutations in the gate and latch residues were performed using Arabidopsis protoplast assays, where ABA-induction of gene expression can be reconstituted by coexpression of a set of components consisting of PYL, PP2C, SnRK2, ABF2 transcription factor and an ABA-responsive promoter reporter construct (Fujii et al., 2009). Mutations in the gate, latch and ligand-binding residues of PYL2 compromised the ability of PYL2 to activate the reporter in response to ABA (Figure 39a).

In addition to the mutational studies of PYL2, functional studies of PYR1 with a mutated latch residue (H115A) were carried out. Consistent with the important role of this latch residue in the PYL2–ABA inhibition of PP2C, the PYR1 H115A protein was defective in ABA-mediated PP2C inhibition *in vitro* (Figure 39b) and was not able to interact with HAB1 in response to ABA (Figure 39c). Furthermore, *in vivo* studies showed that the PYR1 H115A failed to rescue the ABA-response defect of a quadruple *pyr1/pyl1/pyl2/pyl4* mutant in transgenic plants, while the wild type PYR1 did (Figure 39d). Together, these results provide further validation of the critical roles of the receptor gate and latch in ABA signalling.

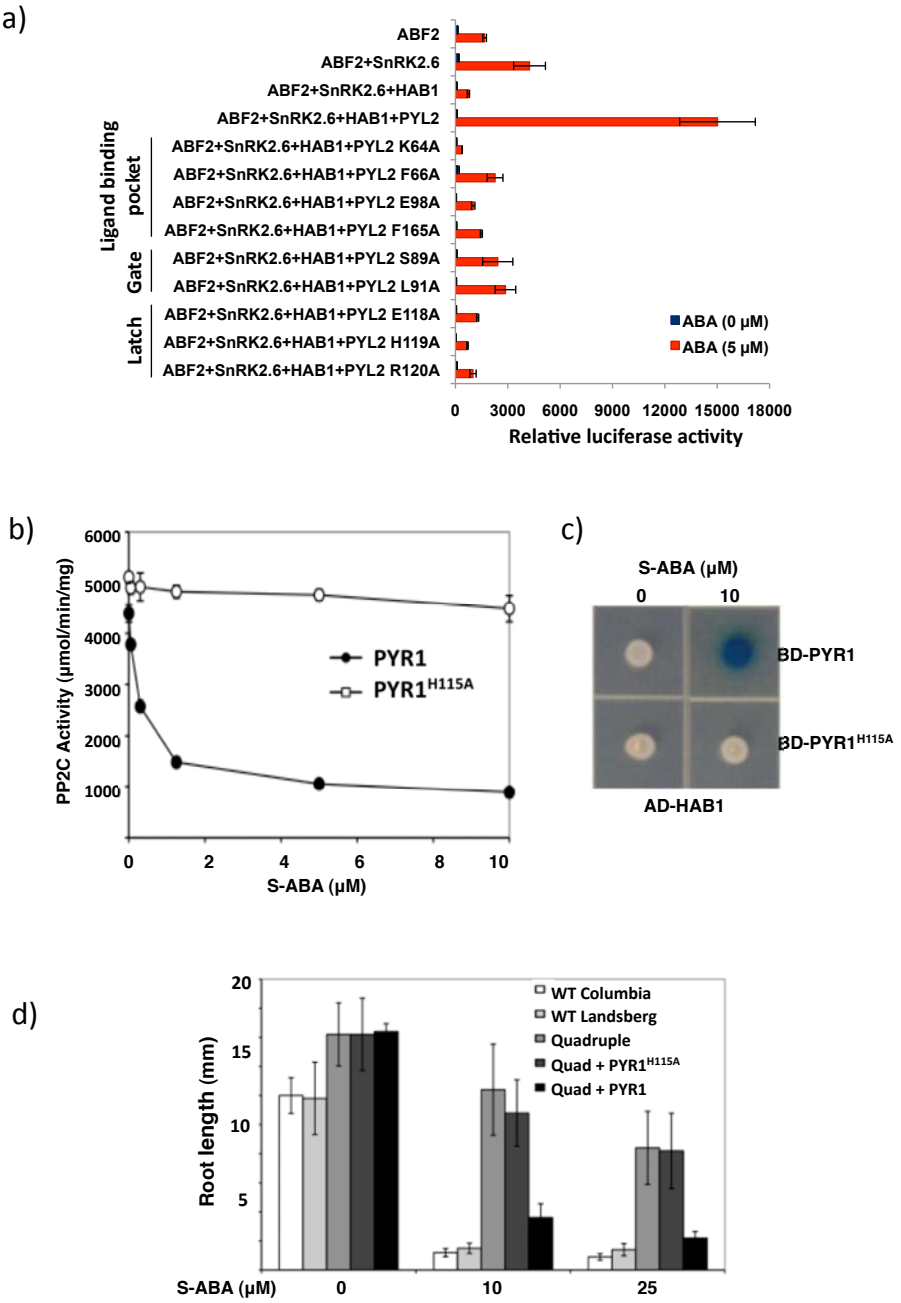

Figure 39. Mutations in the PYR1 latch and gate affect ABA signalling *in vitro* and *in vivo*.

a) Mutations in the PYL2 ligand binding pocket, gate and latch are defective in the reconstituted signalling pathway (n=3, error bars=SEM). **b)** HAB1 phosphatase activity is abolished in H115A PYR1 (n=3, error bars=SD). **c)** The H115A PYR1 mutant is defective in ABA-mediated HAB1 interaction, as shown by yeast two-hybrid assay. AD, activation domain; BD, DNA binding domain. **d)** The H115A PYR1 mutant is defective in inhibiting the root growth of transgenic plants in response to ABA. A quadruple *pyr1/pyl1/pyl2/pyl4* mutant defective in root growth inhibition can be complemented by wild type PYR1, but not by PYR1 (H115A) (n=6–10, error bars=SD). *Nature. 462:602–8* (Melcher et al., 2009)

We further elucidated the mechanistic basis of selective PYL activation and antagonism by pyrabactin. The PYL1–pyrabactin agonist structure revealed that pyrabactin mimics ABA in which its interaction with the receptor gate induces a 'closed-gate' receptor conformation that enables receptor docking into the PP2C active site (Figure 38c). In the antagonist conformation, pyrabactin occupies the ABA-binding pocket but does not interact with the gate residues, lacking the interacting energy to pull the gate into the closed position and therefore leaving the gate in the inactive open conformation (Figure 38d). Here, we provide evidence for the phenomenon of ABA receptor antagonism and its underlying mechanism through combinatorial approaches of structural, biochemical and mutagenesis studies.

Our results are coherent with a series of crystallographic studies of PYLs published in the same period. Collectively, the identification of PYLs as ABA receptors and the following structural studies of the molecular mechanisms of ABA perception and signal transduction by the PYLs has greatly advanced our understanding of hormonal regulation of plant growth and development and as such, has been nominated by *Science Signaling* as one of the signalling breakthroughs of the year 2009 (Adler, 2010). In the following sections, critical aspects of the core ABA signalling pathway provided by our data together with other relevant studies and their potential implications in agriculture as well as human health and diseases will be discussed.

4.1 Collective structural studies of the PYL ABA receptors

In late 2009, five crystallographic studies providing evidence and mechanism of the PYL proteins as ABA receptors (Melcher et al., 2009; Miyazono et al., 2009; Nishimura et al., 2009; Santiago et al., 2009a; Yin et al., 2009), including the study presented in this thesis (Melcher et al., 2009), were published in the same period (listed in Table 5). Collectively, these five groups derived crystal structures for PYR1, PYL1 and PYL2, all exhibiting the helix-grip structure characteristic for START domain/ Bet v 1-fold proteins, in which a seven-stranded anti-parallel β-sheet is surrounded by a long C-terminal α-helix and few smaller α-helices. A large ligand-binding pocket forms between the C-terminal helix and β-sheet and is guarded by two functionally important β-loops that we have named the 'gate' and 'latch' loops (alternatively named Pro-Cap and Leu-Lock (Nishimura et al., 2009), CL2 and CL3 (Yin et al., 2009), and β3–β4 and β5–β6 lid loops (Miyazono et al., 2009)) and whose amino acid sequences (SGLPA and HRL, respectively) are identical for all 14 members of the PYL family, except for PYL12 and PYL13 (Figure 40). Comparisons of the apo and ABA-bound receptor structures revealed the critical role of ABA-induced conformational changes in these two loops in transmitting the hormone binding signal to downstream effectors (Melcher et al., 2009; Nishimura et al., 2009; Santiago et al., 2009a; Yin et al., 2009). In addition to conformational changes in the gate and latch loops, Nishimura et al., 2009 has also identified a "recoil motif" (indicated in Figure 40) in PYR1 that shifts towards the C-terminal helix upon ABA binding.

In the hormone-bound pocket, ABA forms a network of interactions with

conserved residues of PYR1, PYL1 and PYL2 (consolidated and listed in Table 6). Notably, single point mutation of the key lysine residue (K59Q in PYR1, K64A in PYL2), which anchors the carboxylate group of ABA to the deep end of the pocket opposite the entrance, impaired the receptor's ability in ABA binding, PP2C interaction and PP2C inhibition (Melcher et al., 2009; Nishimura et al., 2009; Yin et al., 2009).

Crystal structures of the PYL2–ABA–HAB1 complex in our study (Melcher et al., 2009) and PYL1–ABA–ABI1 complexes (Miyazono et al., 2009; Yin et al., 2009) showed that the ABA-bound receptors bind to the active site of the PP2Cs, thereby inhibiting the PP2C activity by blocking substrate access to the catalytic site. PYL interact with PP2C at the gate-latch interface induced by ABA-binding. In this interface, a conserved PP2C tryptophan residue (W385 in HAB1 and W300 in ABI1) forms a water-mediated contact with ABA and interacts with the receptor gate and latch loops, further locking the loops in a closed conformation. These observations provide structural explanations for the more than 10-fold increase in PYL's ABA binding affinity in the presence of a PP2C (Ma et al., 2009; Miyazono et al., 2009; Santiago et al., 2009b; Yin et al., 2009). These structural studies also explain the previously characterized ABA-insensitive *abi1-1* and *abi2-1* mutations in which a glycine to aspartic acid change in the PP2C active site disrupts receptor-PP2C interactions (Ma et al., 2009; Park et al., 2009; Santiago et al., 2009b; Sheen, 1998). In the PYL–ABA–PP2C structures, this glycine is in close proximity with the receptor gate, and replacement of the glycine hydrogen with the bulky side chain of aspartate sterically interferes with gate

interaction (Melcher et al., 2009; Miyazono et al., 2009; Yin et al., 2009).

Table 5. Structural studies of PYLs in ABA signal transduction.

Aspect of Study	Study Number[#]	Crystal Structures		
		Apo Receptor	Ligand-bound Receptor	Receptor–ligand–PP2C complex
ABA perception and receptor activation	1	PYR1	PYR1–ABA	
	2	PYR1	PYR1–ABA	
	3		PYL1–ABA	PYL1–ABA–ABI1
	4*	PYL1	PYL2–ABA	PYL2–ABA–HAB1
		PYL2		
	5	PYL2	PYL2–ABA	PYL1–ABA–ABI1
Selective receptor activation and antagonism by pyrabactin	6		PYL1–pyr (AG)	
	7		PYL2–pyr (AT)	
	8*		PYL2–pyr (AT)	PYL1–pyr–ABI1 (AG)
			PYL2 (A93F)–pyr (AG)	PYL2 (A93F)–pyr–ABI2 (AG)
				PYL2 (A93F)–pyr–HAB1 (AG)
	9		PYR1 (P88S)–pyr (AG)	
			PYL2–pyr (AT)	
			PYL2 (V114I)–pyr (AG)	
Ligand-independent receptor activation	10	PYL10		PYL10–HAB1

Notes:

[#]Study number 1-(Nishimura et al., 2009); 2-(Santiago et al., 2009a); 3-(Miyazono et al., 2009); 4-(Melcher et al., 2009); 5-(Yin et al., 2009); 6-(Hao et al., 2010); 7-(Yuan et al., 2010); 8-(Melcher et al., 2010); 9-(Peterson et al., 2010); 10-(Hao et al., 2011).

Asterisks indicate publications that include the work presented in this thesis.

The PYL–pyr (pyrabactin) complexes representing agonist and antagonist conformations are denoted by AG and AT respectively.

Table 6. Interactions between functional groups of ABA and pyrabactin with receptor residues.

ABA-PYL interactions					
Type of interaction		Ligand group	Receptor residues		
			PYR1[1,2]	PYL1[3]	PYL2[4,5]
Polar interactions	Direct charged interaction	Carboxylate group	Lys59	Lys86	Lys64
	Water mediated H-bond	Carboxylate group	Glu94	Glu121	Glu98
			Tyr120	Tyr147	Tyr124
			Ser122	Ser149	Ser126
			Glu141	Glu171	Glu147
				Asn197	Asn173
	Water mediated H-bond	Hydroxyl group	Glu94	Glu121	Glu98
	Water mediated H-bond	Ketone group	Arg116	Arg143	Arg120
	Direct interaction	Ketone group	Ala89		Ala93
Non-polar interaction	Hydrophobic interactions or Van der Waals contact	Non-polar groups	Phe61	Phe88	Phe66
			Ser92		Ser96
			Val83	Val110	Val87
					Leu91
				Ala116	Ala93
			Phe108	Phe135	Phe112
			Ile110	Ile137	Val114
					His119
			Leu117	Leu144	Leu121
					Tyr124
			Phe159	Phe189	Phe165
					Val166
			Val163	Val193	Val169
					Val170

Pyrabactin-PYL interactions					
Type of interaction		Ligand group	Receptor residues		
			PYR1[6#]	PYL1[7]	PYL2[8,9]
Polar interactions	Direct interaction and/or Water mediated H-bond	Sulfonamide/ Pyridyl nitrogen	Lys59	Lys86	Lys64
				Arg106	Arg83
			Glu94	Glu121	Glu98
					Tyr124
					Ser126
			Glu141	Glu171	Glu147
					Asn173
Non-polar interactions	Hydrophobic interactions or Van der Waals contact	Non-polar groups		Phe88	Phe66
				Val110	Val87
				Leu114	
				Ala116	
				Phe135	Phe112
				Ile137*	Val114*
				His142	
				Tyr147	Tyr124
				Phe189	Phe165
				Ala190	Val166
				Val193	Val169
				Ile194	

Refer to notes on the following page.

Notes for Table 6:

References: 1-(Nishimura et al., 2009); 2-(Santiago et al., 2009a); 3-(Miyazono et al., 2009); 4-(Melcher et al., 2009); 5-(Yin et al., 2009); 6-(Peterson et al., 2010); 7-(Hao et al., 2010); 8-(Yuan et al., 2010); 9-(Melcher et al., 2010).

[#]In this study, only 3 key residues forming polar interactions were described, although hydrophobic interactions are also involved.

Amino acids listed in the same rows correspond to the same residue positions in PYL alignment. Asterisks indicate the residues involved in pyrabactin-selective receptor activation.

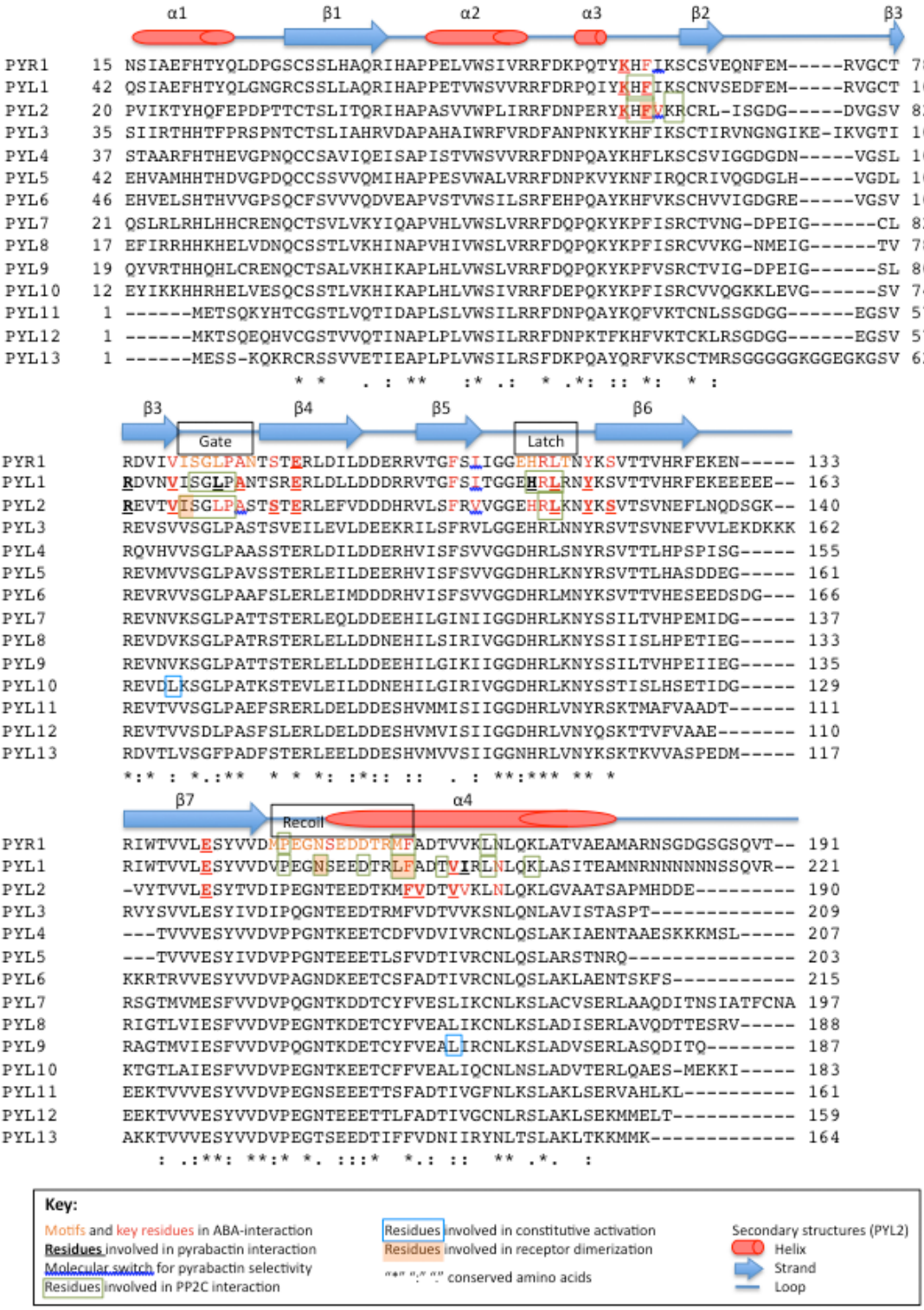

Figure 40. PYL functional motifs and residues in ABA receptor activity.

Sequence alignment of the 14 Arabidopsis PYL members, showing motifs and residues involved in different aspects of the ABA receptor activity, collectively identified in various structural studies.

4.2 Development of novel ABA receptor agonists

We have shown that pyrabactin selectively activates a subset of ABA receptors, including PYR1 and PYL1. Structures of pyrabactin-bound PYR1 and PYL1 reveal that pyrabactin interacts with receptor residues through a similar network of polar and hydrophobic interactions as ABA (Table 6) (Hao et al., 2010; Melcher et al., 2010; Peterson et al., 2010). The sulfonamide group of pyrabactin mimics the carboxylate group of ABA and forms extensive interactions with the receptor. The mechanistic knowledge of how amphipathic modules function in receptor activation provides a rational model to screen for novel PYL agonists. To demonstrate the validity of this concept, Dr Xu Yong from our research team carried out an *in silico* approach to screen chemical libraries for molecules containing the naphthalene-1-sulfonamide group and computationally docked these compounds into the PYL1 ligand binding pocket (Melcher et al., 2010). Of the top docking matches, at least 4 compounds efficiently activated PYR1 in *in vitro* assays with efficacies and EC_{50} values similar to that of pyrabactin (Figure 41). The success of this exercise provides proof of concept for future screening and design of potent ABA receptor ligands for understanding of ABA biology as well as for agriculture applications.

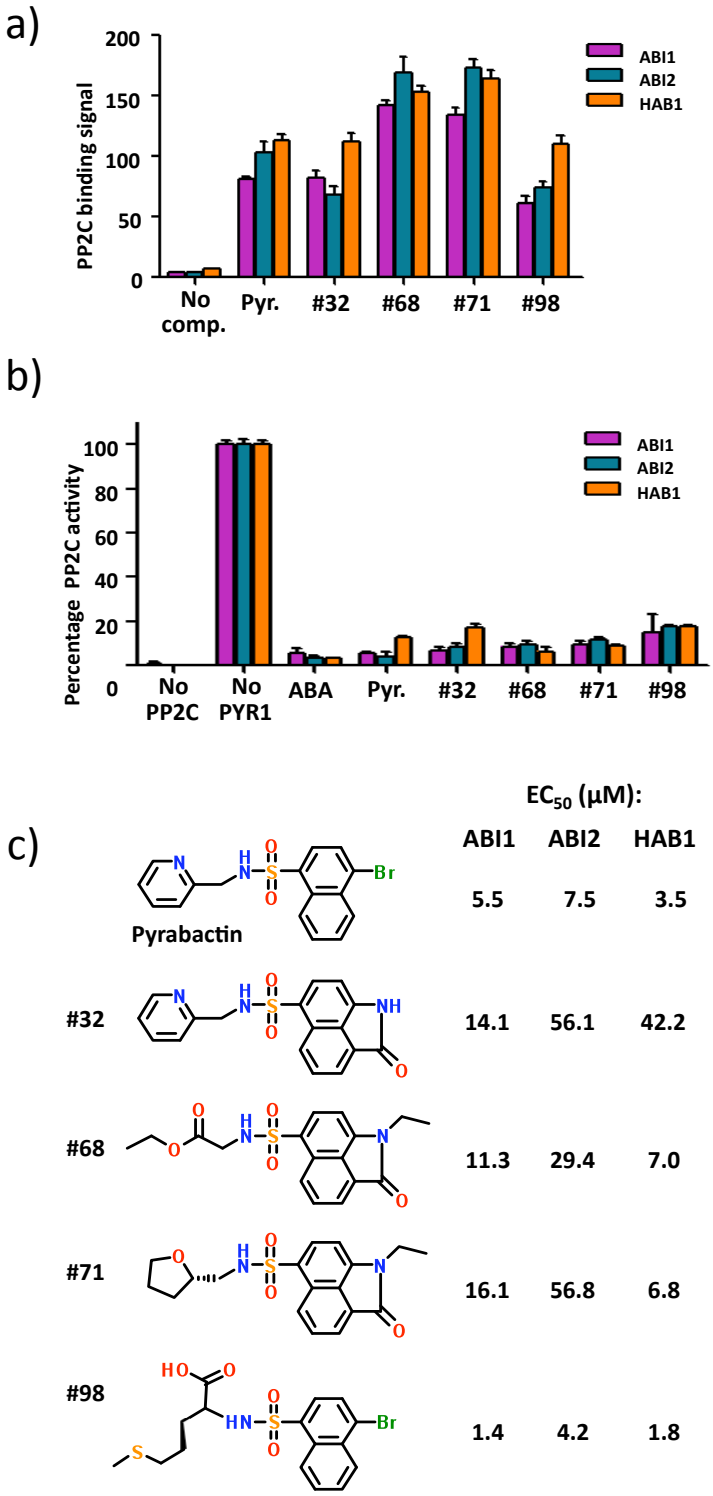

Figure 41. Identification of novel ABA receptor agonists.

Compounds identified in computational screening induce PYR1-PP2C interaction as determined by AlphaScreen assay **(a)** and mediate PYR1 inhibition of PP2Cs **(b)** with EC_{50} values as indicated **(c)**. *Nature structural & molecular biology. 17:1102-1108* (Melcher et al., 2010).

4.3 Identification of ABA receptor antagonism

To understand how pyrabactin selectively antagonizes PYL2 activity, our group and two other groups have independently solved the structures of pyrabactin-bound PYL2 (Melcher et al., 2010; Peterson et al., 2010; Yuan et al., 2010). In all three studies, the gate loop of pyrabactin-bound PYL2 was found to be in the open conformation, in contrast to the closed, active conformation in PYL1–pyrabactin structure, consistent with the notion that gate closure is critical for PYL activation. The orientation of pyrabactin in PYL2 was also rotated relative to that in the agonist structures. However, the extent of pyrabactin rotation in the PYL2–pyrabactin structures varied in the different studies, suggesting that pyrabactin can adopt several unproductive orientations in PYL2. The ability of pyrabactin to antagonize PYL2 raises the possibility that physiological antagonists exist. It has been estimated that the endogenous concentration of ABA in unstressed conditions is 0.7–1.5 fg per guard cell pair (0.7–1.5 μM) (Harris et al., 1988; McCourt and Creelman, 2008; Zhang et al., 2001), a concentration range that is sufficient to bind and activate several different recombinant PYL–PP2C complexes (Ma et al., 2009; Melcher et al., 2009; Park et al., 2009; Santiago et al., 2009b). Moreover, several subtypes of PYLs show ABA-independent interactions with PP2Cs (Hao et al., 2011; Santiago et al., 2009b), but yet the ABA response is kept silenced in unstressed plants. Altogether, these observations lead to the intriguing hypothesis that physiological antagonists exist to inhibit the basal activity of ABA receptors. Thus, the identification of endogenous ABA receptor antagonists will be an exciting avenue for future research.

4.4 Ligand-independent receptor activation

While some members of the PYL family, such as PYR1 and PYL1–PYL4, only interact with PP2Cs in the presence of ABA (Park et al., 2009), other members, including PYL5, PYL6 and PYL8 have been shown in yeast two-hybrid assays to be able to interact with PP2Cs in the absence or presence of exogenous ABA (Santiago et al., 2009b). In agreement with these observations, we were able to detect and isolate the PYL5–HAB1 complex by size exclusion chromatography of a mixture of the individual recombinant proteins without exogenous ABA (Figure 42a,b). To study the mechanism of ABA-independent PYL activation, we crystallized PYL5 in apo form and in ligand-free complex with HAB1 (Figure 42c). However, these crystals diffracted poorly (3.5 Å and 6 Å respectively), which hindered further analysis. The ABA-independent mechanism was later published by another group based on the ligand-free PYL10–HAB1 structure (Hao et al., 2011). This study reported that PYL5–PYL10 (except the untested PYL7) were able to inhibit PP2Cs to some extent in the absence of any ligands. To determine whether receptor monomerization is associated with its constitutive activity, the oligomeric state of each PYL was characterized using static light scattering and analytical ultracentrifugation analyses. It was found that while the ABA-dependent PYR1, PYL1 and PYL2 exist as dimers, PYL4–PYL10 are monomers in solutions. The PYL2 I88K mutant at the dimerization interface eluted as monomer in size exclusion chromatography and exhibited an increased constitutive activity compared to the wild type receptor, suggesting that monomeric state contributes to constitutive receptor activity. Analyses of

the ligand-free PYL10–HAB1 complex structure and amino acid sequence alignment suggested that bulky hydrophobic residues near the opening of the ligand binding pocket facilitate ligand-independent gate closure to allow formation of the active, closed conformation. A second mutation, V87L, which introduces a bulkier residue at the pocket opening in the PYL2 I88K mutant, further increases its constitutive activity, suggesting that both receptor monomeric state and the facilitated gate closing are involved in ligand-independent activation of PYL.

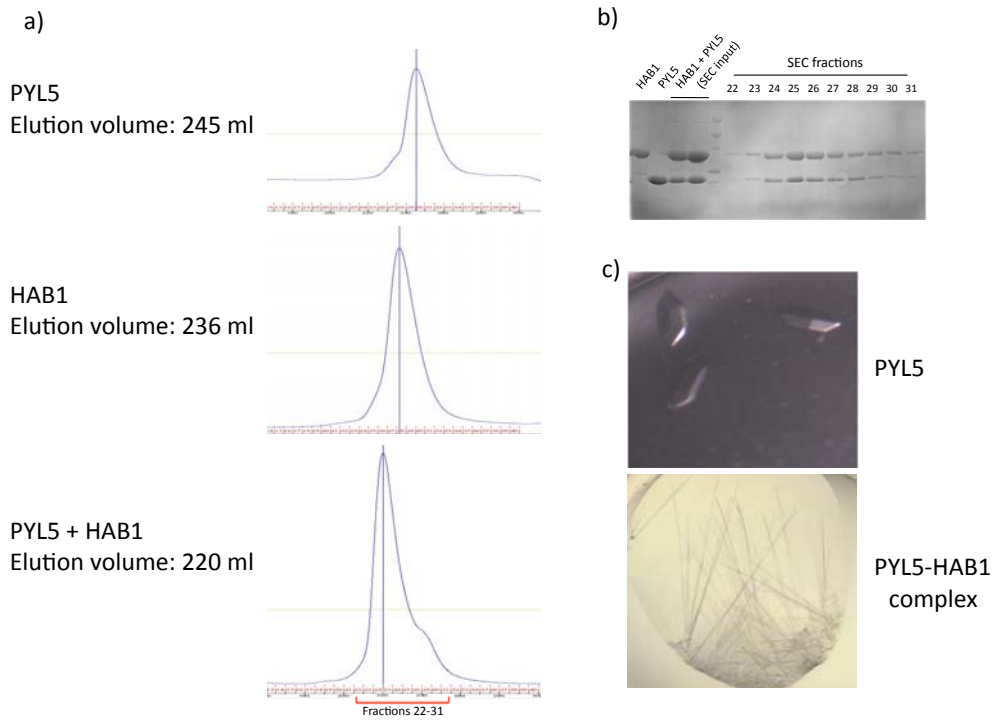

Figure 42. ABA-independent PYL5–HAB1 interaction.

a) Size exclusion chromatography (SEC) profiles of PYL5 and HAB1 as individual proteins as well as a mixture of both proteins, in the absence of ABA. The lower peak elution volume observed in the PYL5–HAB1 mixture compared to that of each individual protein suggests complex formation between the two proteins. **b)** SDS-PAGE analysis of SEC of the PYL5 and HAB1 mixture, confirming the presence of both PYL5 and HAB1 proteins in the peak elute fractions. **c)** Crystals of the apo PYL5 and PYL5–HAB1 complex.

4.5 Agricultural applications

Although the 14 members in the PYL family share a high degree of sequence similarity, different ligand responses have been shown by the different PYLs, suggesting that functional differences exist between PYL members. Since the first reports of the identification of PYLs, several structural studies quickly followed that collectively identified the molecular determinants and mechanisms of the various aspects of PYL activity (consolidated in Figure 40). These studies pave the way for future possibilities to achieve specific molecular control of abiotic stress tolerance responses through targeting at specific PYL activity.

In the view of the rising problems of fresh water shortage and climatic changes, approaches to improve environmental stress tolerance in crops will have valuable impacts on agriculture, which will in turn benefit the livelihood of millions of people especially in developing countries. The direct application of ABA to plants in the fields has been used to improve drought stress tolerance (Hawkins et al., 1987). However, the feasibility of this method is limited by the high production cost and instability of ABA. Pyrabactin, on the other hand, shows greatest effects in seeds as it selectively activates a subset of ABA receptors that are highly expressed in seeds (Park et al., 2009), thus limiting its use in controlling stress tolerance in the field, where effects on vegetative tissues are more relevant. A pressing need is therefore to identify ABA agonists with broad range receptor activity.

To address this, we suggest a combinatorial approach for future development

of ABA agonists that applies our molecular knowledge of ABA receptors in agricultural improvement. In this approach, potential agonists will be identified by computational screens of chemical libraries and tested in *in vitro* assays for their agonist efficacy. Chemical modifications of promising candidates will be performed based on the known ABA/pyrabactin-receptor interactions to improve agonist efficacy. On the other hand, a structure-guided approach will be used to design mutations in the PYL ABA receptor to complement the activity of each candidate agonist for improved efficacy. Transgenic Arabidopsis lines expressing the PYL mutations will be generated and tested with the respective agonist for drought tolerance. With its feasibility demonstrated in Arabidopsis, this orthogonal ligand-receptor approach can subsequently be evaluated in crop plants such as corn and rice.

Our current knowledge of the molecular mechanisms of ABA signalling has been primarily based on the Arabidopsis model. To translate this knowledge into agricultural applications, efforts have been made to evaluate the relevance of the Arabidopsis model of ABA signal transduction in commercial crop plants.

Homologues of the Arabidopsis PYLs, PP2Cs and SnRK2s have been identified in various crop plants. For instance, in the tomato (*Solanum lycopersicum*) genome, eight *SlPYL*, seven *SlPP2C* and eight *SlSnRK2* have been isolated and transcriptional characterization suggested their functional roles in fruit development and dehydration tolerance (Sun et al., 2011). Similarly, in the sweet orange (*Citrus sinesis*) genome, six *CsPYL*, five

CsPP2C and two *CsSnRK2* were identified and transcriptional analysis suggested the involvement of these genes in fruit ripening and water stress (Romero et al., 2012). The grape (*Vitis vinifera*) ABA signalling cascade consists of at least seven ABA receptors (*VvRCAR*) and six PP2Cs (*VvPP2C*), forming twenty-two combinations of receptor-PP2C interactions shown by yeast two-hybrid screens (Boneh et al., 2012). A rice (*Oryza sativa*) ABA signalling unit consisting of rice orthologues of PYL, PP2C, SnRK2 and OREB1, an ABRE-binding transcription factor, has been identified by interaction assays and reconstituted in transient gene expression assay (Kim et al., 2012). These findings suggest that the core ABA signal transduction pathway could be highly conserved across plant species. However, further studies will be necessary to characterize the unique properties of these core components, such as redundancy, in commercial crop species in order to translate the Arabidopsis-based knowledge into diverse agriculture applications.

4.6 Elucidating the complete core ABA signalling pathway

The data presented in this thesis has contributed to the mechanistic understanding of ABA-binding and PP2C inhibition by the PYL ABA receptors. To complete the elucidation of the core ABA signal transduction pathway, the immediate questions that follow are how SnRK2s are regulated by PP2Cs and how they are autoactivated. To address these questions, our group has further solved the crystal structures of two SnRK2s, SnRK2.3 and SnRK2.6, in an active and inactivate state respectively and that of a

PP2C–SnRK2 complex. However, presentation of the full data is beyond the scope of this thesis. A summary of the main findings will be provided here.

4.6.1 Regulation of SnRK2 by PP2C

Our crystal structure of the HAB1–SnRK2.6 complex reveals striking similarity in PP2C recognition by SnRK2 and PYL (Soon et al., 2012). ABA-induced PP2C inhibition leads to SnRK2 activation by autophosphorylation of the kinase activation loop (Belin et al., 2006; Boudsocq et al., 2007). In the HAB1–SnRK2.6 complex structure, this kinase activation loop docks into the active site of the PP2C while the conserved ABA-sensing tryptophan of the PP2C docks into the kinase catalytic cleft (Figure 43a), resembling the PYL–ABA–PP2C interaction (Figure 43b). In addition to steric inhibition by blocking the kinase active site, at sub-stoichiometric levels of PP2C, the phosphatase also inhibits SnRK2 activity by enzymatic dephosphorylation of a critical serine residue in the kinase activation loop (Soon et al., 2012). Thus, in the absence of ABA, PP2C binds to SnRK2 and inhibits the kinase activity in a two-step mechanism by dephosphorylating the activation loop serine and blocking the catalytic cleft (illustrated in Figure 43c). In the presence of ABA, the PYL–ABA complex binds to and inhibits PP2C by physically blocking the PP2C active site. This releases the PP2C from inhibiting SnRK2, allowing activation of the kinase by activation loop autophosphorylation.

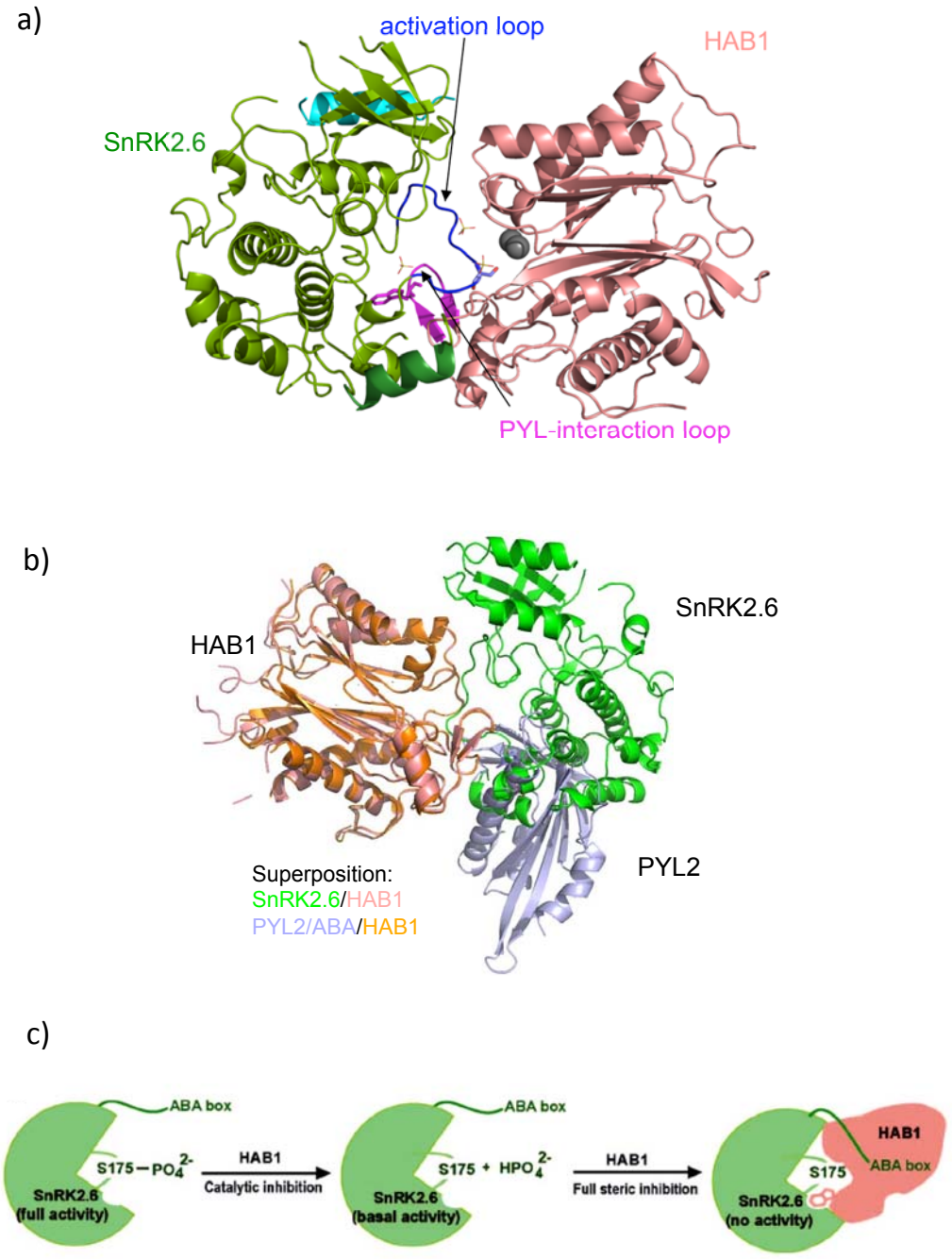

Figure 43. Mechanism of PP2C inhibition of SnRK2.

a) Structure of the SnRK2.6–HAB1 complex. SnRK2.6 is shown in green, with its activation loop in blue. HAB1 is coloured pink and its PYL-interaction loop in magenta. **b)** Overlay of the structures of SnRK2.6–HAB1 and PYL2–ABA–HAB1 complexes. **c)** Cartoon model for the two-step mechanism of the inhibition of SnRK2.6 activity by HAB1. *Science. 335:85-88* (Soon et al., 2012).

4.6.2 PP2C catalytic mechanism

The SnRK2.6–HAB1 structure (Soon et al., 2012) mimics the post-reaction state of PP2C and offers an opportunity to examine the phosphatase catalytic mechanism (Zhou et al., 2012). The SnRK2.6–HAB1 interface contains a dominant density for a sulfate group that is coordinated by two Mg^{2+} ions, resembling the leaving phosphate product of PP2C (Figure 44a).

The two Mg^{2+} ions, which are coordinated by conserved aspartic acid residues of the PP2C, bind to the phosphate group oxygens of phosphorylated S175 of the SnRK2.6, thereby increasing the partial positive charge of the phosphorus atom (Figure 44b). This facilitates a S_N2 nucleophilic attack of the phosphate by a nearby water molecule. The conserved glutamate E203 partly deprotonizes the water molecule and increases its nucleophilicity for attacking the phosphorus atom. The conserved arginine R199 from the PP2C then binds to the leaving phosphate group by charge interaction and promotes the release of this group from the substrate molecule, SnRK2.6.

4.6.3 Mechanism of SnRK2 autoactivation

We then further pursued the mechanism of SnRK2 autoactivation upon relieve of its inhibition by PP2C. Our biochemical analyses show that while autophosphorylation of the activation loop serine is required for full kinase activation, SnRK2s with the serine mutated to alanine retains basal kinase activity (Ng et al., 2011).

a)

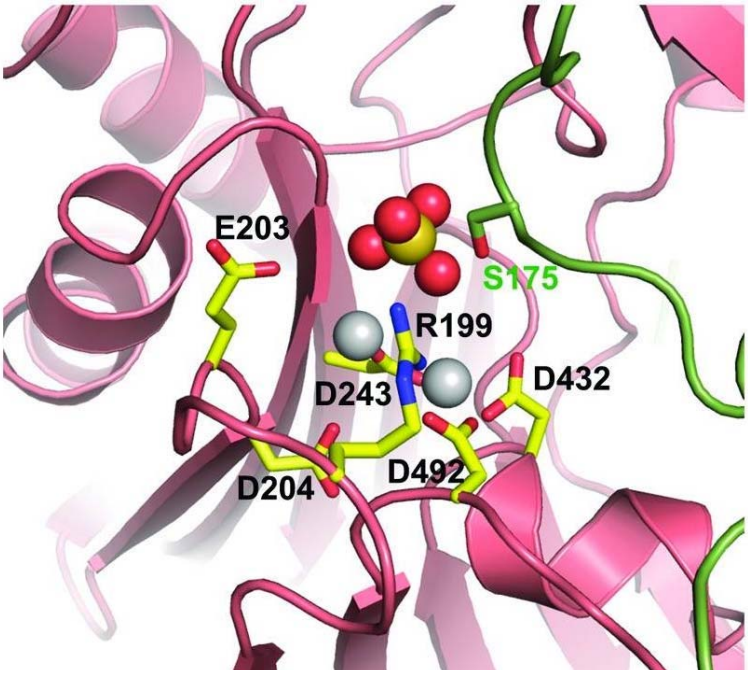

b)

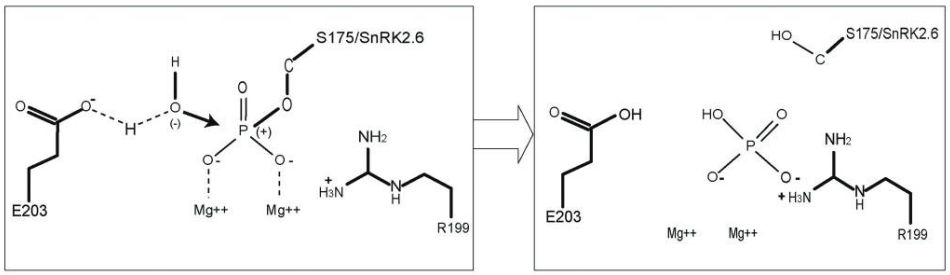

Figure 44. HAB1 catalytic mechanism

a) HAB1 catalytic site in the SnRK2.6–HAB1 structure, in which the sulfate group mimics the phosphate group cleaved from SnRK2.6 S175. This represents the functional correlate of the post-reaction status, at which the phosphate group has been transferred to HAB1 R199. Pink, HAB1; green, SnRK2.6. The sulfate ion is shown in ball presentation, the Mg^{2+}-ions as solid gray balls. **b)** Schematic presentation of the reaction mechanism. *Plant Signaling & Behavior. 7:581–588* (Zhou et al., 2012)

We solved the crystal structures of unphosphorylated SnRK2.3 and SnRK2.6, and observed that while the kinase domain of the SnRK2.3 structure adopts a closed conformation characteristic of active kinases, that of the SnRK2.6 structure adopted an open conformation that is indicative of inactive kinases (Chen et al., 2009; Kornev et al., 2006; Rabiller et al., 2010) (Figure 45). This suggests that unphosphorylated SnRK2s can adopt conformational characteristics of both inactive and active kinases, in agreement with our biochemical detection of basal kinase activities. Detailed structural and mutational analyses indicated that intramolecular interaction between two domains, the SnRK2 box and regulatory αC-helix, is important for kinase activity. Another feature we observed is that the close proximity of the activation loop serine and its adjacent threonine residue (S175 and T176 in SnRK2.6) to the catalytic center puts these residues in a favourable position for efficient phosphorylation which will lead to full kinase activation. Altogether, our data illustrate a two-step mechanism of SnRK2 autoactivation. The first step is an ABA-mediated release of SnRK2 from PP2C-inhibited state to a partially active state. The second step is by autophosphorylation of its activation loop to achieve full kinase activity, allowing it to relay the ABA signal into several distinct pathways by phosphorylation of different possible downstream effectors.

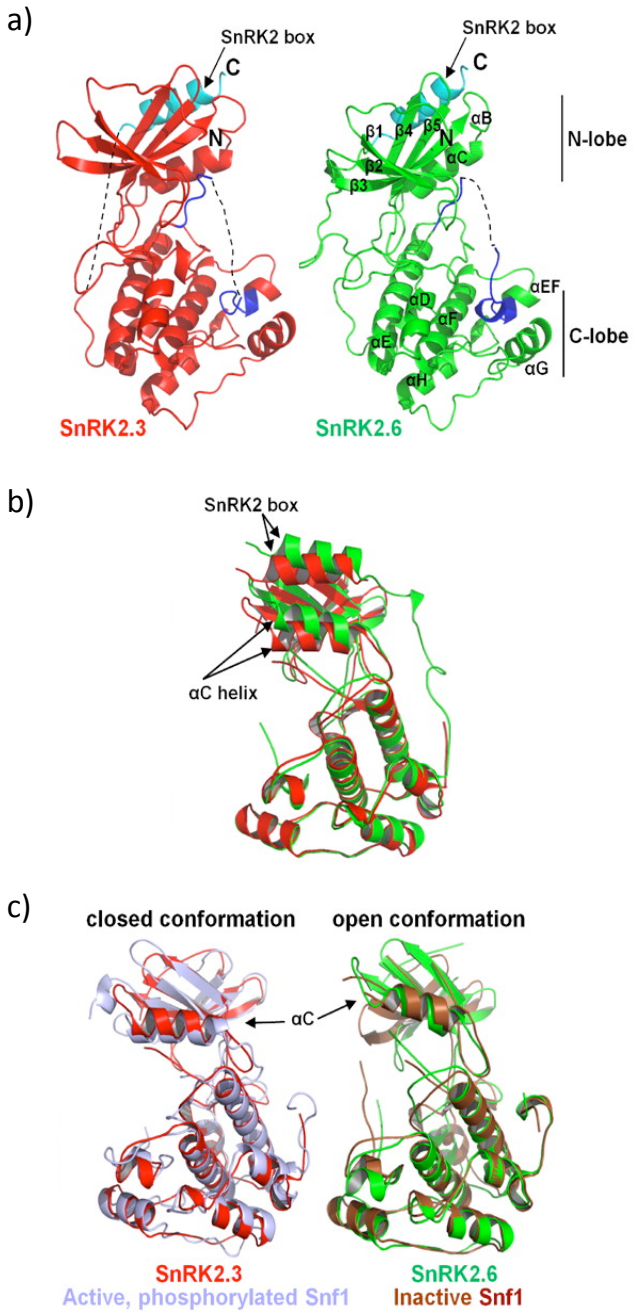

Figure 45. Structures of SnRK2.3 and SnRK2.6.

a) Overview of the SnRK2.3 (red) and SnRK2.6 (green) structures. The SnRK2 box, which is a domain required for the kinase activity, is shown in cyan and the activation loop segment is shown in blue. **b)** Overlay of the SnRK2.3 (red) and SnRK2.6 (blue) structures, showing their closed and open conformations with respect to the relative positions of their SnRK2 boxes and αC-helices. **c)** Overlays of SnRK2.3 (red) with the active Snf1 kinase domain (light blue) (PDB code 3DAE) and of SnRK2.6 (green) with the kinase domain of Snf1 in the inactive, open conformation (brown) (PDB code 2FH9). The SnRK2 boxes were omitted from the overlay for clarity. *PNAS. 108:21259-21264* (Ng et al., 2011).

4.7 Human homologues of the core ABA signalling proteins

The START domain of the PYL ABA receptors, PP2C catalytic domain and SnRK kinase domain are highly conserved through evolution and homologues exists in many species including humans. This raises an interesting speculation that the mammalian form of these proteins may interact in a mechanism similar to the ABA signal transduction pathway in Arabidopsis. In this section, we discuss the potential relevance of the structural studies of the plant PYL, PP2C and SnRK to mammalian signalling pathway through the mammalian homologues of these components.

4.7.1 START domain proteins

Though absent in yeast and Archeae, the START domain is conserved through evolution and are found in bacteria, plant, flies, nematodes and mammals (Schrick et al., 2004). In humans, there are 15 START domain-containing proteins, designated STARD1–STARD15 (Soccio and Breslow, 2003). These proteins are generally known to be involved in lipid metabolism, lipid transfer and cell signalling. The 15 members can be grouped into six subfamilies based on their sequences and ligand similarities (Alpy and Tomasetto, 2005) (Figure 46). In general terms, the subfamilies can be described as the cholesterol- and oxysterol-binding proteins (STARD1/D3 and STARD4/D5/D6 subfamilies), the phospholipid- and sphingolipid- binding proteins (STARD2/D7/D10/D11 subfamily), the Rho-GAP domain-containing proteins (STARD8/D12/D13 subfamily), the thioesterase domain-containing proteins (STARD14/D15

subfamily) and the STARD9 family consisting of a single member of unknown function. Within the cholesterol- and oxysterol-binding subfamily, the biological function of STARD1 has been well established as a regulator of cholesterol transport across mitochondrial membranes in steroidogenesis (Lavigne et al., 2010; Rone et al., 2009). The unique roles of the other members in this subfamily have not been clearly defined. The phospholipid/sphingolipid-binding proteins subfamily appear to have diverse functions from modulating liver insulin sensitivity to intermembrane ceramide transfer and tumour proliferation (Clark, 2012). Although the ligands have been identified for this subfamily, the significance of ligand binding to their functions remains unclear. Ligands for the remaining subfamilies have yet to be identified.

To evaluate the degree of homology between Arabidopsis PYL proteins and human STARD proteins, the sequences of the START domains between these two groups of proteins were compared. The START domains of PYR1, PYL1 and PYL2 shared between 3–12 % amino acid sequence identity with that of the 15 human STARD proteins (Table 7). Multiple sequence alignment reveals that the gate and latch sequences that are functionally important for ABA signal transduction in the PYLs are not conserved in the human STARD domains (Figure 47).

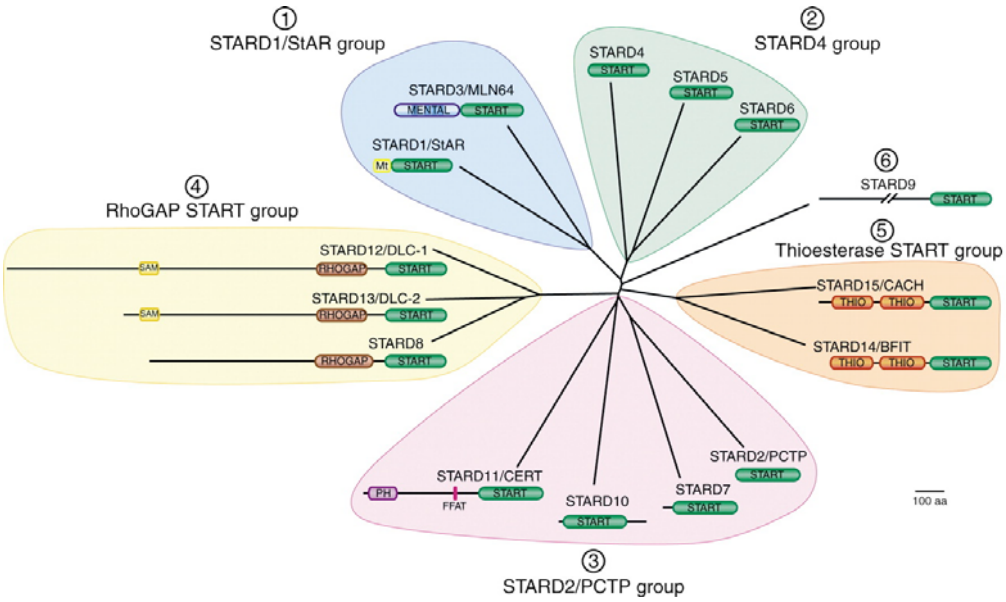

Figure 46. Phylogenetic tree and domain organizations of the 15 human START domain proteins.

Figure taken from *Journal of cell science. 118:2791-2801* (Alpy and Tomasetto, 2005). Abbreviations: Mt, mitochondrial targeting motif; MENTAL, MLN64 N-terminal domain; PH, pleckstrin homology domain; FFAT, two phenylalanines in an acidic tract motif responsible for ER targeting; RHOGAP, Rho-GTPase-activating-protein domain; SAM, sterile alpha motif; THIO, acyl-CoA thioesterase domain.

Table 7. Percent amino sequence identity between START domains of Arabidopsis PYLs and human STARD proteins.

	PYR1	PYL1	PYL2
PYR1	100	77	53
PYL1	77	100	50
PYL2	53	50	100
STARD1	8	8	6
STARD2	8	8	5
STARD3	12	11	10
STARD4	10	10	9
STARD5	7	8	7
STARD6	6	6	4
STARD7	6	7	7
STARD8	7	9	8
STARD9	9	8	12
STARD10	3	3	6
STARD11	6	8	5
STARD12	6	8	7
STARD13	7	11	7
STARD14	5	5	7
STARD15	8	5	8

Analysis was performed using STRAP software (Gille and Frommel, 2001).

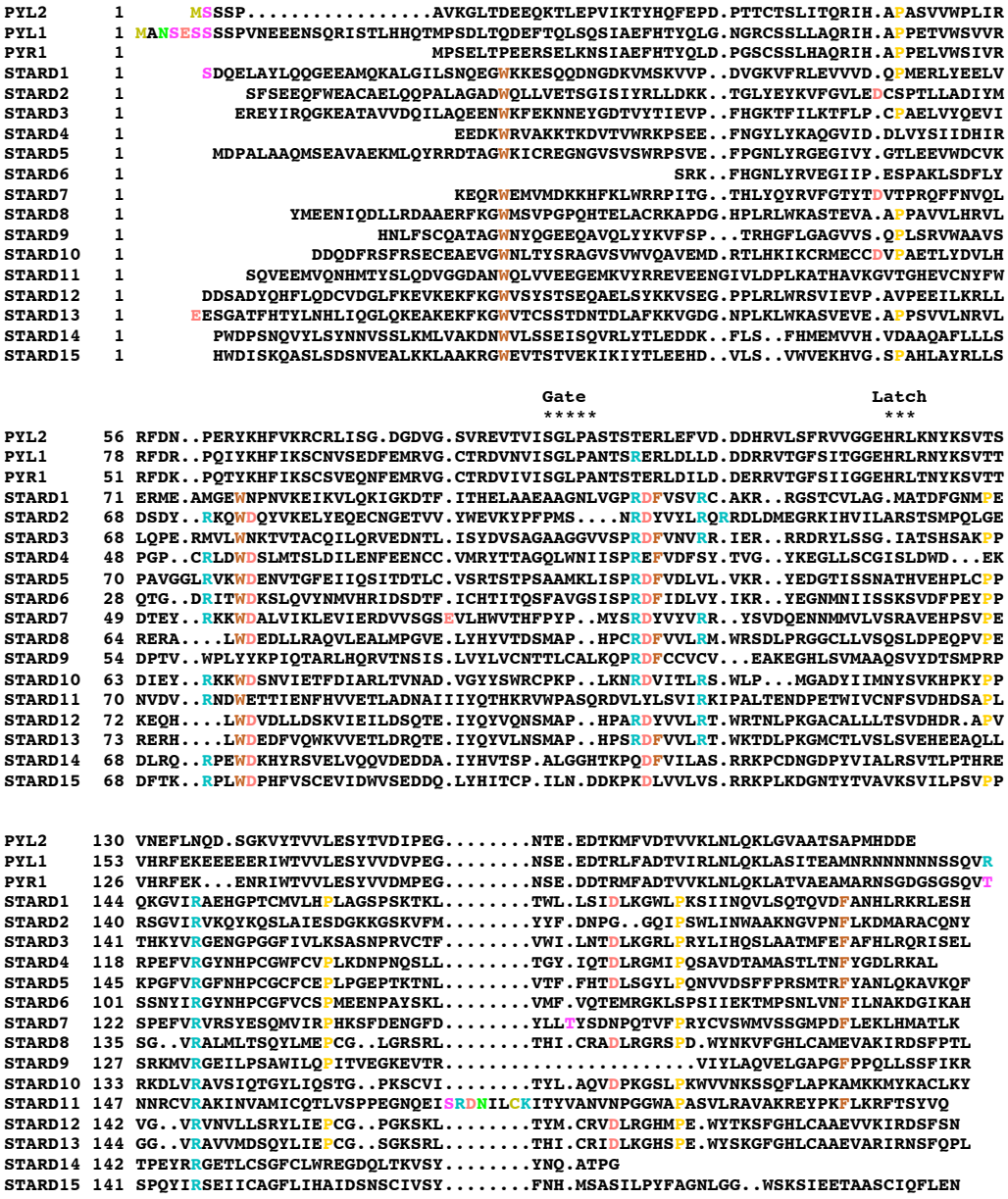

Figure 47. Multiple sequence alignment of the START domains of Arabidopsis PYL and human STARD proteins.

Sequence alignment was performed by STRAP software (Gille and Frommel, 2001). The gate and latch regions of the Arabidopsis PYLs are indicated on top of the asterisks. Conserved amino acids are coloured according to chemical property.

Crystal structures have been reported for the START domains of the human STARD1, STARD2, STARD5, STARD11, STARD13 and STARD14, representing 5 of the 6 human STARD subfamilies (Kudo et al., 2010; Kudo et al., 2008; Roderick et al., 2002; Thorsell et al., 2011). We examined the structures of these six human STARD domains and compared them to the Arabidopsis PYL2 structure. The human STARD structures exhibit the helix-grip fold as expected, with their central β-sheets and surrounding α-helices generally overlapping with that of the PYL2 structure (Figure 48). However, regions in the human STARD structures corresponding to the PYL2 gate and latch loops do not superimpose with that of the PYL2 protein, as suggested by the multiple sequence alignment. Pairwise structural comparison of each human STARD with Arabidopsis PYL2 using DaliLite (Holm and Park, 2000) gave structural alignment scores (Z-scores) of ~8−12 (Table 8), indicating a low but significant degree of homology between the two groups of proteins.

Table 8. Statistics of structural comparison between PYL2 and human STARD proteins.

	Pairwise alignment of PYL2 structure (PDB code 3KAZ) with					
	STARD1	**STARD2**	**STARD5**	**STARD11**	**STARD13**	**STARD14**
STARD PDB code	3P0L	1LN1	2R55	2E3M	2PSO	3FO5
Z score	11.4	8.7	11.8	11.1	12.6	10.6
Aligned residues	148	142	151	160	143	147
RMSD (Å)	3.1	3.6	3.3	4.1	3	3.3
% Sequence Identity	8	13	11	7	12	10

Pairwise structural alignment was performed using DaliLite (Holm and Park, 2000).

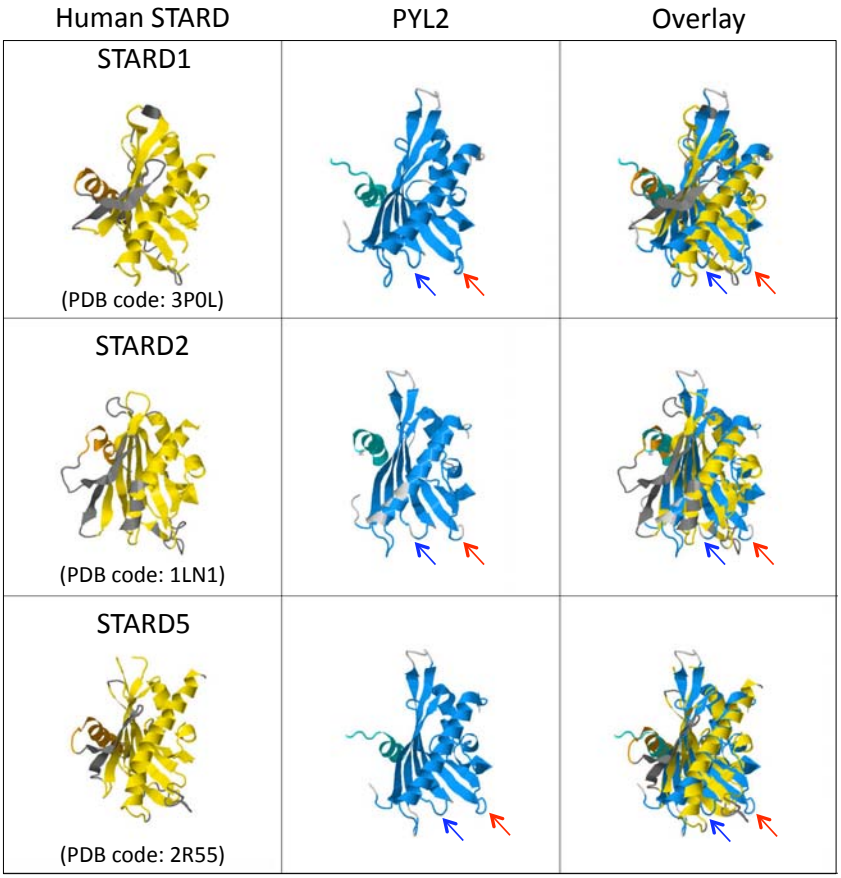

Figure 48. Continued on next page.

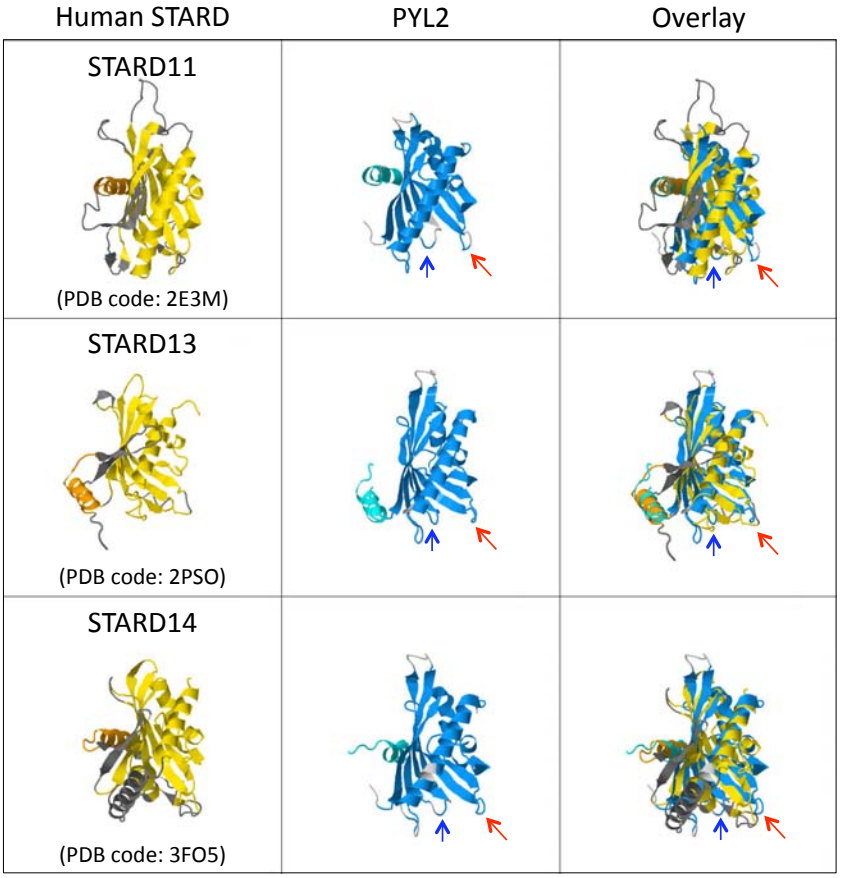

Figure 48. Structures of human STARD proteins and their overlay with Arabidopsis PYL2.

Each human STARD structure was aligned to PYL2 using FATCAT flexible structure alignment (Ye and Godzik, 2003). The gate and latch loops of PYL2 are indicated by red and blue arrows respectively.

4.7.2 Human protein phosphatases

4.7.2.1 Protein phosphatases classification

Reversible protein phosphorylation regulated by the interplay of protein kinases and phosphatases is one of the fundamental mechanisms for controlling cellular signal transduction. While protein kinases, of which more than 500 subtypes have been identified in the human genome (Kostich et al., 2002; Manning et al., 2002), has been extensively characterized, less than 100 subtypes of protein phosphatases have been identified so far (Lammers and Lavi, 2007), with limited knowledge of their regulatory mechanisms (Lu and Wang, 2008). Protein phosphatases can be divided into three broad families based on their substrate specificity and conservation of their catalytic domains (Barford et al., 1998). The protein tyrosine phosphatases (PTP) family consists of phosphatases that specifically dephosphorylate phosphotyrosine residues, as well as a subfamily known as the dual specificity phosphatases (DSP) that are also able to dephosphorylate phosphoserine and phosphothreonine residues. The two other protein phosphatase families, namely the phosphoprotein phosphatases (PPP) and the metal-dependent protein phosphatases (PPM), are only able to dephosphorylate phosphoserine and phosphothreonine residues. Members of the PPP family are further classified into three subfamilies, PP1, PP2A and PP2B, and are known to function as multimeric complexes. The PPM family is solely represented by the PP2C subfamily and its members are known to function as monomers and depend on bivalent cations (Mn^{2+} or Mg^{2+}) for their catalytic activity.

4.7.2.2 Human PP2Cs

PP2C orthologues are found in virtually all organisms ranging from bacteria, yeasts and plants to nematodes, insects and mammals (Schweighofer et al., 2004). In humans, 16 different PP2C genes have been identified so far, encoding at least 22 PP2C isozymes by alternative splicing (Lammers and Lavi, 2007). These members are predominantly implicated in the regulation of cell growth and cellular stress signalling. The most well characterized member of the human PP2C is PP2Cα (PPM1A). A few years after its first identification in 1992 (Mann et al., 1992), the crystal structure of PP2Cα has been solved, revealing a novel PP2C catalytic domain fold that is composed of a central β-sandwich surrounded by α-helices (Das et al., 1996). As the other PP2C members, PP2Cα has been implicated in the regulation of important cellular metabolic, cell cycle and stress signalling pathways (Lammers and Lavi, 2007; Lu and Wang, 2008).

The catalytic domains of human PP2Cs share about 16–36 % sequence identity with that of the Arabidopsis PP2Cs ABI1, ABI2 and HAB1 (Table 9), indicating a high degree of conservation across species. A number of conserved amino acids are seen in a multiple sequence alignment of these PP2C sequences (Figure 49). Comparison of our ABI2 structure with the PP2C domains of three known human PP2C structures, PPM1A, PPM1B and PPM1K, suggested that Arabidopsis and human PP2Cs are highly homologous, as indicated by the statistics of structural alignment (Z-scores >

30, RMSD < 2 Å) (Table 10). The PP2C domains of the Arabidopsis ABI2 and human PP2Cs exhibit the common PP2C-fold that are superimposable (Figure 50), although the conserved tryptophan residue in Arabidopsis PP2Cs that interacts with PYL–ABA is not seen in the corresponding regions in the human PP2Cs (Figure 49 and Figure 50).

While a number of potential human PP2C targets have been reported, which includes AMP-activated protein kinase (AMPK), mitogen-activated protein kinases (MAPKs), cyclin-dependent protein kinases (CDKs) and Bcl-2/Bcl-xL-associated death promoter (BAD) (Lammers and Lavi, 2007), little is known about how the PP2Cs are regulated (Lu and Wang, 2008). Given the high degree of homology between human and plant PP2Cs, we speculated that human PP2Cs could be regulated by START domain proteins in a mechanism similar to the ABA signal transduction pathway. To test this, we obtained cDNA of the START domains of all 15 human STARD genes by DNA synthesis and screened them against the catalytic domains of 5 selected human PP2Cs (PP2Cα, PPM1F, PPM1E, PPM1L and PPM1G) in mammalian two-hybrid assays for any interactions. In this preliminary test, no significant interaction signals were detected between any STARD/PP2C pair (data not shown). It is possible that such regulatory mechanism does not exist in mammalian cells, or that the activating ligands are absent in the experimental conditions tested. Thus, for a more exhaustive evaluation, every possible STARD/PP2C combination could be tested in future high throughput screens with ligand libraries, such as lipid libraries.

Table 9. Percent amino sequence identity between Arabidopsis and human PP2C domains.

		ABI1	ABI2	HAB1
Arabidopsis PP2Cs	**ABI1**	100	87	63
	ABI2	87	100	63
	HAB1	63	63	100
Human PP2Cs	**PPM1A**	35	37	34
	PPM1B	34	34	34
	PPM1G	31	30	32
	PPM1D	28	28	28
	PPM1L	35	34	35
	PPM1J	24	23	22
	PPM1M	28	29	30
	PPM1K	34	34	33
	PPM1F	33	34	30
	PPM1E	33	32	31
	ILKAP	31	30	29
	PHLPP	29	28	25
	PPM1H	30	31	30
	PPTC7	18	18	17
	PDP1	24	23	25
	PDP2	26	26	23

Analysis was performed using STRAP software (Gille and Frommel, 2001).

Table 10. Statistics of structural comparison between Arabidopsis and human PP2C domains.

	Pairwise alignment of Arabidopsis ABI2 structure (PDB code 3UJK) with human PP2Cs		
Human PP2C	**PPM1A**	**PPM1B**	**PPM1K**
PDB code	1A6Q	2P8E	2IQ1
Z score	34	33.5	34.9
Aligned residues	260	252	247
RMSD (Å)	1.8	1.7	1.5
% Sequence Identity	38	38	35

Pairwise structural alignment was performed using DaliLite (Holm and Park, 2000).

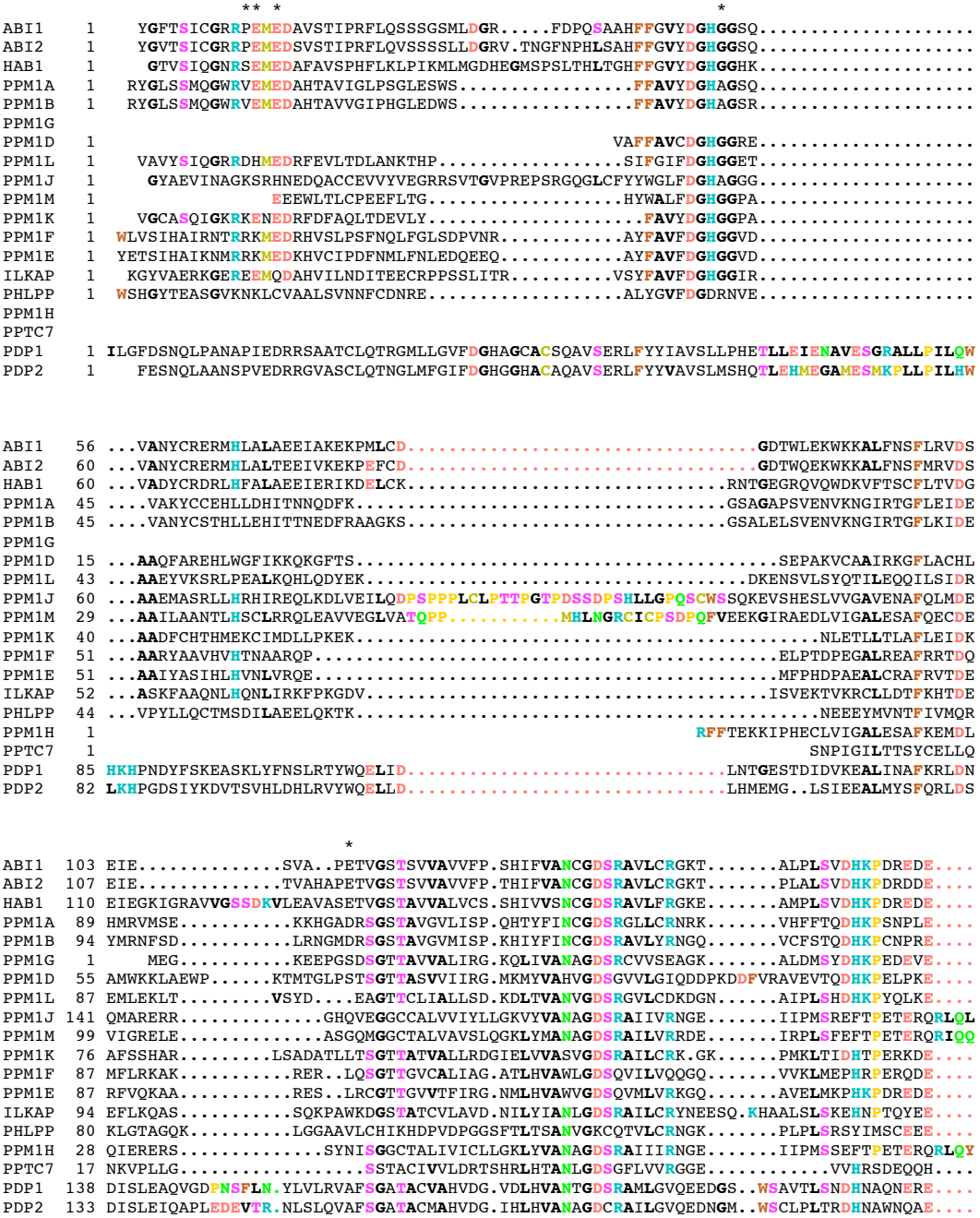

Figure 49. Continued on next page.

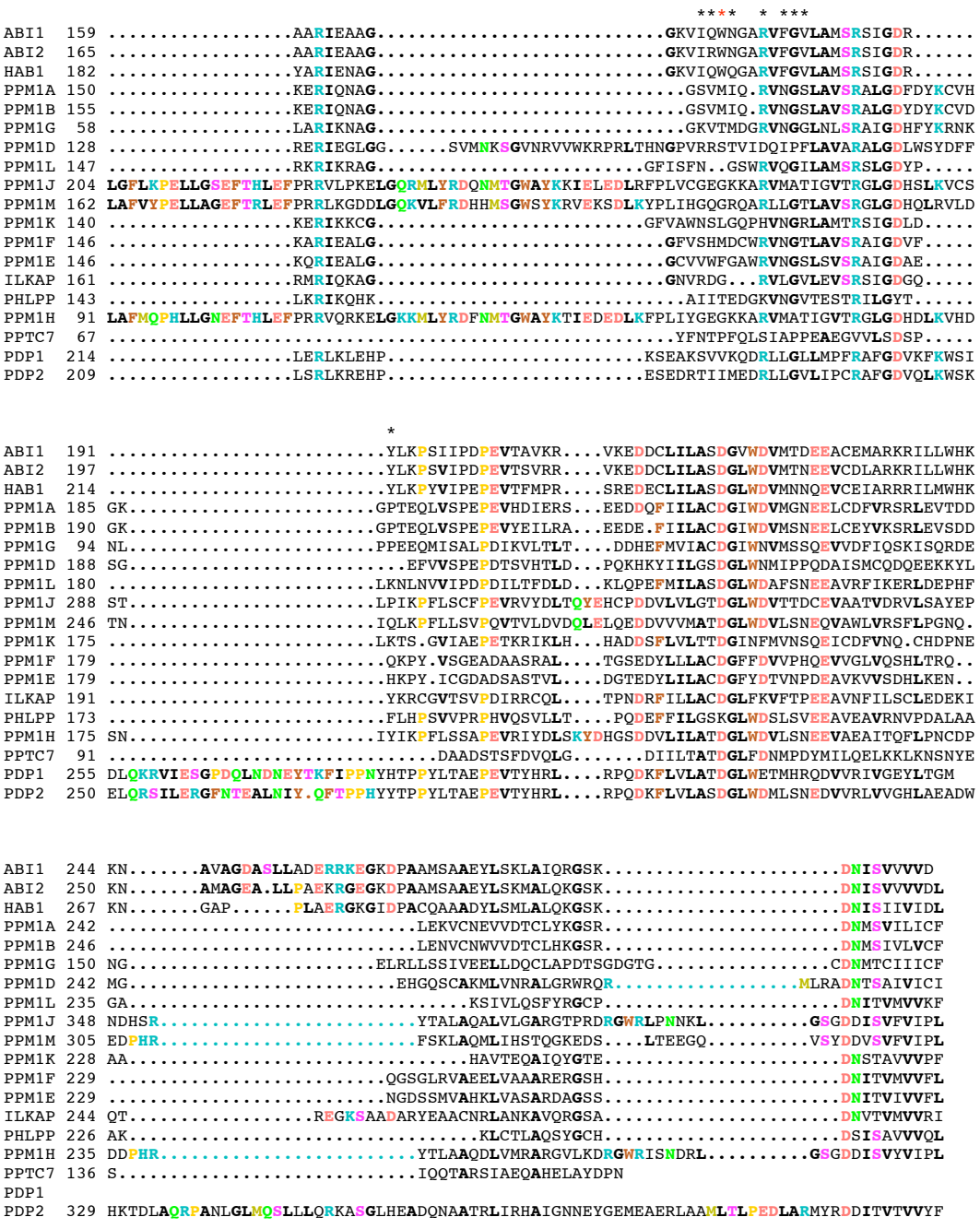

Figure 49. Multiple sequence alignment of the PP2C domains of Arabidopsis and human PP2C proteins.

Sequence alignment was performed by STRAP software (Gille and Frommel, 2001). The Arabidopsis PP2C residues involved in PYL interaction, based on PYL2-ABA-HAB1 structural analysis, are indicated by asterisks. The 'tryptophan lock' residue conserved in Arabidopsis ABA signalling PP2Cs is indicated by a red asterisk. Conserved amino acids are coloured according to chemical property.

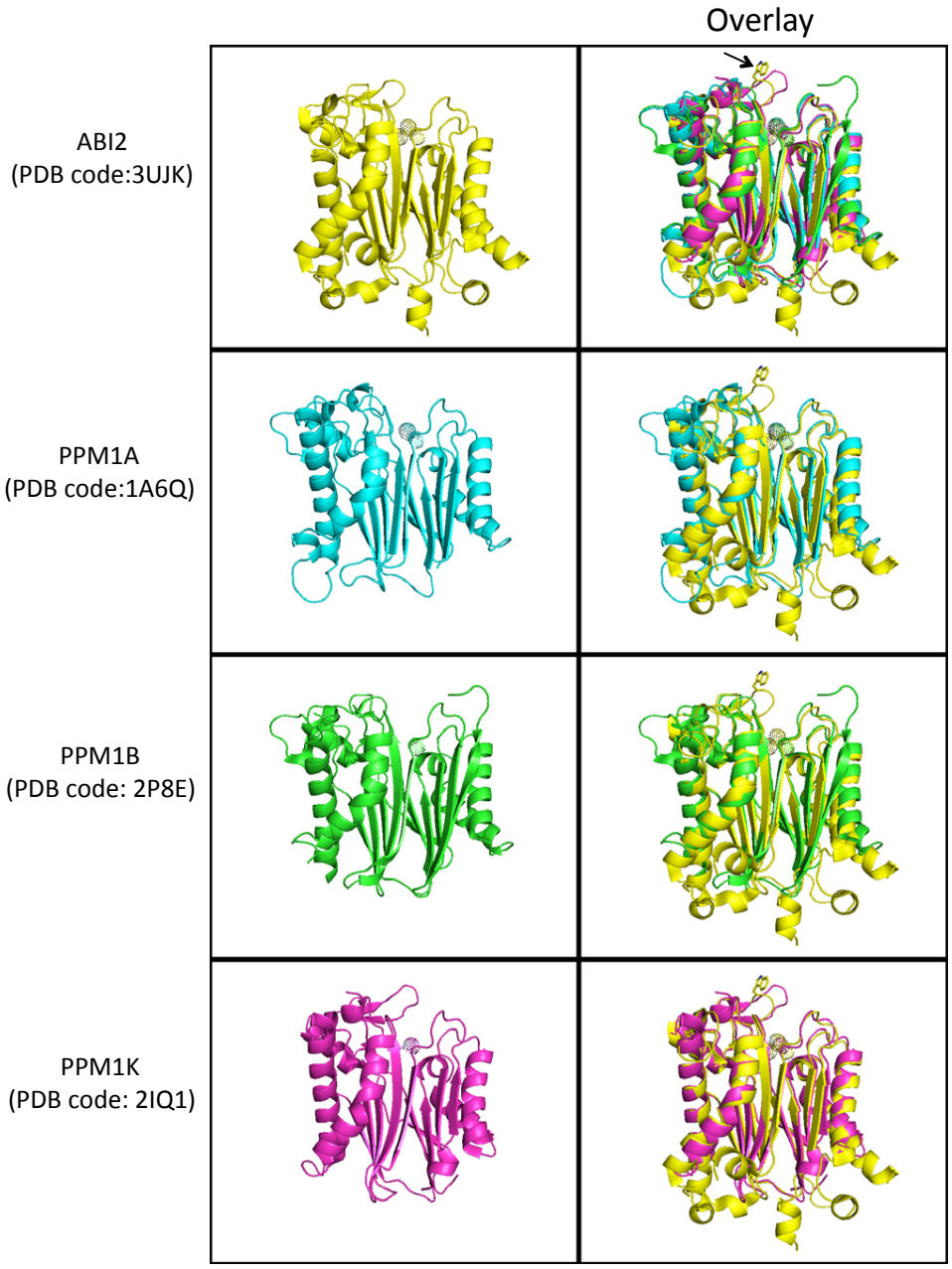

Figure 50. Structural similarity between Arabidopsis ABI2 and human PP2Cs.

Structures of Arabidopsis ABI2 and human PP2Cs are shown on the left panels. Overlay of each human PP2C with ABI2 is shown on the right panels. On the upper right panel, all 4 PP2C structures are superimposed, with an arrow indicating the tryptophan side chain of the ABI2 that is critical for PYL interaction.

4.7.3 AMPK- The mammalian homologue of SnRK

AMPK is a mammalian protein kinase that derived its name from its allosteric activation by AMP. Because of its important role in maintaining energy metabolism, AMPK has been described as a 'fuel-gauge' and 'guardian of energy status' (Hardie, 2003). The kinase is sensitive to an increase in cellular AMP:ATP ratio that is activated by metabolic stresses. Once activated, AMPK switches on ATP-producing catabolic pathways and inhibits ATP-consuming anabolic pathways (Hardie, 2007). AMPK exists as a heterotrimeric enzyme complex that consists of a catalytic α subunit and regulatory β and γ subunits. Each subunit has multiple isoforms encoded by distinct genes (α1, α2, β1, β2, γ1, γ2, γ3), enabling the formation of at least 12 αβγ heterotrimer combinations (Fogarty and Hardie, 2010).

Orthologues of the mammalian AMPK is found in virtually all eukaryotes, including plants, fungi, nematodes and insects (Hardie, 2008). The orthologue of AMPK in budding yeast (*Saccharomyces cerevisiae*) is known as Snf1 (sucrose nonfermenting) (Carling et al., 1994), a protein kinase best known for its role in carbon catabolite repression (Celenza and Carlson, 1986). In plants, there are 3 groups of Snf1-related protein kinases (SnRK1, SnRK2 and SnRK3). The *SnRK1* gene was in fact first identified based on its ability to complement the *snf1* mutation in yeast (Alderson et al., 1991). Of the 3 groups of plant SnRKs, SnRK1 is most closely related with Snf1 and AMPKα, sharing 47 % amino acid sequence identity with the yeast and mammalian orthologues (Halford and Hey, 2009). The SnRK2 and SnRK3 groups have

diverged further in evolution and appear to be unique to plants. Even so, some homology still remains as they share 42–45 % amino acid sequence identity with the SnRK1, Snf1 and AMPK in the catalytic region (Halford and Hey, 2009).

In the mammalian AMPK, phosphorylation of a threonine residue (Thr172) in the α subunit activation loop is required for its activation (Stein et al., 2000), which is a common feature for many protein kinases. Calcium/calmodulin-dependent protein kinase kinase-β (CaMKKβ) and LKB1 are the best known kinases upstream of AMPK (Hawley et al., 2005; Woods et al., 2003). Protein phosphatases PP1, PP2A and PP2C have been shown to dephosphorylate AMPK Thr172 *in vitro* (Davies et al., 1994; Davies et al., 1995). However, the physiological relevance of these phosphatases in AMPK regulation remains to be determined. Other key issues that remain include the roles of the glycogen binding domain (GBD) and β-subunit myristoylation in AMPK regulation. Obtaining the crystal structure of full-length heterotrimeric AMPK will provide insights into elucidating the mechanisms of AMPK regulation. The challenge, however, is that the full-length complexes are resistant to crystallization (Xiao et al., 2007). There has been a growing interest in AMPK as a potential target for treatment of metabolic disorders and cancers (Fogarty and Hardie, 2010). A more complete understanding of the molecular mechanisms of AMPK regulation will be useful for development of novel therapeutics targeting AMPK.

In our studies of the mechanisms of SnRK2 autoactivation and regulation by

PP2Cs, we have successfully used protein engineering techniques to obtain highly diffracting crystals of SnRK2s (Ng et al., 2011) and SnRK2-PP2C complex (Soon et al., 2012), which initially failed to crystallize. Such techniques may be useful to facilitate crystallization of the full-length AMPK. Our findings of SnRK2-PP2C regulation by mutual packing of their catalytic sites (Soon et al., 2012) also leads to the speculation that such a mechanism may exist between AMPK-PP2C in mammals, that remains to be elucidated. Thus, the identification of signalling mechanisms in plants not only has ramifications in agricultural improvement but can also serve as a framework for novel discovery of analogous mechanisms in other species including humans.

4.8 Conclusions and perspectives

We have identified a gate-latch-lock mechanism of ABA binding and signal transduction by the PYL family of ABA receptors. Using our structural knowledge, we have also demonstrated how these receptors can be selectively activated or antagonized. Translation into agricultural applications will require further validation of the Arabidopsis model of the core ABA signalling pathway in commercial crop species. Downstream of PP2C regulation by the PYLs, we have further probed the structural mechanisms of SnRK2s activation and their inhibition by PP2Cs. Discovery of analogous mechanisms of regulation involving mammalian homologues of the PYL, PP2C and SnRKs will be an exciting avenue for future research.

REFERENCES

Adler, E. M. (2010). 2009: signaling breakthroughs of the year. *Sci Signal* **3**, eg1.

Alderson, A., Sabelli, P. A., Dickinson, J. R., Cole, D., Richardson, M., Kreis, M., Shewry, P. R., and Halford, N. G. (1991). Complementation of snf1, a mutation affecting global regulation of carbon metabolism in yeast, by a plant protein kinase cDNA. *Proc Natl Acad Sci U S A* **88**, 8602-5.

Almo, S. C., Bonanno, J. B., Sauder, J. M., Emtage, S., Dilorenzo, T. P., Malashkevich, V., Wasserman, S. R., Swaminathan, S., Eswaramoorthy, S., Agarwal, R., Kumaran, D., Madegowda, M., Ragumani, S., Patskovsky, Y., Alvarado, J., Ramagopal, U. A., Faber-Barata, J., Chance, M. R., Sali, A., Fiser, A., Zhang, Z. Y., Lawrence, D. S., and Burley, S. K. (2007). Structural genomics of protein phosphatases. *J Struct Funct Genomics* **8**, 121-40.

Alpy, F., and Tomasetto, C. (2005). Give lipids a START: the StAR-related lipid transfer (START) domain in mammals. *J Cell Sci* **118**, 2791-801.

Asami, T., Robertson, M., Yamamoto, S., Yoneyama, K., Takeuchi, Y., and Yoshida, S. (1998). Biological Activities of an Abscisic Acid Analog in Barley, Cress, and Rice. *Plant and Cell Physiology* **39**, 342-348.

Barford, D., Das, A. K., and Egloff, M. P. (1998). The structure and mechanism of protein phosphatases: insights into catalysis and regulation. *Annu Rev Biophys Biomol Struct* **27**, 133-64.

Belin, C., de Franco, P. O., Bourbousse, C., Chaignepain, S., Schmitter, J. M., Vavasseur, A., Giraudat, J., Barbier-Brygoo, H., and Thomine, S. (2006). Identification of features regulating OST1 kinase activity and OST1 function in guard cells. *Plant Physiol* **141**, 1316-27.

Bensmihen, S., Giraudat, J., and Parcy, F. (2005). Characterization of three homologous basic leucine zipper transcription factors (bZIP) of the ABI5 family during Arabidopsis thaliana embryo maturation. *J Exp Bot* **56**, 597-603.

Bensmihen, S., Rippa, S., Lambert, G., Jublot, D., Pautot, V., Granier, F., Giraudat, J., and Parcy, F. (2002). The homologous ABI5 and EEL transcription factors function antagonistically to fine-tune gene expression during late embryogenesis. *Plant Cell* **14**, 1391-403.

Boneh, U., Biton, I., Zheng, C., Schwartz, A., and Ben-Ari, G. (2012). Characterization of potential ABA receptors in Vitis vinifera. *Plant Cell Rep* **31**, 311-21.

Boudsocq, M., Barbier-Brygoo, H., and Lauriere, C. (2004). Identification of nine sucrose nonfermenting 1-related protein kinases 2 activated by hyperosmotic and saline stresses in Arabidopsis thaliana. *J Biol Chem* **279**, 41758-66.

Boudsocq, M., Droillard, M. J., Barbier-Brygoo, H., and Lauriere, C. (2007). Different phosphorylation mechanisms are involved in the activation of sucrose non-fermenting 1 related protein kinases 2 by osmotic stresses and abscisic acid. *Plant Mol Biol* **63**, 491-503.

Busk, P. K., and Pages, M. (1998). Regulation of abscisic acid-induced transcription. *Plant Mol Biol* **37**, 425-35.

Cao, Y. J., Wei, Q., Liao, Y., Song, H. L., Li, X., Xiang, C. B., and Kuai, B. K. (2009). Ectopic overexpression of AtHDG11 in tall fescue resulted in enhanced tolerance to drought and salt stress. *Plant Cell Rep* **28**, 579-88.

Carling, D., Aguan, K., Woods, A., Verhoeven, A. J., Beri, R. K., Brennan, C. H., Sidebottom, C., Davison, M. D., and Scott, J. (1994). Mammalian AMP-activated protein kinase is homologous to yeast and plant protein kinases involved in the regulation of carbon metabolism. *J Biol Chem* **269**, 11442-8.

Celenza, J. L., and Carlson, M. (1986). A yeast gene that is essential for release from glucose repression encodes a protein kinase. *Science* **233**, 1175-80.

Chen, L., Jiao, Z. H., Zheng, L. S., Zhang, Y. Y., Xie, S. T., Wang, Z. X., and Wu, J. W. (2009). Structural insight into the autoinhibition mechanism of AMP-activated protein kinase. *Nature* **459**, 1146-9.

Choi, H., Hong, J., Ha, J., Kang, J., and Kim, S. Y. (2000). ABFs, a family of ABA-responsive element binding factors. *J Biol Chem* **275**, 1723-30.

Clark, B. J. (2012). The mammalian START domain protein family in lipid transport in health and disease. *J Endocrinol* **212**, 257-75.

Coello, P., Hey, S. J., and Halford, N. G. (2011). The sucrose non-fermenting-1-related (SnRK) family of protein kinases: potential for manipulation to improve stress tolerance and increase yield. *J Exp Bot* **62**, 883-93.

Cutler, A. J., and Krochko, J. E. (1999). Formation and breakdown of ABA. *Trends Plant Sci* **4**, 472-478.

Cutler, S. R., Rodriguez, P. L., Finkelstein, R. R., and Abrams, S. R. (2010). Abscisic acid: emergence of a core signaling network. *Annu Rev Plant Biol* **61**, 651-79.

Das, A. K., Helps, N. R., Cohen, P. T., and Barford, D. (1996). Crystal structure of the protein serine/threonine phosphatase 2C at 2.0 A resolution. *EMBO J* **15**, 6798-809.

Davies, S. P., Hawley, S. A., Woods, A., Carling, D., Haystead, T. A., and Hardie, D. G. (1994). Purification of the AMP-activated protein kinase on ATP-gamma-sepharose and analysis of its subunit structure. *Eur J Biochem* **223**, 351-7.

Davies, S. P., Helps, N. R., Cohen, P. T., and Hardie, D. G. (1995). 5'-AMP inhibits dephosphorylation, as well as promoting phosphorylation, of the AMP-activated protein kinase. Studies using bacterially expressed human protein phosphatase-2C alpha and native bovine protein phosphatase-2AC. *FEBS Lett* **377**, 421-5.

Dietz, K. J., Sauter, A., Wichert, K., Messdaghi, D., and Hartung, W. (2000). Extracellular beta-glucosidase activity in barley involved in the hydrolysis of ABA glucose conjugate in leaves. *J Exp Bot* **51**, 937-44.

Emsley, P., and Cowtan, K. (2004). Coot: model-building tools for molecular graphics. *Acta Crystallogr D Biol Crystallogr* **60**, 2126-32.

Fernandes, H., Pasternak, O., Bujacz, G., Bujacz, A., Sikorski, M. M., and Jaskolski, M. (2008). Lupinus luteus pathogenesis-related protein as a reservoir for cytokinin. *J Mol Biol* **378**, 1040-51.

Finkelstein, R. R. (1994). Mutations at two new Arabidopsis ABA response loci are similar to the abi3 mutations. *The Plant Journal* **5**, 765-771.

Finkelstein, R. R., and Lynch, T. J. (2000). The Arabidopsis abscisic acid response gene ABI5 encodes a basic leucine zipper transcription factor. *Plant Cell* **12**, 599-609.

Finkelstein, R. R., Wang, M. L., Lynch, T. J., Rao, S., and Goodman, H. M. (1998). The Arabidopsis abscisic acid response locus ABI4 encodes an APETALA 2 domain protein. *Plant Cell* **10**, 1043-54.

Fogarty, S., and Hardie, D. G. (2010). Development of protein kinase activators: AMPK as a target in metabolic disorders and cancer. *Biochim Biophys Acta* **1804**, 581-91.

Fu, D., Uauy, C., Distelfeld, A., Blechl, A., Epstein, L., Chen, X., Sela, H., Fahima, T., and Dubcovsky, J. (2009). A kinase-START gene confers temperature-dependent resistance to wheat stripe rust. *Science* **323**, 1357-60.

Fujii, H., Chinnusamy, V., Rodrigues, A., Rubio, S., Antoni, R., Park, S. Y., Cutler, S. R., Sheen, J., Rodriguez, P. L., and Zhu, J. K. (2009). In vitro reconstitution of an abscisic acid signalling pathway. *Nature* **462**, 660-4.

Fujii, H., Verslues, P. E., and Zhu, J. K. (2007). Identification of two protein kinases required for abscisic acid regulation of seed germination, root growth, and gene expression in Arabidopsis. *Plant Cell* **19**, 485-94.

Fujii, H., Verslues, P. E., and Zhu, J. K. (2011). Arabidopsis decuple mutant reveals the importance of SnRK2 kinases in osmotic stress responses in vivo. *Proc Natl Acad Sci U S A* **108**, 1717-22.

Fujii, H., and Zhu, J. K. (2009). Arabidopsis mutant deficient in 3 abscisic acid-activated protein kinases reveals critical roles in growth, reproduction, and stress. *Proc Natl Acad Sci U S A* **106**, 8380-5.

Fujita, Y., Fujita, M., Satoh, R., Maruyama, K., Parvez, M. M., Seki, M., Hiratsu, K., Ohme-Takagi, M., Shinozaki, K., and Yamaguchi-Shinozaki, K. (2005). AREB1 is a transcription activator of novel ABRE-dependent ABA signaling that enhances drought stress tolerance in Arabidopsis. *Plant Cell* **17**, 3470-88.

Fujita, Y., Nakashima, K., Yoshida, T., Katagiri, T., Kidokoro, S., Kanamori, N., Umezawa, T., Fujita, M., Maruyama, K., Ishiyama, K., Kobayashi, M., Nakasone, S., Yamada, K., Ito, T., Shinozaki, K., and Yamaguchi-Shinozaki, K. (2009). Three SnRK2 protein kinases are the main positive regulators of abscisic acid signaling in response to water stress in Arabidopsis. *Plant Cell Physiol* **50**, 2123-32.

Furihata, T., Maruyama, K., Fujita, Y., Umezawa, T., Yoshida, R., Shinozaki, K., and Yamaguchi-Shinozaki, K. (2006). Abscisic acid-dependent multisite phosphorylation regulates the activity of a transcription activator AREB1. *Proc Natl Acad Sci U S A* **103**, 1988-93.

Gao, Y., Zeng, Q., Guo, J., Cheng, J., Ellis, B. E., and Chen, J. G. (2007). Genetic characterization reveals no role for the reported ABA receptor, GCR2, in ABA control of seed germination and early seedling development in Arabidopsis. *Plant J* **52**, 1001-13.

Geiger, D., Scherzer, S., Mumm, P., Stange, A., Marten, I., Bauer, H., Ache, P., Matschi, S., Liese, A., Al-Rasheid, K. A., Romeis, T., and Hedrich, R. (2009). Activity of guard cell anion channel SLAC1 is controlled by drought-stress signaling kinase-phosphatase pair. *Proc Natl Acad Sci U S A* **106**, 21425-30.

Gille, C., and Frommel, C. (2001). STRAP: editor for STRuctural Alignments of Proteins. *Bioinformatics* **17**, 377-8.

Gomez-Porras, J. L., Riano-Pachon, D. M., Dreyer, I., Mayer, J. E., and Mueller-Roeber, B. (2007). Genome-wide analysis of ABA-responsive elements ABRE and CE3 reveals divergent patterns in Arabidopsis and rice. *BMC Genomics* **8**, 260.

Gosti, F., Beaudoin, N., Serizet, C., Webb, A. A., Vartanian, N., and Giraudat, J. (1999). ABI1 protein phosphatase 2C is a negative regulator of abscisic acid signaling. *Plant Cell* **11**, 1897-910.

Goujon, M., McWilliam, H., Li, W., Valentin, F., Squizzato, S., Paern, J., and Lopez, R. (2010). A new bioinformatics analysis tools framework at EMBL-EBI. *Nucleic Acids Res* **38**, W695-9.

Guo, J., Zeng, Q., Emami, M., Ellis, B. E., and Chen, J. G. (2008). The GCR2 gene family is not required for ABA control of seed germination and early seedling development in Arabidopsis. *PLoS One* **3**, e2982.

Halford, N. G., and Hey, S. J. (2009). Snf1-related protein kinases (SnRKs) act within an intricate network that links metabolic and stress signalling in plants. *Biochem J* **419**, 247-59.

Hao, Q., Yin, P., Li, W., Wang, L., Yan, C., Lin, Z., Wu, J. Z., Wang, J., Yan, S. F., and Yan, N. (2011). The molecular basis of ABA-independent inhibition of PP2Cs by a subclass of PYL proteins. *Mol Cell* **42**, 662-72.

Hao, Q., Yin, P., Yan, C., Yuan, X., Li, W., Zhang, Z., Liu, L., Wang, J., and Yan, N. (2010). Functional mechanism of the abscisic acid agonist pyrabactin. *J Biol Chem* **285**, 28946-52.

Hardie, D. G. (2003). Minireview: the AMP-activated protein kinase cascade: the key sensor of cellular energy status. *Endocrinology* **144**, 5179-83.

Hardie, D. G. (2007). AMP-activated/SNF1 protein kinases: conserved guardians of cellular energy. *Nat Rev Mol Cell Biol* **8**, 774-85.

Hardie, D. G. (2008). Role of AMP-activated protein kinase in the metabolic syndrome and in heart disease. *FEBS Lett* **582**, 81-9.

Harris, M. J., Outlaw, W. H., Mertens, R., and Weiler, E. W. (1988). Water-stress-induced changes in the abscisic acid content of guard cells and other cells of Vicia faba L. leaves as determined by enzyme-amplified immunoassay. *Proc Natl Acad Sci U S A* **85**, 2584-8.

Hawkins, A. F., Stead, A. D., Pinfield, N. J., and Editors (1987). "Plant growth regulators for agricultural and amenity use," British Crop Protection Council.

Hawley, S. A., Pan, D. A., Mustard, K. J., Ross, L., Bain, J., Edelman, A. M., Frenguelli, B. G., and Hardie, D. G. (2005). Calmodulin-dependent protein kinase kinase-beta is an alternative upstream kinase for AMP-activated protein kinase. *Cell Metab* **2**, 9-19.

Holm, L., and Park, J. (2000). DaliLite workbench for protein structure comparison. *Bioinformatics* **16**, 566-7.

Hrabak, E. M., Chan, C. W., Gribskov, M., Harper, J. F., Choi, J. H., Halford, N., Kudla, J., Luan, S., Nimmo, H. G., Sussman, M. R., Thomas, M., Walker-Simmons, K., Zhu, J. K., and Harmon, A. C. (2003). The Arabidopsis CDPK-SnRK superfamily of protein kinases. *Plant Physiol* **132**, 666-80.

Huang, D., Jaradat, M. R., Wu, W., Ambrose, S. J., Ross, A. R., Abrams, S. R., and Cutler, A. J. (2007). Structural analogs of ABA reveal novel features of ABA perception and signaling in Arabidopsis. *Plant J* **50**, 414-28.

Illingworth, C. J., Parkes, K. E., Snell, C. R., Mullineaux, P. M., and Reynolds, C. A. (2008). Criteria for confirming sequence periodicity identified by Fourier transform analysis: application to GCR2, a candidate plant GPCR? *Biophys Chem* **133**, 28-35.

Iyer, L. M., Koonin, E. V., and Aravind, L. (2001). Adaptations of the helix-grip fold for ligand binding and catalysis in the START domain superfamily. *Proteins* **43**, 134-44.

Jakoby, M., Weisshaar, B., Droge-Laser, W., Vicente-Carbajosa, J., Tiedemann, J., Kroj, T., and Parcy, F. (2002). bZIP transcription factors in Arabidopsis. *Trends Plant Sci* **7**, 106-11.

Johnston, C. A., Temple, B. R., Chen, J. G., Gao, Y., Moriyama, E. N., Jones, A. M., Siderovski, D. P., and Willard, F. S. (2007). Comment on "A G protein coupled receptor is a plasma membrane receptor for the plant hormone abscisic acid". *Science* **318**, 914; author reply 914.

Kang, J., Hwang, J. U., Lee, M., Kim, Y. Y., Assmann, S. M., Martinoia, E., and Lee, Y. (2010). PDR-type ABC transporter mediates cellular uptake of the phytohormone abscisic acid. *Proc Natl Acad Sci U S A* **107**, 2355-60.

Kang, J. Y., Choi, H. I., Im, M. Y., and Kim, S. Y. (2002). Arabidopsis basic leucine zipper proteins that mediate stress-responsive abscisic acid signaling. *Plant Cell* **14**, 343-57.

Kanno, Y., Hanada, A., Chiba, Y., Ichikawa, T., Nakazawa, M., Matsui, M., Koshiba, T., Kamiya, Y., and Seo, M. (2012). Identification of an abscisic acid transporter by functional screening using the receptor complex as a sensor. *Proc Natl Acad Sci U S A* **109**, 9653-8.

Kim, H., Hwang, H., Hong, J. W., Lee, Y. N., Ahn, I. P., Yoon, I. S., Yoo, S. D., Lee, S., Lee, S. C., and Kim, B. G. (2012). A rice orthologue of the ABA receptor, OsPYL/RCAR5, is a positive regulator of the ABA signal transduction pathway in seed germination and early seedling growth. *J Exp Bot* **63**, 1013-24.

Kim, S., Kang, J. Y., Cho, D. I., Park, J. H., and Kim, S. Y. (2004). ABF2, an ABRE-binding bZIP factor, is an essential component of glucose signaling and its overexpression affects multiple stress tolerance. *Plant J* **40**, 75-87.

Kim, S. Y. (2006). The role of ABF family bZIP class transcription factors in stress response. *Physiologia Plantarum* **126**, 519-527.

Kim, S. Y., Ma, J., Perret, P., Li, Z., and Thomas, T. L. (2002). Arabidopsis ABI5 subfamily members have distinct DNA-binding and transcriptional activities. *Plant Physiol* **130**, 688-97.

Kim, T. H., Bohmer, M., Hu, H., Nishimura, N., and Schroeder, J. I. (2010). Guard cell signal transduction network: advances in understanding abscisic acid, CO2, and Ca2+ signaling. *Annu Rev Plant Biol* **61**, 561-91.

Kleywegt, G. J., and Jones, T. A. (1994). Detection, delineation, measurement and display of cavities in macromolecular structures. *Acta Crystallogr D Biol Crystallogr* **50**, 178-85.

Kleywegt, G. J., and Jones, T. A. (1996). Efficient rebuilding of protein structures. *Acta Crystallogr D Biol Crystallogr* **52**, 829-32.

Koornneef, M., Reuling, G. & Karssen, C.M. (1984). The isolation and characterization of abscisic acid-insensitive mutants of Arabidopsis thaliana. . *Physiol. Plant.* **61**, 377-383.

Kornev, A. P., Haste, N. M., Taylor, S. S., and Eyck, L. F. (2006). Surface comparison of active and inactive protein kinases identifies a conserved activation mechanism. *Proc Natl Acad Sci U S A* **103**, 17783-8.

Korostelev, A., Bertram, R., and Chapman, M. S. (2002). Simulated-annealing real-space refinement as a tool in model building. *Acta Crystallogr D Biol Crystallogr* **58**, 761-7.

Kostich, M., English, J., Madison, V., Gheyas, F., Wang, L., Qiu, P., Greene, J., and Laz, T. M. (2002). Human members of the eukaryotic protein kinase family. *Genome Biol* **3**, RESEARCH0043.

Koussevitzky, S., Nott, A., Mockler, T. C., Hong, F., Sachetto-Martins, G., Surpin, M., Lim, J., Mittler, R., and Chory, J. (2007). Signals from chloroplasts converge to regulate nuclear gene expression. *Science* **316**, 715-9.

Kudo, N., Kumagai, K., Matsubara, R., Kobayashi, S., Hanada, K., Wakatsuki, S., and Kato, R. (2010). Crystal structures of the CERT START domain with inhibitors provide insights into the mechanism of ceramide transfer. *J Mol Biol* **396**, 245-51.

Kudo, N., Kumagai, K., Tomishige, N., Yamaji, T., Wakatsuki, S., Nishijima, M., Hanada, K., and Kato, R. (2008). Structural basis for specific lipid recognition by CERT responsible for nonvesicular trafficking of ceramide. *Proc Natl Acad Sci U S A* **105**, 488-93.

Kuromori, T., Miyaji, T., Yabuuchi, H., Shimizu, H., Sugimoto, E., Kamiya, A., Moriyama, Y., and Shinozaki, K. (2010). ABC transporter AtABCG25 is involved in abscisic acid transport and responses. *Proc Natl Acad Sci U S A* **107**, 2361-6.

Kushiro, T., Okamoto, M., Nakabayashi, K., Yamagishi, K., Kitamura, S., Asami, T., Hirai, N., Koshiba, T., Kamiya, Y., and Nambara, E. (2004). The Arabidopsis cytochrome P450 CYP707A encodes ABA 8'-hydroxylases: key enzymes in ABA catabolism. *EMBO J* **23**, 1647-56.

Lammers, T., and Lavi, S. (2007). Role of type 2C protein phosphatases in growth regulation and in cellular stress signaling. *Crit Rev Biochem Mol Biol* **42**, 437-61.

Larkin, M. A., Blackshields, G., Brown, N. P., Chenna, R., McGettigan, P. A., McWilliam, H., Valentin, F., Wallace, I. M., Wilm, A., Lopez, R., Thompson, J. D., Gibson, T. J., and Higgins, D. G. (2007). Clustal W and Clustal X version 2.0. *Bioinformatics* **23**, 2947-8.

Lavigne, P., Najmanivich, R., and Lehoux, J. G. (2010). Mammalian StAR-related lipid transfer (START) domains with specificity for cholesterol: structural conservation and mechanism of reversible binding. *Subcell Biochem* **51**, 425-37.

Lee, K. H., Piao, H. L., Kim, H. Y., Choi, S. M., Jiang, F., Hartung, W., Hwang, I., Kwak, J. M., Lee, I. J., and Hwang, I. (2006). Activation of glucosidase via stress-induced polymerization rapidly increases active pools of abscisic acid. *Cell* **126**, 1109-20.

Lee, S. C., Lan, W., Buchanan, B. B., and Luan, S. (2009). A protein kinase-phosphatase pair interacts with an ion channel to regulate ABA signaling in plant guard cells. *Proc Natl Acad Sci U S A* **106**, 21419-24.

Leung, J., Bouvier-Durand, M., Morris, P. C., Guerrier, D., Chefdor, F., and Giraudat, J. (1994). Arabidopsis ABA response gene ABI1: features of a calcium-modulated protein phosphatase. *Science* **264**, 1448-52.

Leung, J., Merlot, S., and Giraudat, J. (1997). The Arabidopsis ABSCISIC ACID-INSENSITIVE2 (ABI2) and ABI1 genes encode homologous protein phosphatases 2C involved in abscisic acid signal transduction. *Plant Cell* **9**, 759-71.

Lin, B. L., Wang, H. J., Wang, J. S., Zaharia, L. I., and Abrams, S. R. (2005). Abscisic acid regulation of heterophylly in Marsilea quadrifolia L.: effects of R-(-) and S-(+) isomers. *J Exp Bot* **56**, 2935-48.

Liu, J.-J., and Ekramoddoullah, A. K. M. (2006). The family 10 of plant pathogenesis-related proteins: Their structure, regulation, and function in response to biotic and abiotic stresses. *Physiological and Molecular Plant Pathology* **68**, 3-13.

Liu, X., Yue, Y., Li, B., Nie, Y., Li, W., Wu, W. H., and Ma, L. (2007). A G protein-coupled receptor is a plasma membrane receptor for the plant hormone abscisic acid. *Science* **315**, 1712-6.

Lopez-Molina, L., Mongrand, S., and Chua, N. H. (2001). A postgermination developmental arrest checkpoint is mediated by abscisic acid and requires the ABI5 transcription factor in Arabidopsis. *Proc Natl Acad Sci U S A* **98**, 4782-7.

Lu, G., and Wang, Y. (2008). Functional diversity of mammalian type 2C protein phosphatase isoforms: new tales from an old family. *Clin Exp Pharmacol Physiol* **35**, 107-12.

Ma, Y., Szostkiewicz, I., Korte, A., Moes, D., Yang, Y., Christmann, A., and Grill, E. (2009). Regulators of PP2C phosphatase activity function as abscisic acid sensors. *Science* **324**, 1064-8.

Mann, D. J., Campbell, D. G., McGowan, C. H., and Cohen, P. T. (1992). Mammalian protein serine/threonine phosphatase 2C: cDNA cloning and comparative analysis of amino acid sequences. *Biochim Biophys Acta* **1130**, 100-4.

Manning, G., Whyte, D. B., Martinez, R., Hunter, T., and Sudarsanam, S. (2002). The protein kinase complement of the human genome. *Science* **298**, 1912-34.

Markovic-Housley, Z., Degano, M., Lamba, D., von Roepenack-Lahaye, E., Clemens, S., Susani, M., Ferreira, F., Scheiner, O., and Breiteneder, H. (2003). Crystal structure of a hypoallergenic isoform of the major birch pollen allergen Bet v 1 and its likely biological function as a plant steroid carrier. *J Mol Biol* **325**, 123-33.

McCourt, P., and Creelman, R. (2008). The ABA receptors -- we report you decide. *Curr Opin Plant Biol* **11**, 474-8.

McCoy, A. J., Grosse-Kunstleve, R. W., Adams, P. D., Winn, M. D., Storoni, L. C., and Read, R. J. (2007). Phaser crystallographic software. *J Appl Crystallogr* **40**, 658-674.

Melcher, K., Ng, L. M., Zhou, X. E., Soon, F. F., Xu, Y., Suino-Powell, K. M., Park, S. Y., Weiner, J. J., Fujii, H., Chinnusamy, V., Kovach, A., Li, J., Wang, Y., Li, J., Peterson, F. C., Jensen, D. R., Yong, E. L., Volkman, B. F., Cutler, S. R., Zhu, J. K., and Xu, H. E. (2009). A gate-latch-lock mechanism for hormone signalling by abscisic acid receptors. *Nature* **462**, 602-8.

Melcher, K., Xu, Y., Ng, L. M., Zhou, X. E., Soon, F. F., Chinnusamy, V., Suino-Powell, K. M., Kovach, A., Tham, F. S., Cutler, S. R., Li, J., Yong, E. L., Zhu, J. K., and Xu, H. E. (2010). Identification and mechanism of ABA receptor antagonism. *Nat Struct Mol Biol* **17**, 1102-8.

Menkens, A. E., Schindler, U., and Cashmore, A. R. (1995). The G-box: a ubiquitous regulatory DNA element in plants bound by the GBF family of bZIP proteins. *Trends Biochem Sci* **20**, 506-10.

Merlot, S., Gosti, F., Guerrier, D., Vavasseur, A., and Giraudat, J. (2001). The ABI1 and ABI2 protein phosphatases 2C act in a negative feedback regulatory loop of the abscisic acid signalling pathway. *Plant J* **25**, 295-303.

Meyer, K., Leube, M. P., and Grill, E. (1994). A protein phosphatase 2C involved in ABA signal transduction in Arabidopsis thaliana. *Science* **264**, 1452-5.

Milborrow, B. V. (1974). The Chemistry and Physiology of Abscisic Acid. *Annual Review of Plant Physiology* **25**, 259-307.

Miyazono, K., Miyakawa, T., Sawano, Y., Kubota, K., Kang, H. J., Asano, A., Miyauchi, Y., Takahashi, M., Zhi, Y., Fujita, Y., Yoshida, T., Kodaira, K. S., Yamaguchi-Shinozaki, K., and Tanokura, M. (2009). Structural basis of abscisic acid signalling. *Nature* **462**, 609-14.

Mochizuki, N., Brusslan, J. A., Larkin, R., Nagatani, A., and Chory, J. (2001). Arabidopsis genomes uncoupled 5 (GUN5) mutant reveals the involvement of Mg-chelatase H subunit in plastid-to-nucleus signal transduction. *Proc Natl Acad Sci U S A* **98**, 2053-8.

Moes, D., Himmelbach, A., Korte, A., Haberer, G., and Grill, E. (2008). Nuclear localization of the mutant protein phosphatase abi1 is required for insensitivity towards ABA responses in Arabidopsis. *Plant J* **54**, 806-19.

Muller, A. H., and Hansson, M. (2009). The barley magnesium chelatase 150-kd subunit is not an abscisic acid receptor. *Plant Physiol* **150**, 157-66.

Murshudov, G. N., Vagin, A. A., Lebedev, A., Wilson, K. S., and Dodson, E. J. (1999). Efficient anisotropic refinement of macromolecular structures using FFT. *Acta Crystallogr D Biol Crystallogr* **55**, 247-55.

Mustilli, A. C., Merlot, S., Vavasseur, A., Fenzi, F., and Giraudat, J. (2002). Arabidopsis OST1 protein kinase mediates the regulation of stomatal aperture by abscisic acid and acts upstream of reactive oxygen species production. *Plant Cell* **14**, 3089-99.

Nakashima, K., Fujita, Y., Kanamori, N., Katagiri, T., Umezawa, T., Kidokoro, S., Maruyama, K., Yoshida, T., Ishiyama, K., Kobayashi, M., Shinozaki, K., and Yamaguchi-Shinozaki, K. (2009a). Three Arabidopsis SnRK2 protein kinases, SRK2D/SnRK2.2, SRK2E/SnRK2.6/OST1 and SRK2I/SnRK2.3, involved in ABA signaling are essential for the control of seed development and dormancy. *Plant Cell Physiol* **50**, 1345-63.

Nakashima, K., Ito, Y., and Yamaguchi-Shinozaki, K. (2009b). Transcriptional regulatory networks in response to abiotic stresses in Arabidopsis and grasses. *Plant Physiol* **149**, 88-95.

Nambara, E., and Marion-Poll, A. (2005). Abscisic acid biosynthesis and catabolism. *Annu Rev Plant Biol* **56**, 165-85.

Negi, J., Matsuda, O., Nagasawa, T., Oba, Y., Takahashi, H., Kawai-Yamada, M., Uchimiya, H., Hashimoto, M., and Iba, K. (2008). CO2 regulator SLAC1 and its homologues are essential for anion homeostasis in plant cells. *Nature* **452**, 483-6.

Ng, L. M., Soon, F. F., Zhou, X. E., West, G. M., Kovach, A., Suino-Powell, K. M., Chalmers, M. J., Li, J., Yong, E. L., Zhu, J. K., Griffin, P. R., Melcher, K.,

and Xu, H. E. (2011). Structural basis for basal activity and autoactivation of abscisic acid (ABA) signaling SnRK2 kinases. *Proc Natl Acad Sci U S A* **108**, 21259-64.

Nishimura, N., Hitomi, K., Arvai, A. S., Rambo, R. P., Hitomi, C., Cutler, S. R., Schroeder, J. I., and Getzoff, E. D. (2009). Structural mechanism of abscisic acid binding and signaling by dimeric PYR1. *Science* **326**, 1373-9.

Nishimura, N., Sarkeshik, A., Nito, K., Park, S. Y., Wang, A., Carvalho, P. C., Lee, S., Caddell, D. F., Cutler, S. R., Chory, J., Yates, J. R., and Schroeder, J. I. (2010). PYR/PYL/RCAR family members are major in-vivo ABI1 protein phosphatase 2C-interacting proteins in Arabidopsis. *Plant J* **61**, 290-9.

Nishimura, N., Yoshida, T., Murayama, M., Asami, T., Shinozaki, K., and Hirayama, T. (2004). Isolation and characterization of novel mutants affecting the abscisic acid sensitivity of Arabidopsis germination and seedling growth. *Plant Cell Physiol* **45**, 1485-99.

Okamoto, M., Tanaka, Y., Abrams, S. R., Kamiya, Y., Seki, M., and Nambara, E. (2009). High humidity induces abscisic acid 8'-hydroxylase in stomata and vasculature to regulate local and systemic abscisic acid responses in Arabidopsis. *Plant Physiol* **149**, 825-34.

Otwinowski, Z., Borek, D., Majewski, W., and Minor, W. (2003). Multiparametric scaling of diffraction intensities. *Acta Crystallogr A* **59**, 228-34.

Pandey, S., and Assmann, S. M. (2004). The Arabidopsis putative G protein-coupled receptor GCR1 interacts with the G protein alpha subunit GPA1 and regulates abscisic acid signaling. *Plant Cell* **16**, 1616-32.

Pandey, S., Nelson, D. C., and Assmann, S. M. (2009). Two novel GPCR-type G proteins are abscisic acid receptors in Arabidopsis. *Cell* **136**, 136-48.

Parcy, F., Valon, C., Raynal, M., Gaubier-Comella, P., Delseny, M., and Giraudat, J. (1994). Regulation of gene expression programs during Arabidopsis seed development: roles of the ABI3 locus and of endogenous abscisic acid. *Plant Cell* **6**, 1567-82.

Park, S. Y., Fung, P., Nishimura, N., Jensen, D. R., Fujii, H., Zhao, Y., Lumba, S., Santiago, J., Rodrigues, A., Chow, T. F., Alfred, S. E., Bonetta, D., Finkelstein, R., Provart, N. J., Desveaux, D., Rodriguez, P. L., McCourt, P., Zhu, J. K., Schroeder, J. I., Volkman, B. F., and Cutler, S. R. (2009). Abscisic acid inhibits type 2C protein phosphatases via the PYR/PYL family of START proteins. *Science* **324**, 1068-71.

Pasternak, O., Bujacz, G. D., Fujimoto, Y., Hashimoto, Y., Jelen, F., Otlewski, J., Sikorski, M. M., and Jaskolski, M. (2006). Crystal structure of Vigna radiata cytokinin-specific binding protein in complex with zeatin. *Plant Cell* **18**, 2622-34.

Peterson, F. C., Burgie, E. S., Park, S. Y., Jensen, D. R., Weiner, J. J., Bingman, C. A., Chang, C. E., Cutler, S. R., Phillips, G. N., Jr., and Volkman, B. F. (2010). Structural basis for selective activation of ABA receptors. *Nat Struct Mol Biol* **17**, 1109-13.

Polge, C., and Thomas, M. (2007). SNF1/AMPK/SnRK1 kinases, global regulators at the heart of energy control? *Trends Plant Sci* **12**, 20-8.

Ponting, C. P., and Aravind, L. (1999). START: a lipid-binding domain in StAR, HD-ZIP and signalling proteins. *Trends Biochem Sci* **24**, 130-2.

Rabiller, M., Getlik, M., Kluter, S., Richters, A., Tuckmantel, S., Simard, J. R., and Rauh, D. (2010). Proteus in the world of proteins: conformational changes in protein kinases. *Arch Pharm (Weinheim)* **343**, 193-206.

Radauer, C., Lackner, P., and Breiteneder, H. (2008). The Bet v 1 fold: an ancient, versatile scaffold for binding of large, hydrophobic ligands. *BMC Evol Biol* **8**, 286.

Razem, F. A., El-Kereamy, A., Abrams, S. R., and Hill, R. D. (2006). The RNA-binding protein FCA is an abscisic acid receptor. *Nature* **439**, 290-4.

Razem, F. A., Luo, M., Liu, J. H., Abrams, S. R., and Hill, R. D. (2004). Purification and characterization of a barley aleurone abscisic acid-binding protein. *J Biol Chem* **279**, 9922-9.

Risk, J. M., Day, C. L., and Macknight, R. C. (2009). Reevaluation of abscisic acid-binding assays shows that G-Protein-Coupled Receptor2 does not bind abscisic Acid. *Plant Physiol* **150**, 6-11.

Risk, J. M., Macknight, R. C., and Day, C. L. (2008). FCA does not bind abscisic acid. *Nature* **456**, E5-6.

Robert, N., Merlot, S., N'Guyen, V., Boisson-Dernier, A., and Schroeder, J. I. (2006). A hypermorphic mutation in the protein phosphatase 2C HAB1 strongly affects ABA signaling in Arabidopsis. *FEBS Lett* **580**, 4691-6.

Roderick, S. L., Chan, W. W., Agate, D. S., Olsen, L. R., Vetting, M. W., Rajashankar, K. R., and Cohen, D. E. (2002). Structure of human phosphatidylcholine transfer protein in complex with its ligand. *Nat Struct Biol* **9**, 507-11.

Rodriguez, P. L., Benning, G., and Grill, E. (1998a). ABI2, a second protein phosphatase 2C involved in abscisic acid signal transduction in Arabidopsis. *FEBS Lett* **421**, 185-90.

Rodriguez, P. L., Leube, M. P., and Grill, E. (1998b). Molecular cloning in Arabidopsis thaliana of a new protein phosphatase 2C (PP2C) with homology to ABI1 and ABI2. *Plant Mol Biol* **38**, 879-83.

Romero, P., Lafuente, M. T., and Rodrigo, M. J. (2012). The Citrus ABA signalosome: identification and transcriptional regulation during sweet orange fruit ripening and leaf dehydration. *J Exp Bot* **63**, 4931-45.

Rone, M. B., Fan, J., and Papadopoulos, V. (2009). Cholesterol transport in steroid biosynthesis: role of protein-protein interactions and implications in disease states. *Biochim Biophys Acta* **1791**, 646-58.

Rubio, S., Rodrigues, A., Saez, A., Dizon, M. B., Galle, A., Kim, T. H., Santiago, J., Flexas, J., Schroeder, J. I., and Rodriguez, P. L. (2009). Triple loss of function of protein phosphatases type 2C leads to partial constitutive response to endogenous abscisic acid. *Plant Physiol* **150**, 1345-55.

Saez, A., Apostolova, N., Gonzalez-Guzman, M., Gonzalez-Garcia, M. P., Nicolas, C., Lorenzo, O., and Rodriguez, P. L. (2004). Gain-of-function and loss-of-function phenotypes of the protein phosphatase 2C HAB1 reveal its role as a negative regulator of abscisic acid signalling. *Plant J* **37**, 354-69.

Saez, A., Robert, N., Maktabi, M. H., Schroeder, J. I., Serrano, R., and Rodriguez, P. L. (2006). Enhancement of abscisic acid sensitivity and reduction of water consumption in Arabidopsis by combined inactivation of the protein phosphatases type 2C ABI1 and HAB1. *Plant Physiol* **141**, 1389-99.

Saito, S., Hirai, N., Matsumoto, C., Ohigashi, H., Ohta, D., Sakata, K., and Mizutani, M. (2004). Arabidopsis CYP707As encode (+)-abscisic acid 8'-hydroxylase, a key enzyme in the oxidative catabolism of abscisic acid. *Plant Physiol* **134**, 1439-49.

Santiago, J., Dupeux, F., Round, A., Antoni, R., Park, S. Y., Jamin, M., Cutler, S. R., Rodriguez, P. L., and Marquez, J. A. (2009a). The abscisic acid receptor PYR1 in complex with abscisic acid. *Nature* **462**, 665-8.

Santiago, J., Rodrigues, A., Saez, A., Rubio, S., Antoni, R., Dupeux, F., Park, S. Y., Marquez, J. A., Cutler, S. R., and Rodriguez, P. L. (2009b). Modulation of drought resistance by the abscisic acid receptor PYL5 through inhibition of clade A PP2Cs. *Plant J* **60**, 575-88.

Sato, A., Sato, Y., Fukao, Y., Fujiwara, M., Umezawa, T., Shinozaki, K., Hibi, T., Taniguchi, M., Miyake, H., Goto, D. B., and Uozumi, N. (2009). Threonine at position 306 of the KAT1 potassium channel is essential for channel activity and is a target site for ABA-activated SnRK2/OST1/SnRK2.6 protein kinase. *Biochem J* **424**, 439-48.

Schrick, K., Nguyen, D., Karlowski, W. M., and Mayer, K. F. (2004). START lipid/sterol-binding domains are amplified in plants and are predominantly associated with homeodomain transcription factors. *Genome Biol* **5**, R41.

Schweighofer, A., Hirt, H., and Meskiene, I. (2004). Plant PP2C phosphatases: emerging functions in stress signaling. *Trends Plant Sci* **9**, 236-43.

Sheen, J. (1998). Mutational analysis of protein phosphatase 2C involved in abscisic acid signal transduction in higher plants. *Proc Natl Acad Sci U S A* **95**, 975-80.

Shen, Y. Y., Wang, X. F., Wu, F. Q., Du, S. Y., Cao, Z., Shang, Y., Wang, X. L., Peng, C. C., Yu, X. C., Zhu, S. Y., Fan, R. C., Xu, Y. H., and Zhang, D. P. (2006). The Mg-chelatase H subunit is an abscisic acid receptor. *Nature* **443**, 823-6.

Shinozaki, K., Yamaguchi-Shinozaki, K., and Seki, M. (2003). Regulatory network of gene expression in the drought and cold stress responses. *Curr Opin Plant Biol* **6**, 410-7.

Smith, P. A., Tripp, B. C., DiBlasio-Smith, E. A., Lu, Z., LaVallie, E. R., and McCoy, J. M. (1998). A plasmid expression system for quantitative in vivo biotinylation of thioredoxin fusion proteins in Escherichia coli. *Nucleic Acids Res* **26**, 1414-20.

Soccio, R. E., and Breslow, J. L. (2003). StAR-related lipid transfer (START) proteins: mediators of intracellular lipid metabolism. *J Biol Chem* **278**, 22183-6.

Soon, F. F., Ng, L. M., Zhou, X. E., West, G. M., Kovach, A., Tan, M. H., Suino-Powell, K. M., He, Y., Xu, Y., Chalmers, M. J., Brunzelle, J. S., Zhang, H., Yang, H., Jiang, H., Li, J., Yong, E. L., Cutler, S., Zhu, J. K., Griffin, P. R., Melcher, K., and Xu, H. E. (2012). Molecular mimicry regulates ABA signaling by SnRK2 kinases and PP2C phosphatases. *Science* **335**, 85-8.

Stein, S. C., Woods, A., Jones, N. A., Davison, M. D., and Carling, D. (2000). The regulation of AMP-activated protein kinase by phosphorylation. *Biochem J* **345 Pt 3**, 437-43.

Sun, L., Wang, Y. P., Chen, P., Ren, J., Ji, K., Li, Q., Li, P., Dai, S. J., and Leng, P. (2011). Transcriptional regulation of SlPYL, SlPP2C, and SlSnRK2 gene families encoding ABA signal core components during tomato fruit development and drought stress. *J Exp Bot* **62**, 5659-69.

Tamura, K., Peterson, D., Peterson, N., Stecher, G., Nei, M., and Kumar, S. (2011). MEGA5: molecular evolutionary genetics analysis using maximum likelihood, evolutionary distance, and maximum parsimony methods. *Mol Biol Evol* **28**, 2731-9.

Thorsell, A. G., Lee, W. H., Persson, C., Siponen, M. I., Nilsson, M., Busam, R. D., Kotenyova, T., Schuler, H., and Lehtio, L. (2011). Comparative structural analysis of lipid binding START domains. *PLoS One* **6**, e19521.

Tsuzuki, T., Takahashi, K., Inoue, S., Okigaki, Y., Tomiyama, M., Hossain, M. A., Shimazaki, K., Murata, Y., and Kinoshita, T. (2011). Mg-chelatase H subunit affects ABA signaling in stomatal guard cells, but is not an ABA receptor in Arabidopsis thaliana. *J Plant Res* **124**, 527-38.

Ullah, H., Chen, J. G., Wang, S., and Jones, A. M. (2002). Role of a heterotrimeric G protein in regulation of Arabidopsis seed germination. *Plant Physiol* **129**, 897-907.

Umezawa, T., Nakashima, K., Miyakawa, T., Kuromori, T., Tanokura, M., Shinozaki, K., and Yamaguchi-Shinozaki, K. (2010). Molecular basis of the core regulatory network in ABA responses: sensing, signaling and transport. *Plant Cell Physiol* **51**, 1821-39.

Umezawa, T., Okamoto, M., Kushiro, T., Nambara, E., Oono, Y., Seki, M., Kobayashi, M., Koshiba, T., Kamiya, Y., and Shinozaki, K. (2006). CYP707A3, a major ABA 8'-hydroxylase involved in dehydration and rehydration response in Arabidopsis thaliana. *Plant J* **46**, 171-82.

Umezawa, T., Sugiyama, N., Mizoguchi, M., Hayashi, S., Myouga, F., Yamaguchi-Shinozaki, K., Ishihama, Y., Hirayama, T., and Shinozaki, K. (2009). Type 2C protein phosphatases directly regulate abscisic acid-activated protein kinases in Arabidopsis. *Proc Natl Acad Sci U S A* **106**, 17588-93.

Uno, Y., Furihata, T., Abe, H., Yoshida, R., Shinozaki, K., and Yamaguchi-Shinozaki, K. (2000). Arabidopsis basic leucine zipper transcription factors involved in an abscisic acid-dependent signal transduction pathway under drought and high-salinity conditions. *Proc Natl Acad Sci U S A* **97**, 11632-7.

Vahisalu, T., Kollist, H., Wang, Y. F., Nishimura, N., Chan, W. Y., Valerio, G., Lamminmaki, A., Brosche, M., Moldau, H., Desikan, R., Schroeder, J. I., and Kangasjarvi, J. (2008). SLAC1 is required for plant guard cell S-type anion channel function in stomatal signalling. *Nature* **452**, 487-91.

Vlad, F., Rubio, S., Rodrigues, A., Sirichandra, C., Belin, C., Robert, N., Leung, J., Rodriguez, P. L., Lauriere, C., and Merlot, S. (2009). Protein phosphatases 2C regulate the activation of the Snf1-related kinase OST1 by abscisic acid in Arabidopsis. *Plant Cell* **21**, 3170-84.

Walker-Simmons, M. K., Rose, P. A., Shaw, A. C., and Abrams, S. R. (1994). The 7[prime]-Methyl Group of Abscisic Acid Is Critical for Biological Activity in Wheat Embryo Germination. *Plant Physiol* **106**, 1279-1284.

Wallace, A. C., Laskowski, R. A., and Thornton, J. M. (1995). LIGPLOT: a program to generate schematic diagrams of protein-ligand interactions. *Protein Eng* **8**, 127-34.

Weiner, J. J., Peterson, F. C., Volkman, B. F., and Cutler, S. R. (2010). Structural and functional insights into core ABA signaling. *Curr Opin Plant Biol* **13**, 495-502.

Wilen, R. W., Hays, D. B., Mandel, R. M., Abrams, S. R., and Moloney, M. M. (1993). Competitive Inhibition of Abscisic Acid-Regulated Gene Expression by Stereoisomeric Acetylenic Analogs of Abscisic Acid. *Plant Physiol* **101**, 469-476.

Woods, A., Johnstone, S. R., Dickerson, K., Leiper, F. C., Fryer, L. G., Neumann, D., Schlattner, U., Wallimann, T., Carlson, M., and Carling, D. (2003). LKB1 is the upstream kinase in the AMP-activated protein kinase cascade. *Curr Biol* **13**, 2004-8.

Xiao, B., Heath, R., Saiu, P., Leiper, F. C., Leone, P., Jing, C., Walker, P. A., Haire, L., Eccleston, J. F., Davis, C. T., Martin, S. R., Carling, D., and Gamblin, S. J. (2007). Structural basis for AMP binding to mammalian AMP-activated protein kinase. *Nature* **449**, 496-500.

Xiong, L., Ishitani, M., Lee, H., and Zhu, J. K. (2001). The Arabidopsis LOS5/ABA3 locus encodes a molybdenum cofactor sulfurase and modulates cold stress- and osmotic stress-responsive gene expression. *Plant Cell* **13**, 2063-83.

Xiong, L., Schumaker, K. S., and Zhu, J. K. (2002). Cell signaling during cold, drought, and salt stress. *Plant Cell* **14 Suppl**, S165-83.

Yamazaki, D., Yoshida, S., Asami, T., and Kuchitsu, K. (2003). Visualization of abscisic acid-perception sites on the plasma membrane of stomatal guard cells. *Plant J* **35**, 129-39.

Ye, Y., and Godzik, A. (2003). Flexible structure alignment by chaining aligned fragment pairs allowing twists. *Bioinformatics* **19 Suppl 2**, ii246-55.

Yin, P., Fan, H., Hao, Q., Yuan, X., Wu, D., Pang, Y., Yan, C., Li, W., Wang, J., and Yan, N. (2009). Structural insights into the mechanism of abscisic acid signaling by PYL proteins. *Nat Struct Mol Biol* **16**, 1230-6.

Yoshida, R., Hobo, T., Ichimura, K., Mizoguchi, T., Takahashi, F., Aronso, J., Ecker, J. R., and Shinozaki, K. (2002). ABA-activated SnRK2 protein kinase is required for dehydration stress signaling in Arabidopsis. *Plant Cell Physiol* **43**, 1473-83.

Yoshida, R., Umezawa, T., Mizoguchi, T., Takahashi, S., Takahashi, F., and Shinozaki, K. (2006). The regulatory domain of SRK2E/OST1/SnRK2.6 interacts with ABI1 and integrates abscisic acid (ABA) and osmotic stress signals controlling stomatal closure in Arabidopsis. *J Biol Chem* **281**, 5310-8.

Yoshida, T., Fujita, Y., Sayama, H., Kidokoro, S., Maruyama, K., Mizoi, J., Shinozaki, K., and Yamaguchi-Shinozaki, K. (2010). AREB1, AREB2, and ABF3 are master transcription factors that cooperatively regulate ABRE-dependent ABA signaling involved in drought stress tolerance and require ABA for full activation. *Plant J* **61**, 672-85.

Yu, H., Chen, X., Hong, Y. Y., Wang, Y., Xu, P., Ke, S. D., Liu, H. Y., Zhu, J. K., Oliver, D. J., and Xiang, C. B. (2008). Activated expression of an Arabidopsis HD-START protein confers drought tolerance with improved root system and reduced stomatal density. *Plant Cell* **20**, 1134-51.

Yuan, X., Yin, P., Hao, Q., Yan, C., Wang, J., and Yan, N. (2010). Single amino acid alteration between valine and isoleucine determines the distinct pyrabactin selectivity by PYL1 and PYL2. *J Biol Chem* **285**, 28953-8.

Zhang, D. P., Wu, Z. Y., Li, X. Y., and Zhao, Z. X. (2002). Purification and identification of a 42-kilodalton abscisic acid-specific-binding protein from epidermis of broad bean leaves. *Plant Physiol* **128**, 714-25.

Zhang, S. Q., Outlaw, W. H., Jr., and Aghoram, K. (2001). Relationship between changes in the guard cell abscisic-acid content and other stress-related physiological parameters in intact plants. *J Exp Bot* **52**, 301-8.

Zhang, W., Ruan, J., Ho, T. H., You, Y., Yu, T., and Quatrano, R. S. (2005). Cis-regulatory element based targeted gene finding: genome-wide identification of abscisic acid- and abiotic stress-responsive genes in Arabidopsis thaliana. *Bioinformatics* **21**, 3074-81.

Zhou, X. E., Soon, F. F., Ng, L. M., Kovach, A., Suino-Powell, K. M., Li, J., Yong, E. L., Zhu, J. K., Xu, H. E., and Melcher, K. (2012). Catalytic mechanism and kinase interactions of ABA-signaling PP2C phosphatases. *Plant Signal Behav* **7**.

Zhu, J. K. (2002). Salt and drought stress signal transduction in plants. *Annu Rev Plant Biol* **53**, 247-73.

Zou, J., Abrams, G. D., Barton, D. L., Taylor, D. C., Pomeroy, M. K., and Abrams, S. R. (1995). Induction of Lipid and Oleosin Biosynthesis by (+)-Abscisic Acid and Its Metabolites in Microspore-Derived Embryos of Brassica napus L.cv Reston (Biological Responses in the Presence of 8[prime]-Hydroxyabscisic Acid). *Plant Physiol* **108**, 563-571.